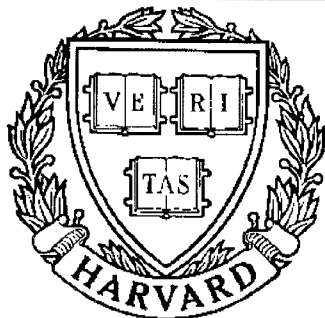


THESIS REPORT

Ph.D.



S Y S T E M S
R E S E A R C H
C E N T E R



*Supported by the
National Science Foundation
Engineering Research Center
Program (NSFD CD 8803012),
the University of Maryland,
Harvard University,
and Industry*

Tendon-Driven Manipulators: Analysis, Synthesis, and Control

*by J.J. Lee
Advisor: L.W. Tsai*

ABSTRACT

Title of Dissertation: **Tendon-Driven Manipulators: Analysis,
Synthesis, and Control**

Name of degree candidate: Jyh-Jone Lee, Doctor of Philosophy, 1991

Dissertation directed by: Professor Lung-Wen Tsai

Department of Mechanical Engineering

and

Systems Research Center

As the development of light-weight, small volume and versatile manipulators has grown in the field of robotics, the need for more efficient and relevant power transmission systems in the manipulators has become increasingly apparent. It is clear that the advent of efficient, low friction, and backlash-free actuation systems promises to provide significant gains in manipulator performance. Tendon transmission has been widely used to actuate small volume and light-weight articulated manipulators, such as dextrous mechanical hands, for it permits actuators to be installed remotely from the end-effector, thus reducing the bulk and inertia of the manipulator system. Current research on such actuation systems is accomplished on the basis of specialized designs. The lack of systematic approaches has limited our scope in realizing performance of such transmission systems. Therefore, when associated with systematic methodologies, the study of tendon-driven manipulators promises to be of major importance in the field of robotics.

This dissertation is concerned with four issues to enhance our use and understanding of tendon-driven manipulators. First, a systematic approach for the kinematic analysis of tendon-driven manipulators is established. Graph is used to represent the kinematic structure of tendon-driven manipulators. It is

shown that the kinematic structure of tendon-driven manipulators is in every way similar to that of epicyclic gear trains. The fundamental circuit equation developed for the kinematic analysis of epicyclic gear trains can thus be applied to this type of mechanism. The displacement equation governing joint angle space and tendon space can be easily obtained.

Secondly, the concept of structural isomorphism and the structural characteristics of tendon-driven manipulators are investigated. Based on the explored properties, a methodology for the enumeration of tendon-driven manipulators is developed. By applying the methodology, a class of kinematic structures having pseudo-triangular structure matrix is enumerated.

Thirdly, a method for assessing the kinematic/static performance of tendon-driven manipulators is developed. Transmission ellipsoids of the manipulators are investigated. A criterion for differentiating force transmission characteristics and a procedure for identifying least maximum-tendon-force are established. Based on the rationale developed, it is shown that optimal kinematic structure can be achieved for certain types of tendon routings.

Finally, the dynamic characteristics of tendon-driven manipulators are examined in detail. When integrating with a control algorithm in the manipulator, the dynamic performance of tendon-driven manipulators is realized and identified with more fidelity.

Tendon-Driven Manipulators: Analysis, Synthesis, and Control

by
Jyh-Jone Lee

Dissertation submitted to the Faculty of the Graduate School
of The University of Maryland in partial fulfillment
of the requirements for the degree of
Doctor of Philosophy

Advisory Committee:

Associate Professor Donald B. Barker

Professor P. S. Krishnaprasad

Professor Edward B. Magrab

Assistant Professor Uri Tasch

Professor Lung-Wen Tsai, Principle advisor

*“...Now we see but a poor reflection as in a mirror; then we shall see face to face. Now I know in part; then I shall know fully, even as I am fully known.
...”* I Corinthians 13:12

To Dad and Mom

ACKNOWLEDGEMENTS

This dissertation has been the result of many years of joyful association with the Department of Mechanical Engineering and Systems Research Center at the University of Maryland. It is also dedicated to all those who have stimulated and encouraged me to undertake this work. First of all, I would like to express most sincere thanks to Professor Lung-Wen Tsai, my thesis advisor, for his guidance, patience, and inspiration throughout this work. Special thanks are also due to Drs. Barker, Krishnaprasad, Magrab, and Tasch for their serving my advisory committee, reading this thesis, and providing informative comments.

Most of all, I would like to dedicate this work to my parents who guided me through my studies. Without their immeasurable love and encouragement, this thesis would not have been possible.

Financial support for this work was provided in part by the U.S. Department of Energy under grant DEF05-88ER13977 and in part by the NSF Engineering Research Centers program, NSF CDR 8500108.

TABLE OF CONTENTS

Acknowledgements	ii
List of Tables	vii
List of Figures	viii
1 Introduction	1
1.1 Robot And Its Transmissions	1
1.2 Overview of Tendon-Driven Robotic Systems	2
1.3 Motivation	4
1.4 Contributions	5
1.5 Preview	5
2 Kinematic Analysis	8
2.1 Introduction	8
2.2 General Assumptions	9
2.3 Structural Representations	10
2.3.1 Functional Representation	10
2.3.2 Planar Schematic Representation	11
2.3.3 Graph Representation	13
2.4 Topological Characteristics	13
2.5 Basic Equations	15

2.5.1 Fundamental Circuit Equation	15
2.5.2 Coaxiality Condition	15
2.5.3 Pulley Trains	15
2.6 Kinematics of Tendon-Driven Robotic Mechanisms	18
2.6.1 A Three-DOF Robotic Arm Driven by Endless Tendons	19
2.6.2 The Stanford/JPL Finger	22
2.6.3 A Six-DOF Manipulator	26
2.7 Summary	29
3 Structural Synthesis	30
3.1 Introduction	30
3.2 General Principle of Operation	31
3.3 Structural Characteristics	32
3.4 Structural Isomorphism	36
3.5 Structure Synthesis	38
3.6 Summary	44
4 Topological Analysis and Performance Evaluation	64
4.1 Introduction	64
4.2 Basic Equations	65
4.3 Transmission Ellipsoids	66

4.3.1 Force Ellipsoid	68
4.3.2 Velocity Ellipsoid	69
4.4 Isotropy of the Transmission Ellipsoid	70
4.5 Maximum Tendon Force	73
4.6 Application to Three-DOF Systems	75
4.7 Summary	79
5 Control and Simulation	81
5.1 Introduction	81
5.2 Dynamic Modelling	82
5.2.1 Dynamics of the Open-Loop Chain	82
5.2.2 Kinematic Relationship Between Joint Space and Tendon Space	82
5.2.3 Rotor Dynamics	83
5.2.4 Overall System Dynamics	84
5.3 Computed Torque Controller	85
5.4 Torque Resolver	86
5.5 Implementation and Simulation Results	96
5.5.1 Controller and Torque Resolver Design	96
5.5.2 Feedback Gains Design	97

5.5.3 Motor Inertia and Viscous Friction Effects on Tendon Force	102
5.5.4 Maximum Motor Torque	102
5.6 Summary	105
6 Summary and Conclusions	110
6.1 Review	110
6.2 Suggestions for Future Research	112
References	113
Appendix A Admissible pseudo-triangular structure matrices for six-DOF systems	116
Appendix B Dimensions of the open-loop chain	135

List Of Tables

3.1	Structure matrices for manipulators having three-DOF and four tendons	39
3.2	Homogeneous solutions for five-DOF tendon-driven manipulators having pseudo-triangular structure matrix	50
3.3	Homogeneous solutions for six-DOF tendon-driven manipulators having pseudo-triangular structure matrix	56
4.1	List of B^T , \underline{f}_h , C and θ^*	78
4.2	A comparison of maximum tendon forces	79

List Of Figures

2.1 (a) Open-ended tendon, (b) Endless tendon	11
2.2 (a) Planar schematic of Fig. 2.1(a)	12
(b) Planar schematic of Fig. 2.1(b).	12
2.3 (a) Graph representation of Fig. 2.2(a)	14
(b) Graph representation of Fig. 2.2(b)	14
2.4 (a) A single-tendon-driven articulated mechanism	17
(b) Graph representation of Fig. 2.4(a)	17
2.5 (a) Planar schematic representation of a three-DOF manipulator	20
(b) Canonical graph of Fig. 2.5(a)	20
(c) Two tendon drives	20
2.6 (a) Functional schematic of the Stanford/JPL finger	23
(b) Planar schematic of the Stanford/JPL finger	23
2.7 Planar schematic of a six-DOF manipulator	27
3.1 Two structurally isomorphic, two-DOF, tendon-driven manipulators ..	37
3.2 Two structurally isomorphic, three-DOF, tendon-driven manipulators .	38
3.3 Functional schematic of a one-DOF tendon-driven manipulator	42
3.4 Planar schematic of a two-DOF tendon-driver manipulator	43
3.5 Planar schematic and the associated structure matrices for	

three-DOF tendon-driven manipulators	45
3.6 Planar schematic and the associated structure matrices for	
four-DOF tendon-driven manipulators	46
3.7 Structure matrices for five-DOF tendon-driven manipulators	51
4.1 A two-DOF tendon-driven manipulator	67
4.2 Quadratic joint torque constraint	68
4.3 Tendon force ellipsoid	69
4.4 Tendon velocity ellipsoid	70
4.5 Non-isomorphic kinematic structures having three-DOF	77
5.1 Schematic of the motor-tendon spooling system	83
5.2 Characteristics of $O^+(x)$ and $O^-(x)$	87
5.3 Free-body diagrams of a three-DOF tendon-driven manipulator	90
5.4 Control block diagram of a three-DOF tendon-driven manipulator	97
5.5 (a) Design details of the controller shown in Fig. 5.4	98
5.5 (b) Design details of the resolver shown in Fig. 5.4	99
5.6 Joint angle response vs. various damping ratios	101
5.7 The effect of feedback gain on system stiffness	101
5.8 (a) Motor torque response with $K_p=225$ and $K_v=30$, peak value= 7.64×10^4 dyne-cm, (b) Motor torque response with $K_p=400$ and $K_v=40$, peak	

value= 1.34×10^5 dyne-cm	103
5.9 Motor rates with $K_p=225$ and $K_v=30$	104
5.10 Motor accelerations with $K_p=225$ and $K_v=30$	104
5.11 Tendon force response with $K_p=225$ and $K_v=30$, $B=1.67 \times 10^4$ dyne	106
5.12 Tendon force response with $K_p=400$ and $K_v=40$ $B=1.22 \times 10^4$ dyne .	106
5.13 Motor torque response without considering motor inertia and viscous friction ($K_p=225$ and $K_v=30$)	107
5.14 Tendon force response without considering motor inertia and viscous friction ($K_p=225$ and $K_v=30$)	107
5.15 Motor torque response for the structure shown in Fig. 4.5(a), peak value = 1.47×10^5 dyne-cm	108
5.16 Motor torque response for the structure shown in Fig. 4.5(b), peak value = 2.19×10^5 dyne-cm	108
5.17 Motor torque response for the structure shown in Fig. 4.5(c), peak value = 8.88×10^4 dyne-cm	109
5.18 Motor torque response for the structure shown in Fig. 4.5(e), peak value = 1.11×10^5 dyne-cm	109
A1 Schematic of the open-loop chain	136

Chapter 1

Introduction

1.1 Robot and Its Transmissions

The kinematic structure of a robotic manipulator often takes the form of an open-loop kinematic chain. It commonly consists of serially connected links. For an open-loop manipulator with n -DOF (Degree-Of-Freedom) having n independent joints and $n + 1$ links, the structure is mechanically simple and easy to construct. Actuation of the joint in such a structure usually requires the actuators to be installed along the joint axes. Thus, the introduction of actuators in some way or another increases the inertia of the manipulator system. Although direct drives of electrical motors associated with the joints are becoming more popular, they are found mainly on the lighter duty assembly robots.

To reduce the inertia of a manipulator, it is often necessary to use a transmission system that permits the actuators to be located remotely from the point of application. The components and configurations of the transmission system may vary in forms, such as gear trains using meshing gears, pulley trains using belts, linkages using tie-rod connections, and so on. Note that the major disadvantage of introducing a transmission system is the extra cost of the transmission components or the opportunity for creating some drawbacks such as backlash, vibration and wear in the overall system. The type of transmission system selected depends on the application of the robot and other design constraints. Generally, in a robot transmission system, the power-to-weight ratio must be optimized, backlash and vibration minimized or compensated for, inertia kept as low as possible, and friction reduced every where.

This dissertation addresses one aspect of the transmission system in the robotic manipulator: tendon transmission. The term *tendon* is widely used to imply belts, cables, or similar types of applications. Specifically, this work is concerned with the systematic approaches for the synthesis of tendon routing in a robotic manipulator from the kinematic point of view rather than from the geometric or material point of view. Experience with tendons has pointed out that tendons are commonly used to transmit power between shafts where center distance is too great for gearing or similar power-transmission devices. Thus, tendons greatly simplify a machine and, consequently, are a major cost-reducing element (Faires, 1959; Shigley and Mitchell, 1983).

In recent years, the application of tendons in teleoperator or robot transmission has become more frequent. In robots, tendon transmission permits actuators to be installed remotely from the joints they drive, therefore, reducing the volume and the inertia of the manipulator system. In addition, pretensioned tendons have no backlash. These merits have made tendon transmission more eminent in the transmission design of robots, especially, in a dextrous hand design where the requirements of small volume and light weight are crucial. Hence, a fundamental understanding of tendon transmission is becoming more necessary and important in the field of robotics.

1.2 Overview of Tendon-Driven Robotic Systems

Probably the most frequent occurrence of tendon-driven robotic systems is in the field of anthropomorphic manipulating systems. Researchers used synthetic tendon-driven systems to emulate biological tendon-driven systems in the study of animal movement. Almost without exception, no matter how aes-

thetically the synthetic systems emulate animal movements, graceful behavior of natural systems still can not be well achieved. Nonetheless, some fruitful results can be perceived. An overview of some of the results follows.

One form of tendon transmission in robotic systems is to use one motor acting through a closed-loop belt to drive the mechanism. Okada (1977) used this approach to actuate his three-fingered mechanical hand. This construction is similar to that of the traditional use of belt drives where an endless belt connects two shafts and transmits motion or power. This application requires a pretensioning of the system so the belts will not slacken when the pulleys move at high speeds. However, experience with this type of construction has shown that a significant amount of friction or vibration may be introduced by pretensioning the belts. The result is low efficiency of the system. Another form of tendon transmission is to employ a spring-biased device in which a tendon is pulling against a spring-biased joint. Rovetta (1977) built a mechanical gripper in which return springs were installed in the joints to serve as a bias torque source. This application prohibits the system from fine force control of manipulation since the spring exhibits somewhat nonlinear properties and causes an asymmetric response.

To alleviate the roughness caused by endless belt drives, researchers studied the biokinematics of living animals and found that open-ended (defined in Chapter 2) tendon drives, as in human muscles, might offer more uniform system characteristics. Morecki, et al. (1980) discussed some of the problem encountered in the design of a new drive, which is accordingly open-ended tendon transmission, for an anthropomorphic two-handed manipulator. The authors analyzed the structure of the drive system and identified the kinematic rela-

relationship between joint angular displacement and tendon linear displacement. One interesting result pointed out by the authors is that in order to control an n -DOF manipulator, at least $n + 1$ open-ended tendons are needed. Later, Salisbury (1982) applied this principle to design the actuation system for the Stanford/JPL three-fingered hand. In the Stanford/JPL hand, each finger has three degrees of freedom and is actuated by four open-ended tendons. The kinematics and statics of the tendon transmission system were also addressed.

On the other side, Jacobsen, et al. (1985) designed the Utah/MIT dextrous hand intended for prosthetic hand use. In the Utah/MIT hand, each finger incorporated eight open-ended tendons for the control of four joints where each joint was actuated by two opposing tendons. This hand involved 38 motors for the actuation of 19 independently controlled joints. Various tendon-driven manipulators intended to emulate human functions, are described in the literature by Leaver and McCarthy (1987), Morecki, et al. (1984), Pham and Heginbotham (1986), and others.

1.3 Motivation

This work is intended to extend the author’s realization that tendon transmission systems can be enhanced if more systematic approaches for the synthesis of tendon routing can be developed. While reviewing tendon-driven systems, the author has noticed that these special purpose devices have been used to study the gripping function of human hands and have focused on the mechanics of manipulation and their controls. Although a few attempts have been made to address the kinematic or static analysis of the actuation systems in the devices, there has been a lack of systematic approaches to guide users in ap-

plying such actuation systems. It seems that the construction of the actuation systems was developed by designers' ingenuity. Therefore, a unified approach for the analysis, synthesis, and control of such systems can be promising and contributive to the field of robotics.

1.4 Contributions

This dissertation describes the development of methodologies for the analysis, structural synthesis, performance evaluation, and control issues for the design of tendon-driven manipulators.

Among the principal contributions of this dissertation are:

- 1) A systematic approach for the kinematic analysis of tendon-driven robotic manipulators,
- 2) A methodology for enumeration of the kinematic structures of tendon-driven manipulators,
- 3) Methods for kinematic/static performance evaluation of the kinematic structure, and
- 4) An algorithm for the control and realization of dynamic characteristics of tendon-driven manipulators.

The author anticipates that this research will give better understanding for the mechanical design of tendon-driven manipulators.

1.5 Preview

This dissertation is organized as follows.

In Chapter 2, the graph theory is used to develop a systematic approach

for the kinematic analysis of tendon-driven manipulators. The correspondence between the graph representation of kinematic structure and the mechanism is established. It is shown that the kinematic structure of tendon-driven kinematic chains is similar to that of epicyclic gear trains. It is also shown that, using the concept of fundamental circuits, displacement equations of tendon-driven robotic mechanisms can be systematically derived from the kinematic structure. Several examples are used to illustrate the principle.

In Chapter 3, the structural characteristics of tendon-driven manipulators is explored. The concept of structural isomorphism for tendon-driven manipulators is introduced. Based on the rationale, a systematic methodology for the enumeration of tendon-driven manipulators having a pseudo-triangular structure matrix is developed. Kinematic structures with up to six-DOF are enumerated.

In Chapter 4, a method for the evaluation of kinematic/static performance of the kinematic structure is developed. By looking at the condition number and the homogeneous solution of the structure matrix, we are able to identify the so-called *isotropic transmission* where the magnitude of the tendon force vector is identical in every direction provided that the joint torque vector is confined to a quadratic equation. A method is also introduced for calculating the least maximum-tendon-force from which a criterion for identifying optimal kinematic structure has been established.

In Chapter 5, the computed torque method is used to formalize the control algorithm for tendon-driven manipulators. A technique, called “torque resolver,” is introduced to map the joint torque signals to motor torque signals. In this chapter, the author also simulates the dynamics of tendon-driven manip-

ulators. Some effects that influence the dynamic performance of a tendon-driven manipulator are dictated as the final stage of the research.

Finally, in Chapter 6 the author reviews the dissertation, summarizes his contributions, and suggests further studies.

Chapter 2

Kinematic Analysis

2.1 Introduction

Gear trains are commonly used to transmit power or motion between either parallel or non-parallel shafts with small offset distance. When the center distance between two offset shafts becomes large, it is often necessary to add intermediate shafts and idler gears in order to keep the size of the gears reasonably small. An alternative method of power transmission is to use tendons or belts and pulleys. This type of mechanisms is called tendon-driven mechanisms. Usually, the actuators are attached to a supporting base (or fixed reference frame) while the end-effector of the manipulator is free to manipulate objects. The relative movement of the actuators results in the motion of the links that position the end-effector in a desired position/orientation. Thus, in most applications, we are interested in the motion of the end-effector with respect to the fixed reference frame, in particular the relations between the motor-variable space and the position/orientation of the end-effector. To date, the kinematic or static analysis of such mechanical systems has been accomplished on an individual basis. This chapter addresses a systematic procedure for the kinematic and static analysis of multi-degree-of-freedom, tendon-driven, robotic mechanisms.

Graph theory has been utilized for representing the topology of kinematic chains or mechanisms over a period of time. The use of graph theory may help simplify our task of kinematic and/or static analysis, because it visually clarifies the relationship among the links and joints in a kinematic chain or mechanism.

The application of graph theory to the kinematic analysis and synthesis of epicyclic gear trains has been well established in recent years (Buchsbaum and Freudenstein, 1970; Day, et al., 1983; Freudenstein, 1971; Freudenstein, et al., 1984; Freudenstein and Yang, 1972; and Tsai, 1987). In what follows, the kinematic structure of tendon-driven robotic mechanisms will be investigated via graph representation. It will be shown that the kinematic structure of tendon-driven mechanisms is similar to that of epicyclic gear trains. Therefore, the fundamental circuit equation developed for the kinematic analysis of epicyclic gear trains (Tsai, 1988) can be directly applied to this type of mechanisms. It will also be shown that once the displacement equations are obtained, the input and output torques (or forces) relationship can be easily derived.

2.2 General Assumptions

In this work, only those mechanisms which obey the following assumptions will be considered:

- (i) The tendons are always under tension and the amount of stretch in tendons due to variation of tension is negligible.
- (ii) The friction between pulleys and tendons is large enough to prevent relative sliding to occur.
- (iii) The mechanism shall obey the general DOF equation, i.e., no special proportions are required to ensure the mobility of a tendon-driven mechanism.
- (iv) Each pulley must have a turning pair on its axis and every pair of pulleys connected by a tendon must have a carrier (or arm) in order to maintain a constant center distance between the pulleys.

- (v) The mechanism shall be of articulated type, i.e., after the removal of tendons and pulleys, the mechanism becomes an open-loop chain.

2.3 Structural Representations

Three types of representation, functional, planar schematic, and graph, will be described in this section.

2.3.1 Functional Representation

Functional representation refers to the conventional drawing of a mechanism. Shafts, pulleys, tendons, and other elements are identified as such. For the reasons of clarity and simplicity, only functional elements essential to the kinematic structure are shown. Different functional representation may represent different designs of the same topological structure (e.g., planar versus spatial mechanisms). For tendon-driven robotic mechanisms, there are two basic routing techniques. The first is known as the *open-ended tendons* and the second the *endless tendons*.

In an open-ended routing, one end of the tendon is tied to a driven pulley while the other end is attached to a linear actuator or a driving pulley that is installed on a rotary actuator. The driven pulley is usually attached to a link to be controlled. Fig. 2.1(a) shows two pulleys, i and j , that are connected by an open-ended tendon. Link k , which is used to maintain a constant center distance for the two pulleys, is called the carrier.

In the endless routing, each tendon or belt is wrapped around two or more pulleys of constant center distance in an endless loop. Fig. 2.1(b) shows an endless tendon routed around two pulleys. Again, the carrier k is used to

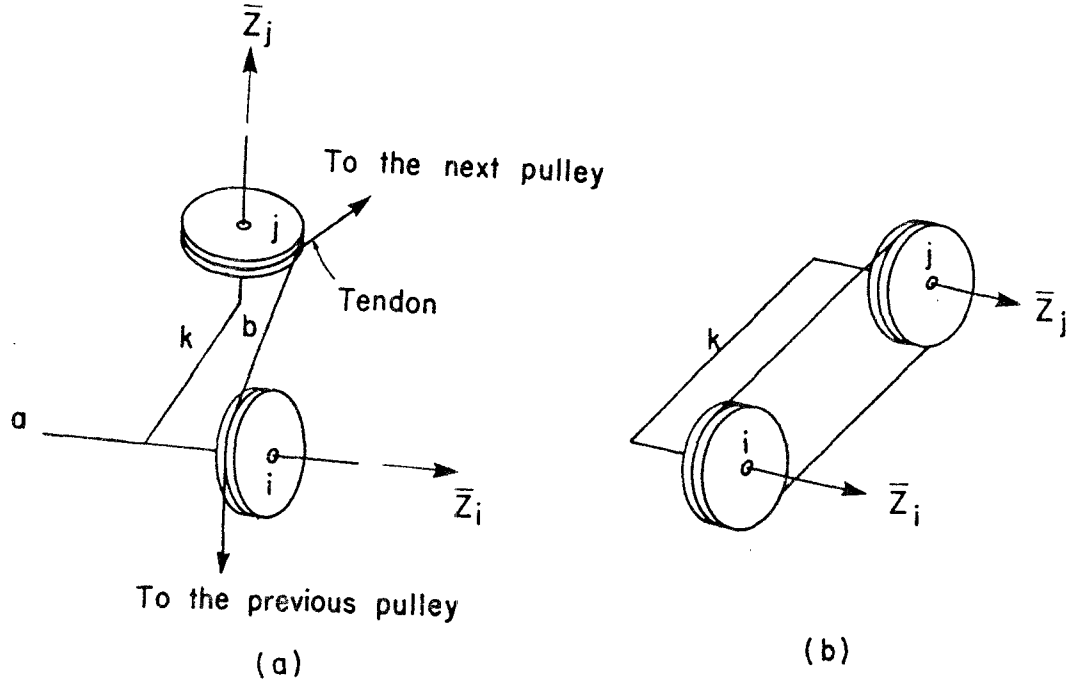


Fig. 2.1 (a) Open-ended tendon, (b) Endless tendon

maintain a constant center distance for the two pulleys.

Note that both kinematic chains (or sub-chains) shown in Figs. 2.1(a) and 2.1(b) consist of three rigid links, links i , j , and k , and a flexible tendon. The geometry of such mechanisms can be defined by the Denavit and Hartenberg's (1955) parameters, i.e., by the offset distance, twist angle, etc., between two joint axes, in addition to the radii of the pulleys.

2.3.2 Planar Schematic Representation

In this representation, a positive direction of rotation is assigned to each joint axis in the mechanism of interest and the joint axis fixed to the reference frame is considered as the first joint axis. Then, starting from the second joint axis, every axis is twisted about the common normal defined by the axis itself and its preceding axis until all the joint axes are parallel to each other and are

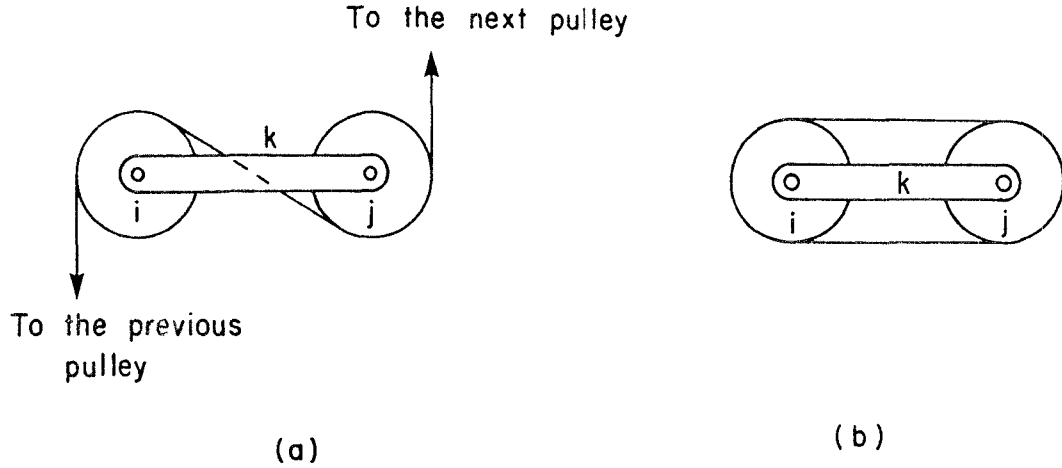


Fig. 2.2 (a) Planar schematic of Fig. 2.1(a), (b) Planar schematic of Fig. 2.1(b)

pointed toward the same positive Z -direction. In this manner, the routing of tendons can be clearly shown without losing the fundamental characteristics of relative rotations among the pulleys and their carriers.

Figures. 2.2(a) and 2.2(b) show the planar schematic of the mechanisms shown in Figs. 2.1(a) and 2.1(b), respectively. The routing method shown in Fig. 2.2(a) is called the *cross-type* while the one shown in Fig. 2.2(b) is called the *parallel-type*. Note that the routing of the kinematic chain shown in Fig. 2.1(a) can also be sketched in a parallel type construction if the definition of the positive Z -direction for either one of the two axes is reversed. Although this change does affect the sign of rotation in the fundamental circuit equation to be described later, it has no effect on the actual motion of the mechanism.

In general, two pulleys are said to have parallel-type routing if a positive rotation of one pulley with respect to its carrier produces a positive rotation of the other, and cross-type routing if a positive rotation of one pulley produces a negative rotation of the other.

2.3.3 Graph Representation

In the graph representation, links are denoted by vertices and joints by edges. The edge connection between vertices corresponds to the joint connection between links. Every pair of pulleys coupled together by a tendon, whether an open-ended or an endless tendon, is considered a pulley pair. In this regard, the tendon has been treated as an element which merely provides the necessary constraints to the two-coupled pulleys. In order to distinguish different types of pair connections, turning pair is denoted by thin edge, parallel-type routing by double-line edge, and cross-type routing by heavy edge. Further, thin edges are labeled according to their axis locations. The graph of a tendon-driven articulated mechanism is, therefore, similar to that of an epicyclic gear train.

Fig. 2.3(a) shows the graph representation for the tendon-driven mechanism shown in Fig. 2.2(a), where the vertices i , j , and k correspond to links i , j , and k ; thin edges $i-k$ and $j-k$ correspond to the turning pairs connecting links i and k , and links j and k ; heavy edge $i-j$ corresponds to cross-type routing between links i and j ; and the edge labels a and b correspond to the axis levels a and b , respectively. Similarly, Fig. 2.3(b) shows the graph representation of the mechanism shown in Fig. 2.2(b) in which the parallel-type routing is denoted by a double-line edge.

2.4 Topological Characteristics

As in epicyclic gear trains, the graph of tendon-driven articulated mechanisms can be characterized by the following fundamental rules:

- (i) For an l -link, n -DOF, tendon-driven articulated mechanism, there are $(l - 1)$ turning pairs and $(l - n - 1)$ pulley pairs.

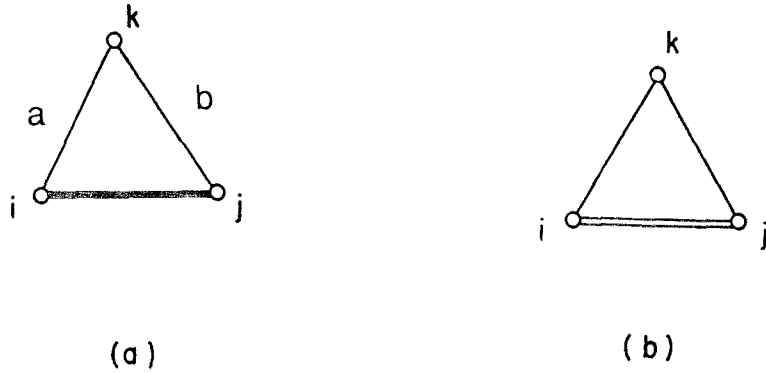


Fig. 2.3 (a) Graph representation of Fig. 2.2(a), (b) Graph representation of Fig. 2.2(b).

- (ii) The subgraph obtained by deleting all the double-line and heavy edges is a tree, and there can be no circuit formed exclusively by thin edges.
- (iii) Any double-line or heavy-edge added to the tree forms a fundamental circuit (f -circuit) having one double-line or heavy edge and several thin edges.
- (iv) The number of f -circuits is equal to the number of double-line and heavy edges.
- (v) Each thin edge can be characterized by a level which identifies the axis location of a turning pair.
- (vi) In each f -circuit, there is a vertex, called the transfer vertex, such that all edges on one side of the transfer vertex are at the same level and edges on the opposite side are at a different level. The transfer vertex corresponds to the carrier in a pulley train.

2.5 Basic Equations

2.5.1 Fundamental Circuit Equation

Let i and j denote the vertices of a pulley pair in an f -circuit for which k is the transfer vertex. Then links i , j and k constitute a simple tendon-and-pulley train. A positive direction of rotation can be assigned to each joint axis of the pulley pair, and a fundamental circuit equation (Tsai, 1988) can be written as follows:

$$r_i\theta_{i,k} = \pm r_j\theta_{j,k} \quad (2.1)$$

where $\theta_{i,k}$ and $\theta_{j,k}$ denote the relative rotations of links i and j with respect to the carrier link k and, r_i and r_j denote the radii of the two matching pulleys i and j , respectively. The sign of Eq. (2.1) is to be determined by the routing of the tendon: positive for the parallel-type routing and negative for the cross-type. Note that Eq. (2.1) is valid whether the carrier is fixed or not.

2.5.2 Coaxiality Condition

Let i , j , and k be three links that share a common joint axis, then similar to epicyclic gear trains (Tsai, 1988), the following chain rule applies

$$\theta_{i,j} = \theta_{i,k} - \theta_{j,k} \quad (2.2)$$

Equation (2.2) is useful for relating the relative rotations among three or more coaxial links.

2.5.3 Pulley Trains

Let links 0, 1, 2, and 3 be connected in series, by turning pairs, to form a spatial open-loop chain; let a , b , and c be the consecutive joint axes; and let pulleys j , $j+1$ and $j+2$ be pivoted about the joint axes a , b and c , respectively,

as shown in Fig. 2.4(a). Pulleys j and $j + 1$ are free to rotate with respect to links 0, 1, and 2 while pulley $j+2$ is rigidly tied to link 3. An endless tendon has been routed around these pulleys as shown in Fig. 2.4(a). We consider link 0 as the base link and link 3 as the link to be controlled, and seek to find a transformation between the rotation of the base pulley, j , and the joint angles, $\theta_{1,0}$, $\theta_{2,1}$, and $\theta_{3,2}$ in the open-loop chain.

Figure 2.4(b) shows the corresponding graph representation of Fig. 2.4(a). This graph consists of two f -circuits: $(j, j + 1, 1)$ and $(j + 1, 3, 2)$, where the first two numbers in the parenthesis denote the link numbers of a pulley pair, and the third denotes the corresponding carrier. Writing Eq. (2.1) once for each of the two f -circuits, yields:

$$r_j \theta_{j,1} = r_{j+1} \theta_{j+1,1} \quad (2.3)$$

and

$$r_{j+1} \theta_{j+1,2} = r_{j+2} \theta_{3,2} \quad (2.4)$$

Since links 0, 1, and j are coaxial, Eq. (2.2) yields

$$\theta_{j,1} = \theta_{j,0} - \theta_{1,0} \quad (2.5)$$

Similarly, writing Eq. (2.2) for links 1, 2, and $j + 1$, yields

$$\theta_{j+1,2} = \theta_{j+1,1} - \theta_{2,1} \quad (2.6)$$

Substituting Eqs. (2.5) and (2.6) into (2.3) and (2.4), respectively, and eliminating $\theta_{j+1,1}$ from the two resulting equations, yields

$$\theta_{j,0} = \theta_{1,0} + (r_{j+1}/r_j) \theta_{2,1} + (r_{j+2}/r_j) \theta_{3,2} \quad (2.7)$$

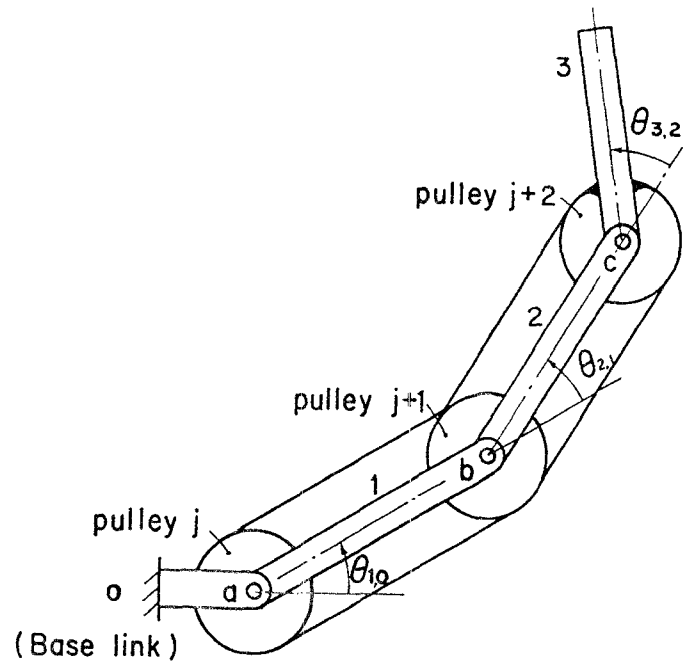


Fig. 2.4(a) A single tendon-driven articulated mechanism

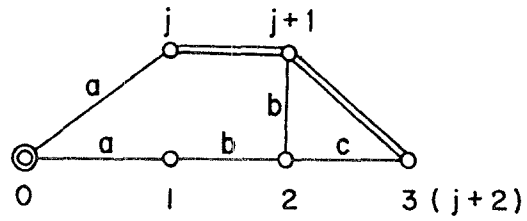


Fig. 2.4(b) Graph representation of Fig. 2.4(a)

Equation (2.7) shows the influence of the joint angles, $\theta_{1,0}$, $\theta_{2,1}$ and $\theta_{3,2}$, on the rotation of the base pulley $\theta_{j,0}$. In general, the relationship between the rotation of a base pulley and the joint angles in an open-loop chain with $(m+1)$ links can be written as follows

$$\begin{aligned}\theta_{j,0} = & \theta_{1,0} \pm (r_{j+1}/r_j)\theta_{2,1} \pm (r_{j+2}/r_j)\theta_{3,2} \\ & \pm \dots \pm (r_{j+m-1}/r_j)\theta_{m,m-1}\end{aligned}\quad (2.8)$$

The sign of each term, $(r_{j+k-1,1}/r_j)\theta_{k,k-1}$, in Eq. (2.8) is to be determined by the number of cross-type routing preceding the k^{th} joint axis. If the number of cross-type routing is even, the sign is positive; otherwise it is negative. This equation can be derived by an inspection of the kinematic structure without going through the graph representation, once one becomes familiar with the subject.

Taking the total derivative of Eq. (2.8), yields

$$\begin{aligned}d\theta_{j,0} = & d\theta_{1,0} \pm (r_{j+1,1}/r_j)d\theta_{2,1} \pm (r_{j+2}/r_j)d\theta_{3,2} \\ & \pm \dots \pm (r_{j+m-1,1}/r_j)d\theta_{m,m-1}\end{aligned}\quad (2.9)$$

where $d()$ denotes the total derivative of $()$. Hence, the coefficients of each derivative on the right-hand-side of Eq. (2.9) may be considered as the partial rate of change of the base pulley rotation with respect to the corresponding joint angle.

2.6 Kinematics of Tendon-Driven Robotic Mechanisms

It has been shown by Tsai (1988) that the graph of a spatial robotic bevel-gear train can be reconstructed into a canonical form from which an equivalent

open-loop chain can be identified. Similarly, a canonical graph can be constructed to represent the topological structure of a tendon-driven robotic mechanism. Hence, the kinematic analysis of articulated, tendon-driven robotic devices can be accomplished in two steps. First, the end-effector position and/or orientation can be related to the joint angles associated with the equivalent open-loop chain. Then, these joint angles can be related to the rotational displacements of the base pulleys. The first step is well-known and will not be discussed in this work. In what follows, a systematic procedure will be described for the derivation of the linear transformation relating the rotational displacements of the base pulleys to the joint angles. Three examples will be used to illustrate the principle.

2.6.1 A Three-DOF Robotic Arm Driven by Endless Tendons

Figure 2.5(a) shows the planar schematic of a spatial robotic arm. Pulleys 4 and 5 are free to rotate about axis a , pulleys 2 and 6 are free to rotate about axis b , and pulley 3 is free to rotate about axis c . The first moving link serves as the carrier for the pulley pairs (4,2), and (5,6); the second moving link which is rigidly tied to pulley 2, serves as the carrier for the pulley pair (6,3); and the third moving link is attached to pulley 3. The first tendon connects pulleys 4 and 2, and the second tendon connects pulleys 5, 6, and 3. Overall, the mechanism consists of seven rigid links and two endless tendons. It has three degrees of freedom. We can designate links 1, 4, and 5 as the inputs and link 3 as the output or end-effector. Note that the mechanism shown in Fig. 2.5(a) has been sketched in its zero *reference position* (Tsai, 1988).

Figure 2.5(b) shows the corresponding canonical graph of the mechanism. It can be seen from Fig. 2.5(b) that the equivalent open-loop chain for the

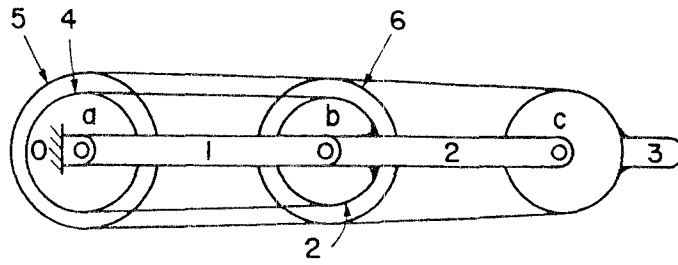


Fig. 2.5(a) Planar schematic representation of a three-DOF manipulator

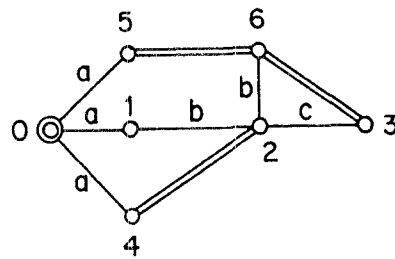


Fig. 2.5(b) Canonical graph of Fig. 2.5(a)

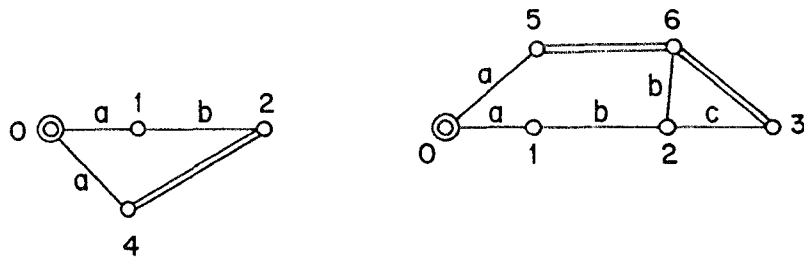


Fig. 2.5(c) Two tendon drives

mechanism consists of links 0-1-2-3, and there are three f -circuits: (2, 4, 1), (5, 6, 1) and (3, 6, 2). Figure 2.5(c) shows the routing of the two tendons with respect to the equivalent open-loop chain. The parallel-type routing is clearly depicted in both Figs. 2.5(b) and 2.5(c). Each of the tendon routings shown in Fig. 2.5(c) is sometimes called a transmission line.

Writing Eq. (2.8) once for each of the two tendon routings shown in Fig. 2.5(c), yields

$$\theta_{4,0} = \theta_{1,0} + (r_2/r_4)\theta_{2,1} \quad (2.10)$$

and

$$\theta_{5,0} = \theta_{1,0} + (r_6/r_5)\theta_{2,1} + (r_3/r_5)\theta_{3,2} \quad (2.11)$$

where r_j , $j=2, 3, 4, \dots$, denote the radii of the pulleys shown in Fig. 2.5(a).

We can add an identity equation, $\theta_{1,0} = \theta_{1,0}$, to Eqs. (2.10) and (2.11) and then rearrange them in a matrix form as shown below:

$$\begin{bmatrix} \theta_{1,0} \\ \theta_{4,0} \\ \theta_{5,0} \end{bmatrix} = \begin{bmatrix} 1 & 0 & 0 \\ 1 & r_2/r_4 & 0 \\ 1 & r_6/r_5 & r_3/r_5 \end{bmatrix} \begin{bmatrix} \theta_{1,0} \\ \theta_{2,1} \\ \theta_{3,2} \end{bmatrix} \quad (2.12)$$

Equation (2.12) provides the necessary transformation between the angular displacements of the input links ($\theta_{1,0}$, $\theta_{4,0}$, $\theta_{5,0}$) and the joint angles ($\theta_{1,0}$, $\theta_{2,1}$, $\theta_{3,2}$). The equations are linear and its inverse transformation can be easily derived.

Let $r_4 = r_2$ and $r_5 = r_6 = r_3$, then Eq. (2.12) becomes,

$$\begin{bmatrix} \theta_{1,0} \\ \theta_{4,0} \\ \theta_{5,0} \end{bmatrix} = \begin{bmatrix} 1 & 0 & 0 \\ 1 & 1 & 0 \\ 1 & 1 & 1 \end{bmatrix} \begin{bmatrix} \theta_{1,0} \\ \theta_{2,1} \\ \theta_{3,2} \end{bmatrix} \quad (2.13)$$

and its inverse transformation is then given by,

$$\begin{bmatrix} \theta_{1,0} \\ \theta_{2,1} \\ \theta_{3,2} \end{bmatrix} = \begin{bmatrix} 1 & 0 & 0 \\ -1 & 1 & 0 \\ 0 & -1 & 1 \end{bmatrix} \begin{bmatrix} \theta_{1,0} \\ \theta_{4,0} \\ \theta_{5,0} \end{bmatrix} \quad (2.14)$$

Note that, for this special proportion, the second joint is locked when links 1 and 4 are driven at the same rate; the third joint is locked when links 4 and 5 are driven at the same rate; and both the second and third joints are locked when links 1, 4, and 5 are all driven at the same rate.

2.6.2 The Stanford/JPL Finger

Figure 2.6(a) shows the functional representation of the Stanford/JPL Finger taken from Mason and Salisbury (1985), where the first joint axis, Z_1 , is fixed to the base link, link 0; the second joint axis, Z_2 , is perpendicular to the first; and the third joint axis, Z_3 , is parallel to the second. Pulleys 4, 5, 6, and 7 are free to rotate about the first joint axis, pulleys 2 and 8 are free to rotate about the second joint axis, and pulley 3 is free to rotate about the third joint axis. The first link, link 1, serves as the carrier for the pulley pairs (4,2), (5,2), (6,8), and (7,8). The second link, which is attached to pulley 2, serves as the carrier for the pulley pair (8,3). The third link is attached to pulley 3. The first tendon, T_4 , connects pulley 2 to 4; the second, T_5 , connects pulley 2 to 5; the third, T_6 , connects pulley 3 to 8 and then 6; and the fourth, T_7 , connects pulley 3 to 8 and then 7 in open-ended routing as shown in Fig. 2.6(a). Overall, the mechanism consists of nine rigid links and four unidirectional tendons. Although it has three degrees of freedom, it requires four open-ended tendons to achieve positive control of the mechanism.

Figure 2.6(b) shows the mechanism in a planar schematic. The equivalent open-loop chain consists of links 0-1-2-3. The routing of the four tendons with

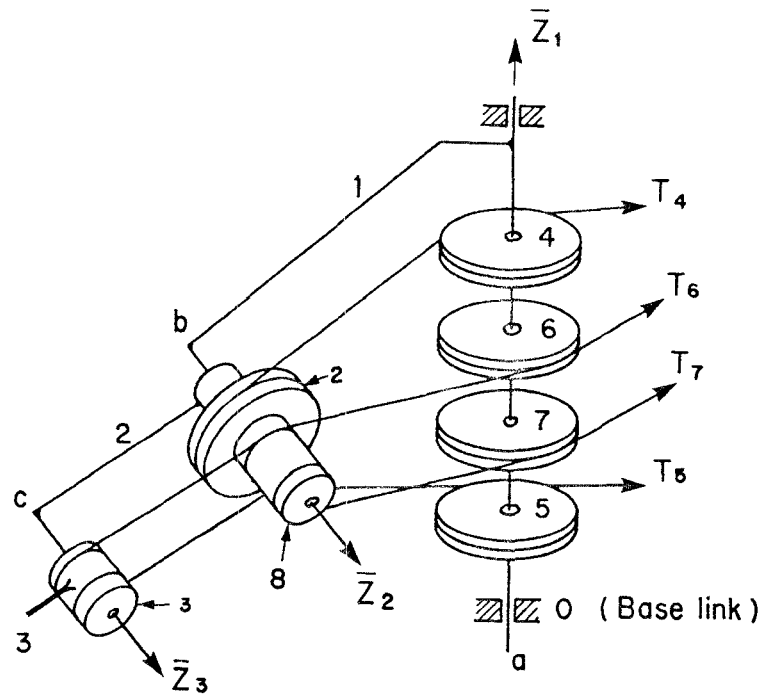


Fig. 2.6(a) Functional schematic of the Stanford/JPL finger

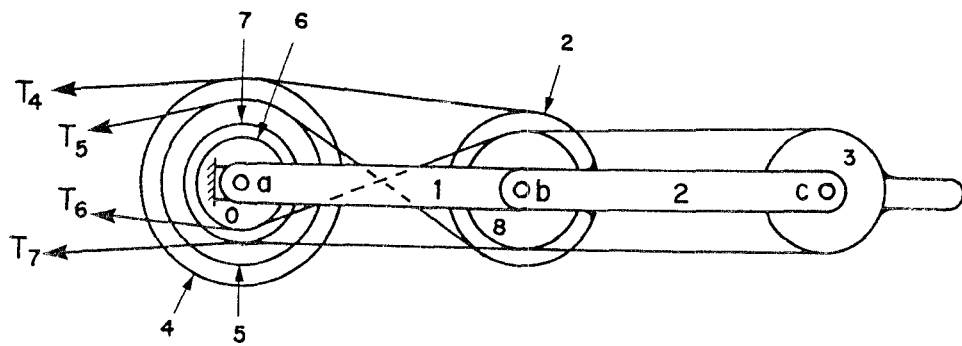


Fig. 2.6(b) Planar schematic of the Stanford/JPL finger

respect to the equivalent open-loop chain is clearly depicted in Fig. 2.6(b).

Writing Eq. (2.8) once for each of the four tendon routings shown in Fig. 2.6(b), yields:

$$\theta_{4,0} = \theta_{1,0} + (r_2/r_4)\theta_{2,1} \quad (2.15)$$

$$\theta_{5,0} = \theta_{1,0} - (r_2/r_5)\theta_{2,1} \quad (2.16)$$

$$\theta_{6,0} = \theta_{1,0} - (r_8/r_6)\theta_{2,1} - (r_3/r_6)\theta_{3,2} \quad (2.17)$$

and

$$\theta_{7,0} = \theta_{1,0} + (r_8/r_7)\theta_{2,1} + (r_3/r_7)\theta_{3,2} \quad (2.18)$$

Equations (2.15)-(2.18) can be written in a matrix form as shown below:

$$\begin{bmatrix} \theta_{4,0} \\ \theta_{5,0} \\ \theta_{6,0} \\ \theta_{7,0} \end{bmatrix} = \begin{bmatrix} 1 & r_2/r_4 & 0 \\ 1 & -r_2/r_5 & 0 \\ 1 & -r_8/r_6 & -r_3/r_6 \\ 1 & r_8/r_7 & r_3/r_7 \end{bmatrix} \begin{bmatrix} \theta_{1,0} \\ \theta_{2,1} \\ \theta_{3,2} \end{bmatrix} \quad (2.19)$$

The linear displacements of the tendons to be pulled away from their neutral positions are given by

$$s_4 = r_4\theta_{4,0} \quad (2.20)$$

$$s_5 = r_5\theta_{5,0} \quad (2.21)$$

$$s_6 = -r_6\theta_{6,0} \quad (2.22)$$

and

$$s_7 = -r_7\theta_{7,0} \quad (2.23)$$

Multiplying the first row of Eq. (2.19) by r_4 , the second row by r_5 , the third row by $-r_6$, and the fourth row by $-r_7$, yields

$$\underline{S} = A \underline{\Theta} \quad (2.24)$$

where $\underline{S}=(s_4, s_5, s_6, s_7)^T$, $\underline{\Theta}=(\theta_{1,0}, \theta_{2,1}, \theta_{3,2})^T$, and

$$A = \begin{bmatrix} r_4 & r_2 & 0 \\ r_5 & -r_2 & 0 \\ -r_6 & r_8 & r_3 \\ -r_7 & -r_8 & -r_3 \end{bmatrix} \quad (2.25)$$

where the superscript T denotes the transpose of the associated matrix.

Furthermore, if $r_4 = r_5 = r_6 = r_7$, and $r_2 = r_8$, then the matrix A can be decomposed into the product of two matrices:

$$A = B R \quad (2.26)$$

where

$$B = \begin{bmatrix} 1 & 1 & 0 \\ 1 & -1 & 0 \\ -1 & 1 & 1 \\ -1 & -1 & -1 \end{bmatrix}$$

and

$$R = \begin{bmatrix} r_4 & 0 & 0 \\ 0 & r_2 & 0 \\ 0 & 0 & r_3 \end{bmatrix}$$

Matrix B which depends on the routing of tendons, is called the structure matrix. Matrix R , under the condition that all pulleys on the same joint axis are of the same size, is a diagonal matrix whose non-zero elements are the radii of the pulleys installed at the consecutive axes of the equivalent open-loop chain.

It can be concluded that, once the joint angles, $\theta_{1,0}$, $\theta_{2,1}$, and $\theta_{3,2}$ are known, linear displacements of the tendons are uniquely determined. On the other hand, the four linear displacements, s_1 , s_2 , s_3 , and s_4 can not be specified arbitrarily. Once three of the four linear displacements are specified, the fourth linear displacement and the joint angles are determined by Eq. (2.24).

It can be shown that the vector of forces, \underline{F} , exerted by the tendons are related to the resultant torques, $\underline{\tau}$, in the joints of the open-loop chain by the following relationship:

$$\underline{\tau} = A^T \underline{F} \quad (2.27)$$

where $\underline{\tau} = (\tau_{1,0}, \tau_{2,1}, \tau_{3,2})^T$, and $\underline{F} = (f_4, f_5, f_6, f_7)^T$.

Hence, once tensions in the tendons are specified, torques in the joints are uniquely determined. On the other hand, when torques in the joints are specified, tensions in the tendons are indeterminate. For a given set of joint torques, Equation (2.27) yields three linear equations in four unknowns. The homogeneous solution corresponds to a set of tensions that result in no net joint torque about any of the three joint axes. The general solution is given by the sum of a particular solution plus the homogeneous solution multiplied by an arbitrary constant. Thus positive tension can be maintained by selecting an appropriate multiplier to the homogeneous solution.

2.6.3 A Six-DOF Manipulator

Now let us consider a general six-DOF manipulator as shown in Fig. 2.7 in a planar schematic. The equivalent open-loop chain is made up of links 0-1-2-3-4-5-6. For the sake of clarity, each individual routing of the tendons about the equivalent open-loop chain is sketched on a separate drawing. It can be seen from Fig. 2.7 that there are twenty pulleys and five endless tendons. Pulleys 2 to 6 are rigidly attached to links 2 to 6, respectively. Overall, there are twenty-two rigid links, twenty-one turning pairs and fifteen pulley pairs. Hence, the mechanism has six degrees of freedom. We can designate pulleys 7 to 11 and the first moving link as the input links and seek for the transformation between the rotational displacements of these inputs and the joint angles associated with

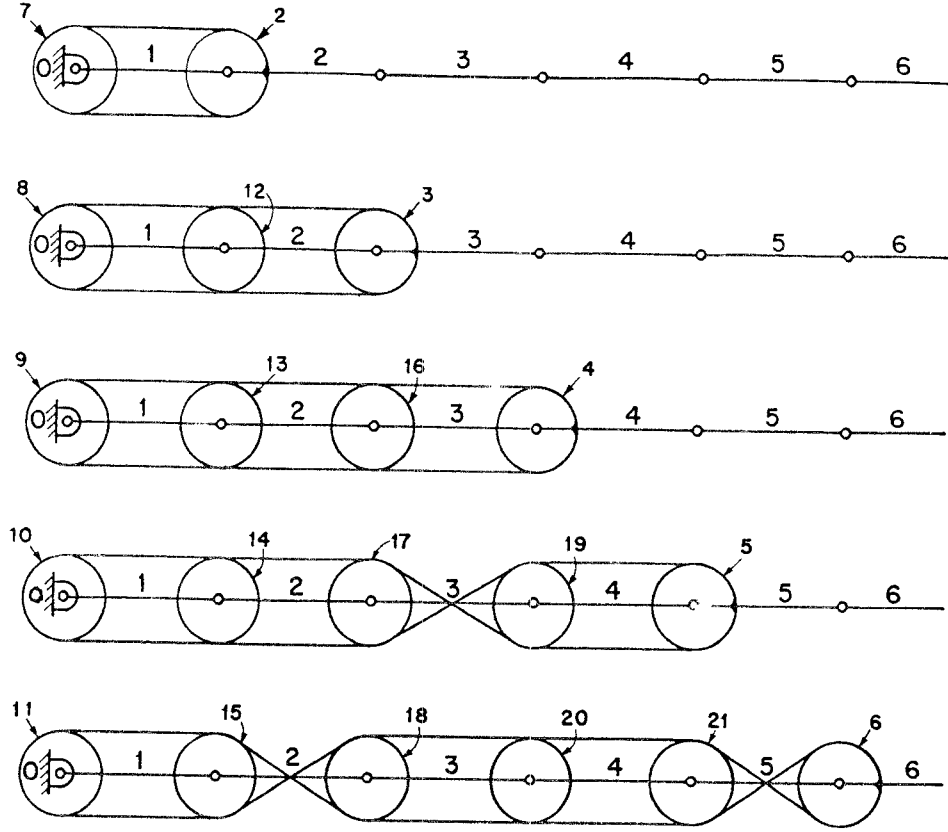


Fig. 2.7 Planar schematic of a six-DOF manipulator

the equivalent open-loop chain.

Writing Eq. (2.8) once for each of the tendon routing shown in Fig. 2.7, yields the following linear transformation in matrix form:

$$\underline{\Phi} = A \underline{\Theta} \quad (2.28)$$

where

$$\underline{\Phi} = (\theta_{1,0}, \theta_{7,0}, \theta_{8,0}, \theta_{9,0}, \theta_{10,0}, \theta_{11,0})^T : \text{input angles}$$

$$\underline{\Theta} = (\theta_{1,0}, \theta_{2,1}, \theta_{3,2}, \theta_{4,3}, \theta_{5,4}, \theta_{6,5})^T : \text{joint angles}$$

and

$$A = \begin{bmatrix} 1 & 0 & 0 & 0 & 0 & 0 \\ 1 & r_2/r_7 & 0 & 0 & 0 & 0 \\ 1 & r_{12}/r_8 & r_3/r_8 & 0 & 0 & 0 \\ 1 & r_{13}/r_9 & r_{16}/r_9 & r_4/r_9 & 0 & 0 \\ 1 & r_{14}/r_{10} & r_{17}/r_{10} & -r_{19}/r_{10} & -r_5/r_{10} & 0 \\ 1 & r_{15}/r_{11} & -r_{18}/r_{11} & -r_{20}/r_{11} & -r_{21}/r_{11} & r_6/r_{11} \end{bmatrix} \quad (2.29)$$

Again, let $r_7 = r_8 = r_9 = r_{10} = r_{11}$, $r_2 = r_{12} = r_{13} = r_{14} = r_{15}$, $r_3 = r_{16} = r_{17} = r_{18}$, $r_4 = r_{19} = r_{20}$, and $r_5 = r_{21}$, then the matrix A can be decomposed into the product of two matrices as shown below:

$$A = B R \quad (2.30)$$

where

$$B = \begin{bmatrix} 1 & 0 & 0 & 0 & 0 & 0 \\ 1 & 1 & 0 & 0 & 0 & 0 \\ 1 & 1 & 1 & 0 & 0 & 0 \\ 1 & 1 & 1 & 1 & 0 & 0 \\ 1 & 1 & 1 & -1 & -1 & 0 \\ 1 & 1 & -1 & -1 & -1 & 1 \end{bmatrix}$$

and,

$$R = \begin{bmatrix} 1 & 0 & 0 & 0 & 0 & 0 \\ 0 & r_2/r_7 & 0 & 0 & 0 & 0 \\ 0 & 0 & r_3/r_8 & 0 & 0 & 0 \\ 0 & 0 & 0 & r_4/r_9 & 0 & 0 \\ 0 & 0 & 0 & 0 & r_5/r_{10} & 0 \\ 0 & 0 & 0 & 0 & 0 & r_6/r_{11} \end{bmatrix}$$

The matrix B is the structure matrix and matrix R the radius matrix. This example illustrates how easily we can derive the transformation matrix merely by inspecting the kinematic structure of the mechanism.

2.7 Summary

The kinematic structure of tendon-driven robotic mechanisms has been investigated with the aid of graph theory. The correspondence between the graph representation of a kinematic structure and the mechanism has been established. It is shown that the routing of tendons in a spatial robotic device can be best represented by the planar schematic. It is also shown that the kinematic structure of tendon-driven robotic mechanisms is similar to that of epicyclic gear trains.

Using the concept of fundamental circuit, a general expression relating the rotational displacement of a base pulley to the joint angles of a pulley train in a tendon-driven mechanism has been derived. It has been shown that the displacement equations of a tendon-driven robotic mechanism can be readily obtained by an inspection of its kinematic structure. The theory has been demonstrated by the kinematic analysis of three articulated robotic devices.

Chapter 3

Structural Synthesis

3.1 Introduction

One of the fundamental phases in mechanical design is the conceptual design phase, i.e., the creation of a mechanism to satisfy certain desired functional requirements. Conventionally, this is accomplished by designers' intuition and experience. Recently, there has been considerable interest in the creation of mechanisms in a systematic manner. A promising approach is to separate the structure of a mechanism from its function. Then, kinematic structures of the same type, same number of degrees of freedom, number of links, and nature of the desired function, can be enumerated systematically. Finally, each kinematic structure obtained can be evaluated according to the functional requirements of a mechanism. This methodology of synthesis has been successfully applied to the creation of epicyclic gear trains (Buchsbaum and Freudenstein, 1970; and Tsai and Lin, 1989).

So far the kinematic and static relations between the joint angle space and tendon/actuator space have been investigated. In the previous chapter, it has been shown that the routing of tendons in a spatial robotic device can be best understood by the planar schematic, the kinematic structure of tendon-driven robotic mechanisms is similar to that of epicyclic gear trains, and the transformation between the actuator space and the joint space can be easily derived by an inspection of the kinematic structure. In order to facilitate the synthesis of tendon-driven manipulators in a systematic manner, first the structural characteristics will be investigated thoroughly, then the structural isomorphism of

tendon-driven manipulators will be defined, and finally a systematic methodology for the enumeration of such mechanisms will be developed in this chapter.

3.2 General Principle of Operation

In what follows, the research will be concentrated on the kinematic structures with open-ended tendon routing only. Generally, for an n -DOF manipulator with m open-ended tendons, the equation of transformation can be written as

$$\underline{S} = A \underline{\Theta} \quad (3.1a)$$

where $\underline{S} = (s_1, s_2, \dots, s_m)^T$ is an $m \times 1$ column matrix representing linear displacements of the tendons, $\underline{\Theta} = (\theta_1, \theta_2, \dots, \theta_n)^T$ is an $n \times 1$ column matrix for the joint angles, and A is an $m \times n$ matrix. If we assume that all pulleys pivoted about one joint axis are of the same radius, then matrix A can be decomposed into the following form:

$$A = B R \quad (3.1b)$$

Here, the matrix B whose elements consist of -1, 0 and +1, is an $m \times n$ matrix describing the routing of the tendons, and the matrix R is an $n \times n$ diagonal matrix whose non-zero elements are the radii of the pulleys.

As to the force transformation, resultant torques, $\underline{\tau}$, about the joint axes in the equivalent open-loop chain, can be related to tendon forces \underline{F} , through the principle of energy conservation:

$$\dot{\underline{\Theta}}^T \underline{\tau} = \dot{\underline{S}}^T \underline{F} \quad (3.2)$$

Substituting the time derivative of Eq. (3.1a) into (3.2), yields

$$\underline{\tau} = A^T \underline{F} \quad (3.3a)$$

or

$$\underline{\tau} = R^T B^T \underline{F}, \quad \text{provided } A = B R \quad (3.3b)$$

Equations (3.1a,b) and (3.3a,b) describe the basic relationships necessary for the kinematic and force control of open-ended tendon-driven manipulators. In the displacement (or velocity) domain, once the joint angles (or joint rates) are known, linear displacements (or velocities) of the tendons can be uniquely determined. Conversely, linear displacements (or velocities) of the tendons can not be specified independently. The attainable tendon displacements (or velocities) are contained in an n -dimensional column space of A .

In the force domain, once tensions in the tendons are specified, torques in the joints are uniquely determined. Conversely, for a given set of joint torques, Eq. (3.3) constitutes n linear equations in m unknowns. In order to achieve positive tensions in the tendons, m should be greater than n . Thus, the solution for the forces in tendons consists of a particular solution plus an $(m - n)$ -dimensional homogeneous solution. The particular solution can be determined by, for example, the generalized inverse transformation of Eq. (3.3). The homogeneous solution corresponds to certain sets of tendon tensions that result in no net joint torques. The homogeneous solution can be expressed as a sum of $(m - n)$ basis vectors each of them being multiplied by an arbitrary constant. The $(m - n)$ basis vectors span the null space of B^T . The components in the homogeneous solution must be of the same sign. Thus, by adjusting the constants, positive tension can be maintained in all of the tendons.

3.3 Structural Characteristics

In this work, it is assumed that all the actuators are installed at the base.

Thus, every tendon regardless of which link it is attached to, must be routed through the base joint of the manipulator and connected to its actuator on the base link.

To facilitate the analysis, the Degree-of-Incidence (DOI) of a tendon is defined as the number of joints the tendon has been routed over. For example, if a tendon has been routed over five consecutive joints, then we say the DOI of the tendon is five.

Let n be the number of DOF of a robotic system, m the total number of tendons, and m_i the number of tendons with i DOI. Then, it can be concluded that

$$\sum_{i=1}^n m_i = m, \quad (3.4)$$

and

$$m \geq n + 1 \quad (3.5)$$

Note that m_i defines the number of columns with i non-zero elements in the matrix B^T .

Because the robotic system is maneuverable, a subsystem containing any number of links and their associated joints taken from the distal end of the original system should also be maneuverable. This means the number of tendons contained in the subsystem should also be greater than the number of joints by a minimum of one. Taking the distal link and its associated joint as a subsystem, we can conclude that there should be at least two tendons routed over the distal joint. Since these two tendons must be routed over all the joints of the original system, the sum of the DOI for these two tendons is equal to $2n$. Likewise, the subsystem consisting of the last two moving links (distal and its adjacent link)

should contain at least 3 tendons, and the minimum number of total DOI is $2n + (n - 1)$. Following the same argument, it can be concluded that the lower limit for the sum of DOI for an n -DOF robotic system with m tendons is given by:

$$2n + (n - 1) + (n - 2) + \dots + 1 + (m - n - 1) \leq m_1 + 2m_2 + 3m_3 + \dots + nm_n \quad (3.6a)$$

The upper limit for the total DOI is reached when all the tendons are attached to the distal moving link. Hence,

$$m_1 + 2m_2 + 3m_3 + \dots + nm_n \leq nm \quad (3.6b)$$

Combining Eqs. (3.6a) and (3.6b), yields

$$n(n + 3)/2 + (m - n - 1) \leq m_1 + 2m_2 + \dots + nm_n \leq nm \quad (3.6c)$$

These m_i 's are also subjected to the following constraints:

$$\begin{aligned} m_n &\geq 2 \\ m_n + m_{n-1} &\geq 3 \\ &\vdots \\ m_n + m_{n-1} + \dots + m_1 &\geq n + 1 \end{aligned} \quad (3.7)$$

Note that the set $(m_n, m_{n-1}, \dots, m_1)$, when assembled into a structure matrix, takes the following form:

$$B^T = \begin{bmatrix} \# & \# & \dots & \# & 0 & 0 & \dots & 0 & \dots & 0 & 0 & \dots & 0 \\ \# & \# & \dots & \# & \# & \# & \dots & \# & \dots & 0 & 0 & \dots & 0 \\ \vdots & \vdots & \ddots & \vdots & \vdots & \vdots & \ddots & \vdots & \ddots & \vdots & \vdots & \ddots & \vdots \\ \# & \# & \dots & \# & \# & \# & \dots & \# & \dots & \# & 0 & \dots & 0 \\ \# & \# & \dots & \# & \# & \# & \dots & \# & \dots & \# & \# & \dots & \# \end{bmatrix} \quad (3.8)$$

where the “#” sign represents the existence of a non-zero element.

In Eq. (3.8), the existence of a non-zero element at the i^{th} row and j^{th} column implies that the j^{th} tendon is incident with the $(n - i + 1)^{th}$ joint, and the sign of the element is determined by the type of the tendon routing. In this notation, the rows have been arranged in a reversed sequence, i.e., the first row represents the distal (n^{th}) joint in a manipulator. This will facilitate the structural synthesis to be discussed next.

Based on the above discussion, the structural characteristics for the tendon-driven manipulators can be summarized as follows:

- C1. There is a minimum of two non-zero elements and one sign change between elements in each row. This guarantees every joint can be manipulated in both directions.
- C2. Exchanging any two columns, which is equivalent to the renaming of two tendons, does not affect the function and structure of the system.
- C3. The structure matrix can always be arranged in a form such that all the zero elements appear on the upper-right-hand corner of the matrix.
- C4. Changing the sign of every element in a row does not affect the generic characteristics of the structure. This is equivalent to a change in the definition of positive direction of a joint axis.
- C5. The rank of the structure matrix is equal to the degrees of freedom of the system. Hence, for an n -DOF system with m tendons, at least one determinant of a submatrix formed by deleting $(m - n)$ columns from the structure matrix shall not be equal to zero. Furthermore, if $m = n + 1$,

then the determinant of a submatrix formed by deleting any column shall not be equal to zero.

- C6. There exists one $(m - n)$ -dimensional homogeneous solution to Eq. (3.3) such that all the elements in the homogeneous solution are of the same sign.

3.4 Structural Isomorphism

To define isomorphic structures, a positive direction of rotation is assigned to each joint axis and then the mechanism is sketched as a planar schematic defined in Chapter Two. It has been shown in Eq. (2.8) that the elements of the structure matrix are determined by the tendon routing and the definition of positive direction of rotation for the joint axes. If the direction of rotation for a joint axis is defined in the reverse manner, then the sign for each element in the corresponding row of the structure matrix is reversed. Since the definition of the positive direction for a joint axis has no effect on the function of a mechanism, two tendon-driven manipulators are said to be structurally isomorphic if

- (a) the structure matrices of the two systems are identical, or
- (b) they become identical after a change of sign for every element in one or more rows, or
- (c) they become identical after rearranging certain columns, or
- (d) a combination of both (b) and (c).

For example, if we define the axes of positive rotation to be pointing out of the page, the structure matrices for the manipulators shown in Figs. 3.1(a)

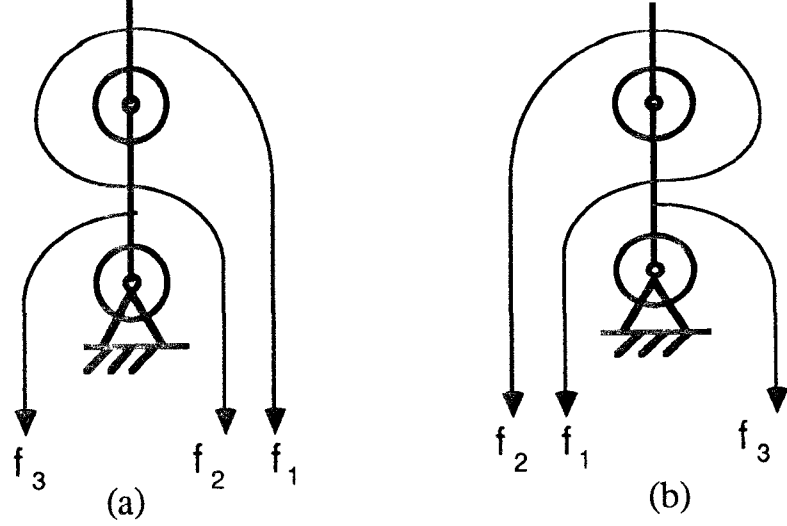


Fig. 3.1 Two structurally isomorphic, two-DOF, tendon-driven manipulators and 3.1(b) are given by

$$B_1^T = \begin{bmatrix} -1 & 1 & 0 \\ -1 & -1 & 1 \end{bmatrix}, \quad \text{and} \quad B_2^T = \begin{bmatrix} -1 & 1 & 0 \\ 1 & 1 & -1 \end{bmatrix},$$

respectively. It can be seen that after switching the sign of each element in the second row of B_2^T , B_2^T becomes identical to B_1^T . Physically, if we reverse the direction of the proximal joint axis of the mechanism shown in Fig. 3.1(b), then it becomes identical to that of Fig. 3.1(a). Therefore, the two mechanisms are said to be structurally isomorphic.

Another example is shown in Fig. 3.2. The structure matrices for the mechanisms shown in Figs. 3.2(a) and 3.2(b) are given by:

$$B_1^T = \begin{bmatrix} -1 & 1 & 0 & 0 \\ -1 & -1 & 1 & 0 \\ -1 & 1 & -1 & 1 \end{bmatrix}, \quad \text{and} \quad B_2^T = \begin{bmatrix} -1 & 1 & 0 & 0 \\ -1 & -1 & 1 & 0 \\ 1 & -1 & -1 & 1 \end{bmatrix},$$

respectively. By switching the sign of each element in the first row of B_2^T ,

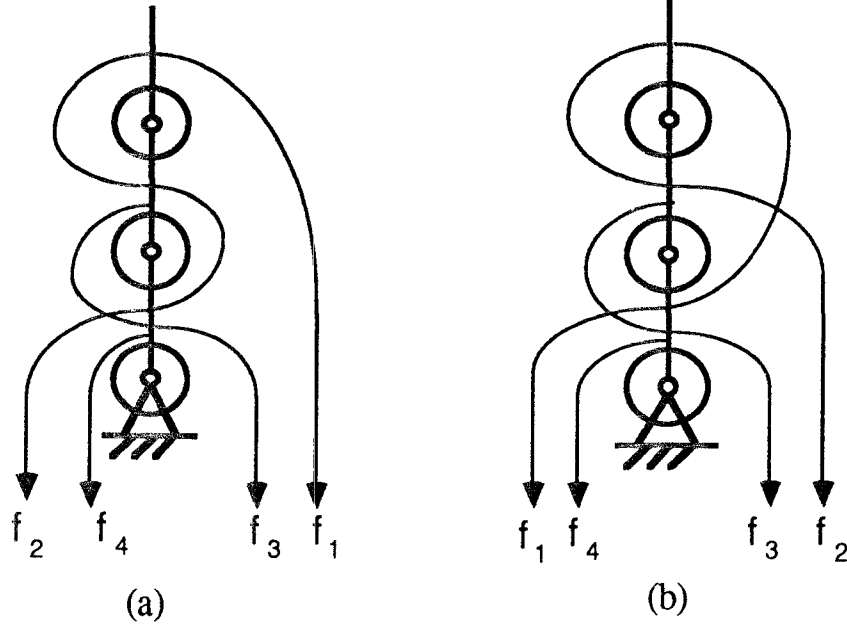


Fig. 3.2 Two structurally isomorphic, three-DOF, tendon-driven manipulators and then exchanging the first and second columns, B_2^T becomes identical to B_1^T . This can also be explained as follows. If we reverse the direction of the distal joint axis in Fig. 3.2(b) and rename f_1 to f_2 and f_2 to f_1 , then the two mechanisms become identical. Therefore, the two mechanisms are said to be structurally isomorphic.

3.5 Structure Synthesis

In what follows, the research shall focus on those tendon-driven robotic systems with the number of tendons greater than the number of DOF by one; that is $m = n + 1$. Writing Eqs. (3.4), (3.6.c), and (3.7) for $n = 3$ and $m = 4$, yields

$$m_1 + m_2 + m_3 = 4 \tag{3.9a}$$

(m_1, m_2, m_3)	(1, 1, 2)	(0, 2, 2)	(1, 0, 3)	(0, 1, 3)	(0, 0, 4)
B^T	$\begin{matrix} \# \# 0 0 \\ \# \# \# 0 \\ \# \# \# \# \end{matrix}$	$\begin{matrix} \# \# 0 0 \\ \# \# \# \# \\ \# \# \# \# \end{matrix}$	$\begin{matrix} \# \# \# 0 \\ \# \# \# 0 \\ \# \# \# \# \end{matrix}$	$\begin{matrix} \# \# \# 0 \\ \# \# \# \# \\ \# \# \# \# \end{matrix}$	$\begin{matrix} \# \# \# \# \\ \# \# \# \# \\ \# \# \# \# \end{matrix}$
admissible solution	$\begin{matrix} -1 & 1 & 0 & 0 \\ -1 & -1 & 1 & 0 \\ -1 & -1 & -1 & 1 \end{matrix}$	$\begin{matrix} -1 & 1 & 0 & 0 \\ -1 & 1 & -1 & 1 \\ -1 & -1 & 1 & 1 \end{matrix}$	no solution	$\begin{matrix} -1 & -1 & 1 & 0 \\ 1 & -1 & -1 & 1 \\ -1 & 1 & -1 & 1 \end{matrix}$	$\begin{matrix} -1 & -1 & 1 & 1 \\ 1 & -1 & -1 & 1 \\ -1 & 1 & -1 & 1 \end{matrix}$

Table 3.1 Structure matrices for manipulators having three-DOF and four tendons.

$$9 \leq m_1 + 2m_2 + 3m_3 \leq 12 \quad (3.9b)$$

$$m_3 \geq 2 \quad (3.9c)$$

$$m_3 + m_2 \geq 3 \quad (3.9d)$$

Solving Eq. (3.9a) for m_1 , m_2 and m_3 subjected to the inequality constraints, Eqs. (3.9b - 3.9d), yields $(m_1, m_2, m_3) = (1, 1, 2)$, or $(0, 2, 2)$, or $(1, 0, 3)$, or $(0, 1, 3)$, or $(0, 0, 4)$. Table 3.1 shows the admissible structure matrices corresponding to the above possible solutions. Note that the structure matrix for those systems with $m - n = 1$ must have a positive homogeneous solution \underline{F} to Eq. (3.3). Otherwise, it is not controllable and, hence, not admissible.

The number of admissible structure matrices increases as the number of degrees of freedom increases. Morecki, et al. (1980) predicted there could exist up to 23040 admissible structures for six-DOF manipulators having seven

tendons. Note that the Stanford/JPL hand has a structure matrix of the form $(m_1, m_2, m_3)=(0, 2, 2)$ as shown in Table 3.1 while the manipulator designed by Morecki, et al. (1980) has a pseudo-triangular structure matrix. In what follows, only those systems whose structure matrix takes the following pseudo-triangular form will be considered:

$$B^T = \begin{bmatrix} e_{11} & e_{12} & 0 & 0 & \cdots & 0 \\ e_{21} & e_{22} & e_{23} & 0 & \cdots & 0 \\ \vdots & \vdots & \vdots & \vdots & \ddots & \vdots \\ e_{n-1,1} & e_{n-1,2} & \cdot & \cdot & \cdots & 0 \\ e_{n1} & e_{n2} & \cdot & \cdot & \cdots & e_{n,n+1} \end{bmatrix}, \quad (3.10)$$

or $(m_1, m_2, m_3, \dots, m_n) = (1, 1, 1, \dots, 2)$, where

$$\sum_{i=1}^n m_i = m = n + 1.$$

Each non-zero element in Eq. (3.10) can assume the value of +1 or -1 provided that the resulting matrix satisfies the structural characteristics C1 - C6 outlined in the previous section. Since there are $n(n+3)/2$ non-zero elements in a robotic system having n -DOF and $(n+1)$ tendons, the number of possible structure matrices is equal to 2 to the $[n(n+3)/2]^{th}$ order. It would be very difficult if not impossible, to identify the admissible structures from such a large number of possible combinations. In what follows, a simpler approach will be presented.

The synthesis starts with a known n by $(n+1)$ structure, called the generic structure, and increases the complexity of the structure by adding one degree of freedom at a time. In view of Eq. (3.10), it can be concluded that each time the degree of freedom is increased by one, both the number of links and the number of joints in the equivalent open-loop chain should also be increased by one. Let

the new link be connected to the base-link of the generic structure by a turning pair and let the added link be the base-link for the new mechanism. In this way the base-link of the generic structure becomes the first moving link. All the tendons in the generic structure must now be extended over the newly added joint to allow all actuators be connected to the base. Moreover, an additional tendon is required to connect the first moving link to the new base-link.

From the structure matrix point of view, this procedure implies that the matrix of a generic structure is to be supplemented by an additional column and an additional row. All the elements in the supplemented column, except the last, are to be set to zero. The new elements in the supplemented row can assume the value of $+1$ or -1 . Without losing generality, one can let the last element of supplemented column (and row) be $+1$. Hence, there are potentially 2^n combinations for assigning the signs of the remaining elements in the supplemented row. However, some of the combinations may be rejected due to the violation of the structural characteristics, C1 through C6, or may be eliminated due to the reason of structural isomorphism. So the number of admissible non-isomorphic structure matrices is usually much less than 2^n . This procedure can be automated by a computer program. The systematic procedure and the results can be summarized as follows:

One-DOF system. The simplest one-DOF manipulator has one moving link and one fixed link connected together by a turning pair. The only possible structure is shown in Fig. 3.3 where two cables are routed through different sides of the joint. The corresponding structure matrix is also shown in Fig. 3.3. Note that the $(1, 2)$ element has been chosen to be $+1$. The homogeneous solution to this structure matrix is given by $\underline{F} = (1, 1)^T$.

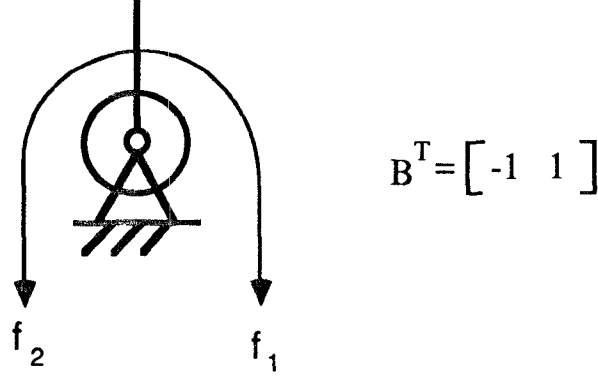


Fig. 3.3 Functional schematic of a one-DOF tendon-driven manipulator

Two-DOF system. There are $2^2 = 4$ possible combinations to form an additional row of non-zero elements to the structure matrix of a one-DOF system. Only one form as shown in Fig. 3.4 satisfies the structural characteristics C1 through C6. The corresponding structure matrix is shown in Fig. 3.4. The homogeneous solution is given by $\underline{F} = (1, 1, 2)^T$.

Three-DOF systems. There are $2^3 = 8$ possible combinations to form an additional row to the matrix shown in Fig. 3.4. Only three were found to satisfy C1 through C6, however, two of them were structurally isomorphic. Hence, there exist only two nonisomorphic structures as shown in Figs. 3.5(a) and 3.5(b) (in page 45). Their associated structure matrices are also shown in the figures.

Four-DOF systems. There are $2^4 = 16$ possible ways to form one additional row to each of the matrices shown in Figs. 3.5(a) and 3.5(b). Since there are two structurally nonisomorphic structures for the three-DOF systems, totally, $16 \times 2 = 32$ possible structures can be generated for four-DOF systems. Thirteen

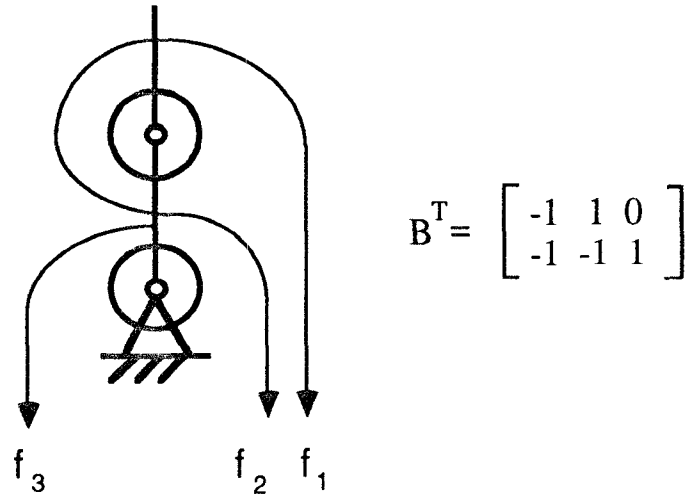


Fig. 3.4 Planar schematic of a two-DOF tendon-driven manipulator

of them satisfy structural characteristics C1 through C6. But, only eleven are structurally nonisomorphic as shown in Figs. 3.6(a) - 3.6(k) (in pages 46-49). The corresponding structure matrices are also shown in these figures.

Five-DOF systems. There are $2^5 = 32$ possible ways to form one additional row to each of the matrices shown in Figs. 3.6(a) - 3.6(k). Since there are eleven structurally nonisomorphic four-DOF systems, a total of $11 \times 32 = 352$ structures can be generated for five-DOF systems. After applying structural characteristics, C1 through C6, and checking for structural isomorphism, 141 nonisomorphic kinematic structures were obtained. Table 3.2 (in page 50) categorizes the numbers of non-isomorphic structures according to their homogeneous solutions. Fig. 3.7 (in pages 51-55) shows the corresponding structure matrices.

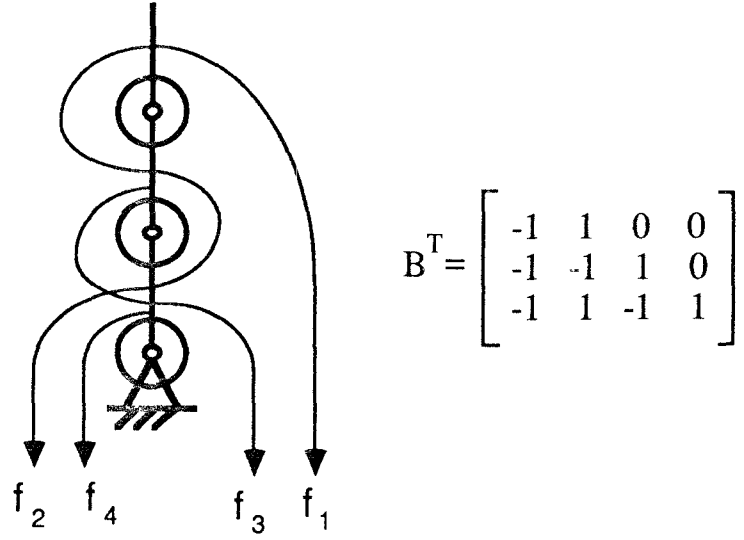
Six-DOF systems. There are $2^6 = 64$ possible ways to form one additional row to each of the matrices of five-DOF systems. A total of $64 \times 141 = 9024$ possible structures can be generated. Again, after checking for structural char-

acteristics, C1 through C6, and structural isomorphism, 3905 structurally non-isomorphic drives were obtained. Table 3.3 (in pages 56-63) categorizes the numbers of non-isomorphic structures according to their homogeneous solutions. Appendix A shows one example of an admissible structure matrix for each category of kinematic structures listed in Table 3.3. Note that this result is different from the 23040 solutions obtained earlier by Morecki, et al. (1980). It is believed that a certain number of those structures given by Morecki, et al. contain isomorphic structures.

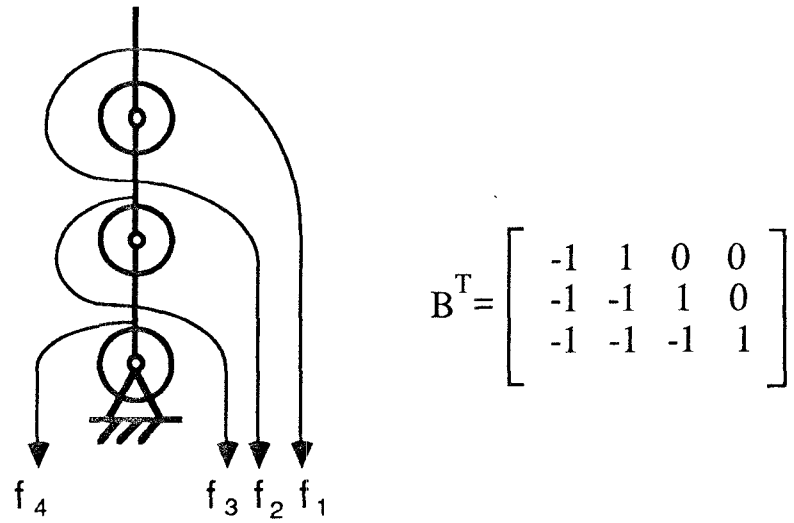
3.6 Summary

The structural characteristics of tendon-driven manipulator system have been investigated. A set of criteria for the identification of structure isomorphism has been established and a methodology for the enumeration of tendon-driven manipulators having pseudo-triangular structure matrix has been developed. All the admissible structure matrices with up to six-DOF have been enumerated.

There is a planar schematic corresponding to each structure matrix. However, each planar schematic can be converted into various different spatial mechanisms depending on the twist angle chosen for every pair of adjacent joint axes. This is also true for the construction of planar mechanisms, for which the twist angles can be either 0° or 180° . Hence, the number of functional mechanisms is much larger than that of nonisomorphic structures.

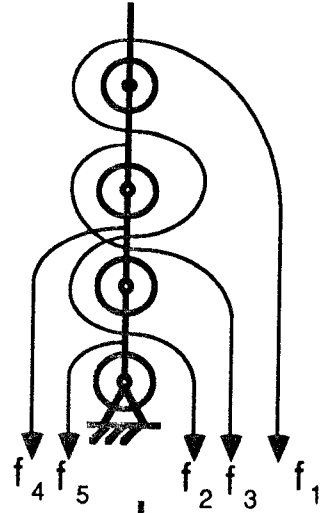


(a)



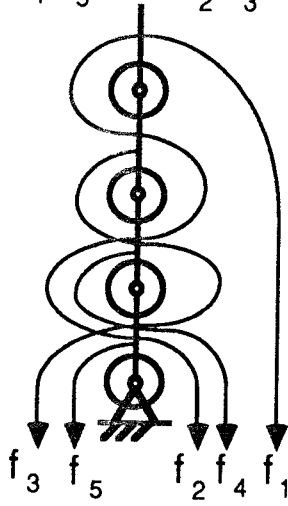
(b)

Fig. 3.5 Planar schematic and the associated structure matrices for three-DOF tendon-driven manipulators



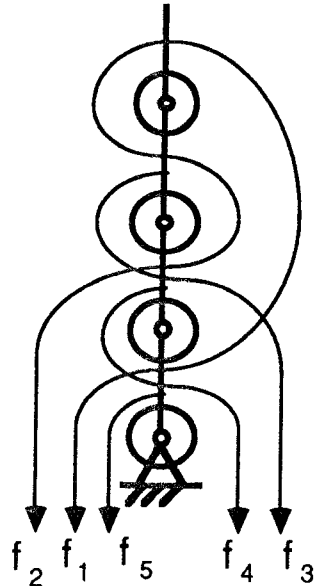
$$B^T = \begin{bmatrix} -1 & 1 & 0 & 0 & 0 \\ -1 & -1 & 1 & 0 & 0 \\ -1 & 1 & -1 & 1 & 0 \\ -1 & -1 & -1 & 1 & 1 \end{bmatrix}$$

(a)



$$B^T = \begin{bmatrix} -1 & 1 & 0 & 0 & 0 \\ -1 & -1 & 1 & 0 & 0 \\ -1 & 1 & -1 & 1 & 0 \\ -1 & -1 & 1 & -1 & 1 \end{bmatrix}$$

(b)



$$B^T = \begin{bmatrix} -1 & 1 & 0 & 0 & 0 \\ -1 & -1 & 1 & 0 & 0 \\ -1 & 1 & -1 & 1 & 0 \\ 1 & 1 & -1 & -1 & 1 \end{bmatrix}$$

(c)

Fig. 3.6 Planar schematic and the associated structure matrices for four-DOF tendon-driven manipulators

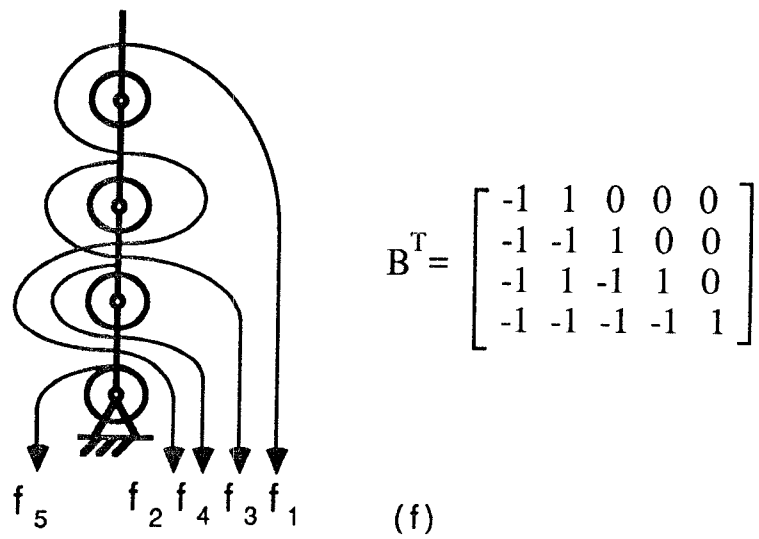
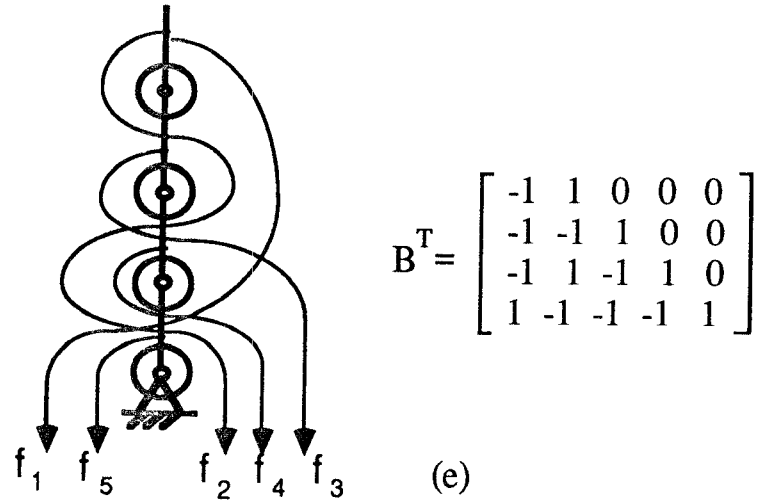
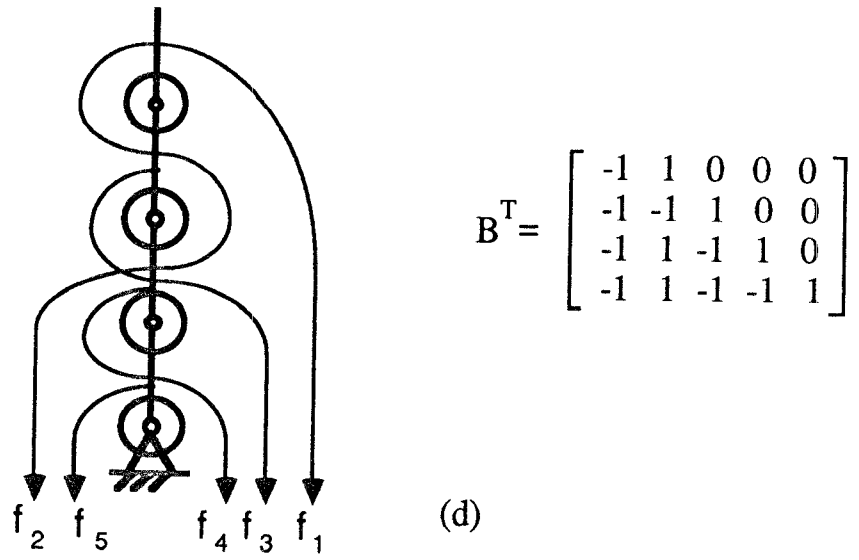
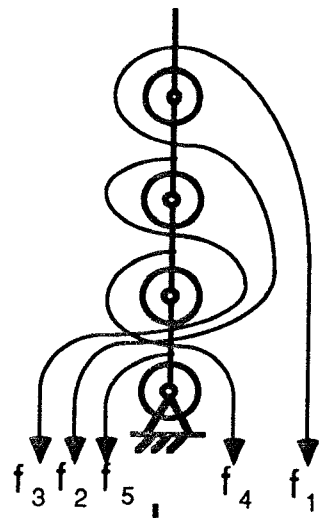
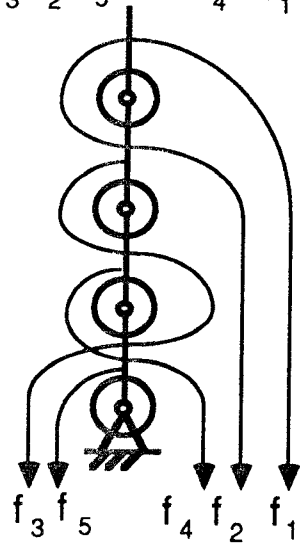


Fig. 3.6 continued



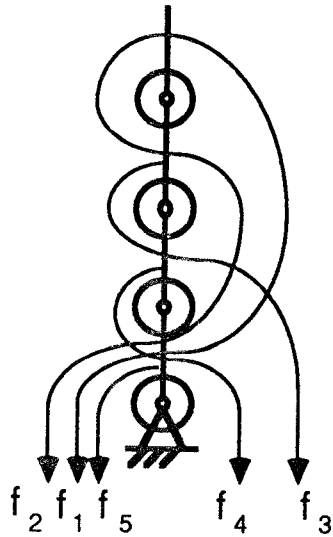
$$B^T = \begin{bmatrix} -1 & 1 & 0 & 0 & 0 \\ -1 & -1 & 1 & 0 & 0 \\ -1 & -1 & -1 & 1 & 0 \\ -1 & 1 & 1 & -1 & 1 \end{bmatrix}$$

(g)



$$B^T = \begin{bmatrix} -1 & 1 & 0 & 0 & 0 \\ -1 & -1 & 1 & 0 & 0 \\ -1 & -1 & -1 & 1 & 0 \\ -1 & -1 & 1 & -1 & 1 \end{bmatrix}$$

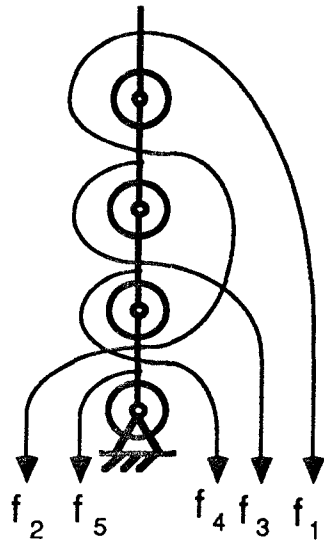
(h)



$$B^T = \begin{bmatrix} -1 & 1 & 0 & 0 & 0 \\ -1 & -1 & 1 & 0 & 0 \\ -1 & -1 & -1 & 1 & 0 \\ 1 & 1 & -1 & -1 & 1 \end{bmatrix}$$

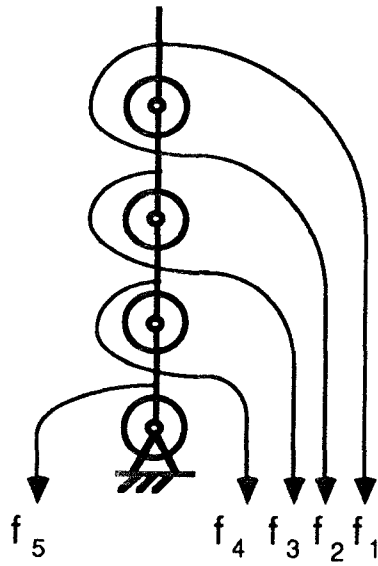
(i)

Fig. 3.6 continued



$$B^T = \begin{bmatrix} -1 & 1 & 0 & 0 & 0 \\ -1 & -1 & 1 & 0 & 0 \\ -1 & -1 & -1 & 1 & 0 \\ -1 & 1 & -1 & -1 & 1 \end{bmatrix}$$

(j)



$$B^T = \begin{bmatrix} -1 & 1 & 0 & 0 & 0 \\ -1 & -1 & 1 & 0 & 0 \\ -1 & -1 & -1 & 1 & 0 \\ -1 & -1 & -1 & -1 & 1 \end{bmatrix}$$

(k)

Fig. 3.6 continued

DOF= 5		total number= 141					
category	homogeneous solution					no. of structures	
5- 1	1	1	2	2	2	2	18
5- 2	1	1	2	2	2	4	12
5- 3	1	1	2	2	2	6	6
5- 4	1	1	2	2	2	8	3
5- 5	1	1	2	2	4	2	8
5- 6	1	1	2	2	4	4	8
5- 7	1	1	2	2	4	6	6
5- 8	1	1	2	2	4	8	4
5- 9	1	1	2	2	4	10	2
5-10	1	1	2	2	6	2	2
5-11	1	1	2	2	6	4	3
5-12	1	1	2	2	6	6	4
5-13	1	1	2	2	6	8	3
5-14	1	1	2	2	6	10	2
5-15	1	1	2	2	6	12	1
5-16	1	1	2	4	2	2	4
5-17	1	1	2	4	2	4	4
5-18	1	1	2	4	2	6	3
5-19	1	1	2	4	2	8	2
5-20	1	1	2	4	2	10	1
5-21	1	1	2	4	4	2	4
5-22	1	1	2	4	4	4	6
5-23	1	1	2	4	4	6	2
5-24	1	1	2	4	4	8	4
5-25	1	1	2	4	4	10	2
5-26	1	1	2	4	4	12	2
5-27	1	1	2	4	6	2	3
5-28	1	1	2	4	6	4	2
5-29	1	1	2	4	6	6	2
5-30	1	1	2	4	6	8	2
5-31	1	1	2	4	6	10	2
5-32	1	1	2	4	6	12	2
5-33	1	1	2	4	6	14	1
5-34	1	1	2	4	8	2	1
5-35	1	1	2	4	8	4	2
5-36	1	1	2	4	8	6	1
5-37	1	1	2	4	8	8	2
5-38	1	1	2	4	8	10	1
5-39	1	1	2	4	8	12	2
5-40	1	1	2	4	8	14	1
5-41	1	1	2	4	8	16	1

Table 3.2 Homogeneous solutions for five-DOF tendon-driven manipulators having pseudo-triangular structure matrix

rank= 5

-1 1 0 0 0 0 -1 -1 1 0 0 0 -1 1 -1 1 0 0 -1 -1 -1 1 1 0 -1 1 -1 -1 1 1 5- 1- 1	-1 1 0 0 0 0 -1 -1 1 0 0 0 -1 1 -1 1 0 0 -1 -1 1 -1 1 0 -1 1 -1 1 -1 1 5- 1- 9	-1 1 0 0 0 0 -1 -1 1 0 0 0 -1 1 -1 1 0 0 1 1 -1 -1 1 0 -1 1 1 -1 -1 1 5- 1-17	-1 1 0 0 0 0 -1 -1 1 0 0 0 -1 1 -1 1 0 0 -1 -1 1 -1 1 0 -1 -1 1 -1 -1 1 5- 2- 7
-1 1 0 0 0 0 -1 -1 1 0 0 0 -1 1 -1 1 0 0 -1 -1 -1 1 1 0 1 -1 -1 -1 1 1 5- 1- 2	-1 1 0 0 0 0 -1 -1 1 0 0 0 -1 1 -1 1 0 0 -1 -1 1 -1 1 0 1 -1 -1 1 -1 1 5- 1-10	-1 1 0 0 0 0 -1 -1 1 0 0 0 -1 1 -1 1 0 0 1 1 -1 -1 1 0 1 -1 1 -1 -1 1 5- 1-18	-1 1 0 0 0 0 -1 -1 1 0 0 0 -1 1 -1 1 0 0 -1 -1 1 -1 1 0 1 1 -1 -1 -1 1 5- 2- 8
-1 1 0 0 0 0 -1 -1 1 0 0 0 -1 1 -1 1 0 0 -1 -1 -1 1 1 0 -1 1 -1 1 -1 1 5- 1- 3	-1 1 0 0 0 0 -1 -1 1 0 0 0 -1 1 -1 1 0 0 -1 -1 1 -1 1 0 -1 1 1 -1 -1 1 5- 1-11	-1 1 0 0 0 0 -1 -1 1 0 0 0 -1 1 -1 1 0 0 -1 -1 -1 1 1 0 -1 -1 -1 -1 1 1 5- 2- 1	-1 1 0 0 0 0 -1 -1 1 0 0 0 -1 1 -1 1 0 0 1 1 -1 -1 1 0 -1 -1 -1 -1 1 1 5- 2- 9
-1 1 0 0 0 0 -1 -1 1 0 0 0 -1 1 -1 1 0 0 -1 -1 -1 1 1 0 1 -1 -1 1 -1 1 5- 1- 4	-1 1 0 0 0 0 -1 -1 1 0 0 0 -1 1 -1 1 0 0 -1 -1 1 -1 1 0 1 -1 1 -1 -1 1 5- 1-12	-1 1 0 0 0 0 -1 -1 1 0 0 0 -1 1 -1 1 0 0 -1 -1 -1 1 1 0 -1 -1 -1 1 -1 1 5- 2- 2	-1 1 0 0 0 0 -1 -1 1 0 0 0 -1 1 -1 1 0 0 1 1 -1 -1 1 0 -1 -1 -1 1 -1 1 5- 2-10
-1 1 0 0 0 0 -1 -1 1 0 0 0 -1 1 -1 1 0 0 -1 -1 -1 1 1 0 -1 1 1 -1 -1 1 5- 1- 5	-1 1 0 0 0 0 -1 -1 1 0 0 0 -1 1 -1 1 0 0 1 1 -1 -1 1 0 -1 1 -1 -1 1 1 5- 1-13	-1 1 0 0 0 0 -1 -1 1 0 0 0 -1 1 -1 1 0 0 -1 -1 -1 1 1 0 -1 -1 1 -1 -1 1 5- 2- 3	-1 1 0 0 0 0 -1 -1 1 0 0 0 -1 1 -1 1 0 0 1 1 -1 -1 1 0 -1 -1 1 -1 -1 1 5- 2-11
-1 1 0 0 0 0 -1 -1 1 0 0 0 -1 1 -1 1 0 0 -1 -1 -1 1 1 0 1 -1 1 -1 -1 1 5- 1- 6	-1 1 0 0 0 0 -1 -1 1 0 0 0 -1 1 -1 1 0 0 1 1 -1 -1 1 0 1 -1 -1 -1 1 1 5- 1-14	-1 1 0 0 0 0 -1 -1 1 0 0 0 -1 1 -1 1 0 0 -1 -1 -1 1 1 0 1 1 -1 -1 -1 1 5- 2- 4	-1 1 0 0 0 0 -1 -1 1 0 0 0 -1 1 -1 1 0 0 1 1 -1 -1 1 0 1 1 -1 -1 -1 1 5- 2-12
-1 1 0 0 0 0 -1 -1 1 0 0 0 -1 1 -1 1 0 0 -1 -1 1 -1 1 0 -1 1 -1 -1 1 1 5- 1- 7	-1 1 0 0 0 0 -1 -1 1 0 0 0 -1 1 -1 1 0 0 1 1 -1 -1 1 0 -1 1 -1 1 -1 1 5- 1-15	-1 1 0 0 0 0 -1 -1 1 0 0 0 -1 1 -1 1 0 0 -1 -1 1 -1 1 0 -1 -1 -1 -1 1 1 5- 2- 5	-1 1 0 0 0 0 -1 -1 1 0 0 0 -1 1 -1 1 0 0 -1 -1 -1 1 1 0 -1 1 -1 -1 -1 1 5- 3- 1
-1 1 0 0 0 0 -1 -1 1 0 0 0 -1 1 -1 1 0 0 -1 -1 1 -1 1 0 1 -1 -1 -1 1 1 5- 1- 8	-1 1 0 0 0 0 -1 -1 1 0 0 0 -1 1 -1 1 0 0 1 1 -1 -1 1 0 1 -1 -1 1 -1 1 5- 1-16	-1 1 0 0 0 0 -1 -1 1 0 0 0 -1 1 -1 1 0 0 -1 -1 1 -1 1 0 -1 -1 -1 1 -1 1 5- 2- 6	-1 1 0 0 0 0 -1 -1 1 0 0 0 -1 1 -1 1 0 0 -1 -1 -1 1 1 0 1 -1 -1 -1 -1 1 5- 3- 2

Fig. 3.7 Structure matrices for five-DOF tendon-driven manipulators

-1 1 0 0 0 0 -1 -1 1 0 0 0 -1 1 -1 1 0 0 -1 -1 1 -1 1 0 -1 1 -1 -1 -1 1 5- 3- 3	-1 1 0 0 0 0 -1 -1 1 0 0 0 -1 1 -1 1 0 0 -1 1 -1 -1 1 0 -1 -1 1 1 -1 1 5- 5- 2	-1 1 0 0 0 0 -1 -1 1 0 0 0 -1 1 -1 1 0 0 -1 1 -1 -1 1 0 1 -1 -1 1 -1 1 5- 6- 2	-1 1 0 0 0 0 -1 -1 1 0 0 0 -1 1 -1 1 0 0 -1 1 -1 -1 1 0 -1 -1 1 -1 -1 1 5- 7- 2
-1 1 0 0 0 0 -1 -1 1 0 0 0 -1 1 -1 1 0 0 -1 -1 1 -1 1 0 1 -1 -1 -1 -1 1 5- 3- 4	-1 1 0 0 0 0 -1 -1 1 0 0 0 -1 1 -1 1 0 0 -1 1 -1 -1 1 0 1 1 -1 1 -1 1 5- 5- 3	-1 1 0 0 0 0 -1 -1 1 0 0 0 -1 1 -1 1 0 0 -1 1 -1 -1 1 0 -1 1 1 -1 -1 1 5- 6- 3	-1 1 0 0 0 0 -1 -1 1 0 0 0 -1 1 -1 1 0 0 -1 1 -1 -1 1 0 1 1 -1 -1 -1 1 5- 7- 3
-1 1 0 0 0 0 -1 -1 1 0 0 0 -1 1 -1 1 0 0 1 1 -1 -1 1 0 -1 1 -1 -1 -1 1 5- 3- 5	-1 1 0 0 0 0 -1 -1 1 0 0 0 -1 1 -1 1 0 0 -1 1 -1 -1 1 0 1 1 1 -1 -1 1 5- 5- 4	-1 1 0 0 0 0 -1 -1 1 0 0 0 -1 1 -1 1 0 0 -1 1 -1 -1 1 0 1 -1 1 -1 -1 1 5- 6- 4	-1 1 0 0 0 0 -1 -1 1 0 0 0 -1 1 -1 1 0 0 1 -1 -1 -1 1 0 -1 -1 -1 1 -1 1 5- 7- 4
-1 1 0 0 0 0 -1 -1 1 0 0 0 -1 1 -1 1 0 0 1 1 -1 -1 1 0 1 -1 -1 -1 -1 1 5- 3- 6	-1 1 0 0 0 0 -1 -1 1 0 0 0 -1 1 -1 1 0 0 1 -1 -1 -1 1 0 -1 -1 -1 -1 1 1 5- 5- 5	-1 1 0 0 0 0 -1 -1 1 0 0 0 -1 1 -1 1 0 0 1 -1 -1 -1 1 0 -1 1 -1 1 -1 1 5- 6- 5	-1 1 0 0 0 0 -1 -1 1 0 0 0 -1 1 -1 1 0 0 1 -1 -1 -1 1 0 -1 -1 1 -1 -1 1 5- 7- 5
-1 1 0 0 0 0 -1 -1 1 0 0 0 -1 1 -1 1 0 0 -1 -1 -1 1 1 0 -1 -1 -1 -1 -1 1 5- 4- 1	-1 1 0 0 0 0 -1 -1 1 0 0 0 -1 1 -1 1 0 0 1 -1 -1 -1 1 0 -1 -1 1 1 -1 1 5- 5- 6	-1 1 0 0 0 0 -1 -1 1 0 0 0 -1 1 -1 1 0 0 1 -1 -1 -1 1 0 1 -1 -1 1 -1 1 5- 6- 6	-1 1 0 0 0 0 -1 -1 1 0 0 0 -1 1 -1 1 0 0 1 -1 -1 -1 1 0 1 1 -1 -1 -1 1 5- 7- 6
-1 1 0 0 0 0 -1 -1 1 0 0 0 -1 1 -1 1 0 0 -1 -1 1 -1 1 0 -1 -1 -1 -1 -1 1 5- 4- 2	-1 1 0 0 0 0 -1 -1 1 0 0 0 -1 1 -1 1 0 0 1 -1 -1 -1 1 0 1 1 -1 1 -1 1 5- 5- 7	-1 1 0 0 0 0 -1 -1 1 0 0 0 -1 1 -1 1 0 0 1 -1 -1 -1 1 0 -1 1 1 -1 -1 1 5- 6- 7	-1 1 0 0 0 0 -1 -1 1 0 0 0 -1 1 -1 1 0 0 -1 1 -1 -1 1 0 -1 1 -1 -1 -1 1 5- 8- 1
-1 1 0 0 0 0 -1 -1 1 0 0 0 -1 1 -1 1 0 0 1 1 -1 -1 1 0 -1 -1 -1 -1 -1 1 5- 4- 3	-1 1 0 0 0 0 -1 -1 1 0 0 0 -1 1 -1 1 0 0 1 -1 -1 -1 1 0 1 1 1 -1 -1 1 5- 5- 8	-1 1 0 0 0 0 -1 -1 1 0 0 0 -1 1 -1 1 0 0 1 -1 -1 -1 1 0 1 -1 1 -1 -1 1 5- 6- 8	-1 1 0 0 0 0 -1 -1 1 0 0 0 -1 1 -1 1 0 0 -1 1 -1 -1 1 0 1 -1 -1 -1 -1 1 5- 8- 2
-1 1 0 0 0 0 -1 -1 1 0 0 0 -1 1 -1 1 0 0 -1 1 -1 -1 1 0 -1 -1 -1 -1 1 1 5- 5- 1	-1 1 0 0 0 0 -1 -1 1 0 0 0 -1 1 -1 1 0 0 -1 1 -1 -1 1 0 -1 1 -1 1 -1 1 5- 6- 1	-1 1 0 0 0 0 -1 -1 1 0 0 0 -1 1 -1 1 0 0 -1 1 -1 -1 1 0 -1 -1 -1 1 -1 1 5- 7- 1	-1 1 0 0 0 0 -1 -1 1 0 0 0 -1 1 -1 1 0 0 1 -1 -1 -1 1 0 -1 1 -1 -1 -1 1 5- 8- 3

Fig. 3.7 continued

-1 1 0 0 0 0 -1 -1 1 0 0 0 -1 1 -1 1 0 0 1 -1 -1 -1 1 0 1 -1 -1 -1 -1 1 5- 8- 4	-1 1 0 0 0 0 -1 -1 1 0 0 0 -1 1 -1 1 0 0 -1 -1 -1 -1 1 0 -1 1 -1 1 -1 1 5-12- 1	-1 1 0 0 0 0 -1 -1 1 0 0 0 -1 1 -1 1 0 0 -1 -1 -1 -1 1 0 1 -1 -1 -1 -1 1 5-14- 2	-1 1 0 0 0 0 -1 -1 1 0 0 0 -1 -1 -1 1 0 0 -1 1 1 -1 1 0 -1 1 1 -1 -1 1 5-17- 3
-1 1 0 0 0 0 -1 -1 1 0 0 0 -1 1 -1 1 0 0 -1 1 -1 -1 1 0 -1 -1 -1 -1 -1 1 5- 9- 1	-1 1 0 0 0 0 -1 -1 1 0 0 0 -1 1 -1 1 0 0 -1 -1 -1 -1 1 0 1 -1 -1 1 -1 1 5-12- 2	-1 1 0 0 0 0 -1 -1 1 0 0 0 -1 1 -1 1 0 0 -1 -1 -1 -1 1 0 -1 -1 -1 -1 -1 1 5-15- 1	-1 1 0 0 0 0 -1 -1 1 0 0 0 -1 -1 -1 1 0 0 -1 -1 -1 -1 1 0 1 -1 1 -1 -1 1 5-17- 4
-1 1 0 0 0 0 -1 -1 1 0 0 0 -1 1 -1 1 0 0 1 -1 -1 -1 1 0 -1 -1 -1 -1 -1 1 5- 9- 2	-1 1 0 0 0 0 -1 -1 1 0 0 0 -1 1 -1 1 0 0 -1 -1 -1 -1 1 0 -1 1 1 -1 -1 1 5-12- 3	-1 1 0 0 0 0 -1 -1 1 0 0 0 -1 -1 -1 1 0 0 -1 1 1 -1 1 0 -1 -1 1 -1 1 1 5-16- 1	-1 1 0 0 0 0 -1 -1 1 0 0 0 -1 -1 -1 1 0 0 -1 1 1 -1 1 0 -1 -1 -1 -1 1 1 5-18- 1
-1 1 0 0 0 0 -1 -1 1 0 0 0 -1 1 -1 1 0 0 -1 -1 -1 -1 1 0 -1 1 1 1 -1 1 5-10- 1	-1 1 0 0 0 0 -1 -1 1 0 0 0 -1 1 -1 1 0 0 -1 -1 -1 -1 1 0 1 -1 1 -1 -1 1 5-12- 4	-1 1 0 0 0 0 -1 -1 1 0 0 0 -1 -1 -1 1 0 0 -1 1 1 -1 1 0 1 1 -1 -1 1 1 5-16- 2	-1 1 0 0 0 0 -1 -1 1 0 0 0 -1 -1 -1 1 0 0 -1 1 1 -1 1 0 -1 -1 1 -1 -1 1 5-18- 2
-1 1 0 0 0 0 -1 -1 1 0 0 0 -1 1 -1 1 0 0 -1 -1 -1 -1 1 0 1 -1 1 1 -1 1 5-10- 2	-1 1 0 0 0 0 -1 -1 1 0 0 0 -1 1 -1 1 0 0 -1 -1 -1 -1 1 0 -1 -1 -1 1 -1 1 5-13- 1	-1 1 0 0 0 0 -1 -1 1 0 0 0 -1 -1 -1 1 0 0 -1 1 1 -1 1 0 -1 -1 -1 1 -1 1 5-16- 3	-1 1 0 0 0 0 -1 -1 1 0 0 0 -1 -1 -1 1 0 0 -1 1 1 -1 1 0 1 1 -1 -1 -1 1 5-18- 3
-1 1 0 0 0 0 -1 -1 1 0 0 0 -1 1 -1 1 0 0 -1 -1 -1 -1 1 0 -1 -1 1 1 -1 1 5-11- 1	-1 1 0 0 0 0 -1 -1 1 0 0 0 -1 1 -1 1 0 0 -1 -1 -1 -1 1 0 -1 -1 1 -1 -1 1 5-13- 2	-1 1 0 0 0 0 -1 -1 1 0 0 0 -1 -1 -1 1 0 0 -1 1 1 -1 1 0 1 1 1 -1 -1 1 5-16- 4	-1 1 0 0 0 0 -1 -1 1 0 0 0 -1 -1 -1 1 0 0 -1 1 1 -1 1 0 -1 1 -1 -1 -1 1 5-19- 1
-1 1 0 0 0 0 -1 -1 1 0 0 0 -1 1 -1 1 0 0 -1 -1 -1 -1 1 0 1 1 -1 1 -1 1 5-11- 2	-1 1 0 0 0 0 -1 -1 1 0 0 0 -1 1 -1 1 0 0 -1 -1 -1 -1 1 0 1 1 -1 -1 -1 1 5-13- 3	-1 1 0 0 0 0 -1 -1 1 0 0 0 -1 -1 -1 1 0 0 -1 1 1 -1 1 0 -1 1 -1 -1 1 1 5-17- 1	-1 1 0 0 0 0 -1 -1 1 0 0 0 -1 -1 -1 1 0 0 -1 1 1 -1 1 0 1 -1 -1 -1 -1 1 5-19- 2
-1 1 0 0 0 0 -1 -1 1 0 0 0 -1 1 -1 1 0 0 -1 -1 -1 -1 1 0 1 1 1 -1 -1 1 5-11- 3	-1 1 0 0 0 0 -1 -1 1 0 0 0 -1 1 -1 1 0 0 -1 -1 -1 -1 1 0 -1 1 -1 -1 -1 1 5-14- 1	-1 1 0 0 0 0 -1 -1 1 0 0 0 -1 -1 -1 1 0 0 -1 1 1 -1 1 0 1 -1 -1 -1 1 1 5-17- 2	-1 1 0 0 0 0 -1 -1 1 0 0 0 -1 -1 -1 1 0 0 -1 1 1 -1 1 0 -1 -1 -1 -1 -1 1 5-20- 1

Fig. 3.7 continued

-1 1 0 0 0 0 -1 -1 1 0 0 0 -1 -1 -1 1 0 0 -1 -1 1 -1 1 0 -1 1 -1 -1 1 1 5-21- 1	-1 1 0 0 0 0 -1 -1 1 0 0 0 -1 -1 -1 1 0 0 1 1 -1 -1 1 0 -1 -1 -1 1 -1 1 5-22- 5	-1 1 0 0 0 0 -1 -1 1 0 0 0 -1 -1 -1 1 0 0 -1 -1 1 -1 1 0 -1 1 -1 -1 -1 1 5-25- 1	-1 1 0 0 0 0 -1 -1 1 0 0 0 -1 -1 -1 1 0 0 -1 1 -1 -1 1 0 1 -1 -1 1 -1 1 5-28- 2
-1 1 0 0 0 0 -1 -1 1 0 0 0 -1 -1 -1 1 0 0 -1 -1 1 -1 1 0 -1 1 -1 1 -1 1 5-21- 2	-1 1 0 0 0 0 -1 -1 1 0 0 0 -1 -1 -1 1 0 0 1 1 -1 -1 1 0 1 1 1 -1 -1 1 5-22- 6	-1 1 0 0 0 0 -1 -1 1 0 0 0 -1 -1 -1 1 0 0 1 1 -1 -1 1 0 -1 1 -1 -1 -1 1 5-25- 2	-1 1 0 0 0 0 -1 -1 1 0 0 0 -1 -1 -1 1 0 0 -1 1 -1 -1 1 0 -1 -1 -1 1 -1 1 5-29- 1
-1 1 0 0 0 0 -1 -1 1 0 0 0 -1 -1 -1 1 0 0 1 1 -1 -1 1 0 -1 1 -1 -1 1 1 5-21- 3	-1 1 0 0 0 0 -1 -1 1 0 0 0 -1 -1 -1 1 0 0 -1 -1 1 -1 1 0 -1 1 1 -1 -1 1 5-23- 1	-1 1 0 0 0 0 -1 -1 1 0 0 0 -1 -1 -1 1 0 0 -1 -1 1 -1 1 0 -1 -1 -1 -1 -1 1 5-26- 1	-1 1 0 0 0 0 -1 -1 1 0 0 0 -1 -1 -1 1 0 0 -1 1 -1 -1 1 0 1 1 1 -1 -1 1 5-29- 2
-1 1 0 0 0 0 -1 -1 1 0 0 0 -1 -1 -1 1 0 0 1 1 -1 -1 1 0 -1 1 -1 1 -1 1 5-21- 4	-1 1 0 0 0 0 -1 -1 1 0 0 0 -1 -1 -1 1 0 0 1 1 -1 -1 1 0 -1 1 1 -1 -1 1 5-23- 2	-1 1 0 0 0 0 -1 -1 1 0 0 0 -1 -1 -1 1 0 0 1 1 -1 -1 1 0 -1 -1 -1 -1 -1 1 5-26- 2	-1 1 0 0 0 0 -1 -1 1 0 0 0 -1 -1 -1 1 0 0 -1 1 -1 -1 1 0 -1 1 1 -1 -1 1 5-30- 1
-1 1 0 0 0 0 -1 -1 1 0 0 0 -1 -1 -1 1 0 0 -1 -1 1 -1 1 0 -1 -1 -1 -1 1 1 5-22- 1	-1 1 0 0 0 0 -1 -1 1 0 0 0 -1 -1 -1 1 0 0 -1 -1 1 -1 1 0 -1 -1 1 -1 -1 1 5-24- 1	-1 1 0 0 0 0 -1 -1 1 0 0 0 -1 -1 -1 1 0 0 -1 1 -1 -1 1 0 -1 -1 -1 -1 1 1 5-27- 1	-1 1 0 0 0 0 -1 -1 1 0 0 0 -1 -1 -1 1 0 0 -1 1 -1 -1 1 0 1 -1 1 -1 -1 1 5-30- 2
-1 1 0 0 0 0 -1 -1 1 0 0 0 -1 -1 -1 1 0 0 -1 -1 1 -1 1 0 -1 -1 -1 1 -1 1 5-22- 2	-1 1 0 0 0 0 -1 -1 1 0 0 0 -1 -1 -1 1 0 0 -1 -1 1 -1 1 0 1 1 -1 -1 -1 1 5-24- 2	-1 1 0 0 0 0 -1 -1 1 0 0 0 -1 -1 -1 1 0 0 -1 1 -1 -1 1 0 -1 -1 1 1 -1 1 5-27- 2	-1 1 0 0 0 0 -1 -1 1 0 0 0 -1 -1 -1 1 0 0 -1 1 -1 -1 1 0 -1 -1 1 -1 -1 1 5-31- 1
-1 1 0 0 0 0 -1 -1 1 0 0 0 -1 -1 -1 1 0 0 -1 -1 1 -1 1 0 1 1 1 -1 -1 1 5-22- 3	-1 1 0 0 0 0 -1 -1 1 0 0 0 -1 -1 -1 1 0 0 1 1 -1 -1 1 0 -1 -1 1 -1 -1 1 5-24- 3	-1 1 0 0 0 0 -1 -1 1 0 0 0 -1 -1 -1 1 0 0 -1 1 -1 -1 1 0 1 1 -1 1 -1 1 5-27- 3	-1 1 0 0 0 0 -1 -1 1 0 0 0 -1 -1 -1 1 0 0 -1 1 -1 -1 1 0 1 1 -1 -1 -1 1 5-31- 2
-1 1 0 0 0 0 -1 -1 1 0 0 0 -1 -1 -1 1 0 0 1 1 -1 -1 1 0 -1 -1 -1 -1 1 1 5-22- 4	-1 1 0 0 0 0 -1 -1 1 0 0 0 -1 -1 -1 1 0 0 1 1 -1 -1 1 0 1 1 -1 -1 -1 1 5-24- 4	-1 1 0 0 0 0 -1 -1 1 0 0 0 -1 -1 -1 1 0 0 -1 1 -1 -1 1 0 -1 1 -1 1 -1 1 5-28- 1	-1 1 0 0 0 0 -1 -1 1 0 0 0 -1 -1 -1 1 0 0 -1 1 -1 -1 1 0 -1 1 -1 -1 -1 1 5-32- 1

Fig. 3.7 continued

-1 1 0 0 0 0	-1 1 0 0 0 0
-1 -1 1 0 0 0	-1 -1 1 0 0 0
-1 -1 -1 1 0 0	-1 -1 -1 1 0 0
-1 1 -1 -1 1 0	-1 -1 -1 -1 1 0
1 -1 -1 -1 -1 1	-1 1 1 -1 -1 1
5-32- 2	5-38- 1
-1 1 0 0 0 0	-1 1 0 0 0 0
-1 -1 1 0 0 0	-1 -1 1 0 0 0
-1 -1 -1 1 0 0	-1 -1 -1 1 0 0
-1 1 -1 -1 1 0	-1 -1 -1 -1 1 0
-1 -1 -1 -1 -1 1	-1 -1 1 -1 -1 1
5-33- 1	5-39- 1
-1 1 0 0 0 0	-1 1 0 0 0 0
-1 -1 1 0 0 0	-1 -1 1 0 0 0
-1 -1 -1 1 0 0	-1 -1 -1 1 0 0
-1 1 -1 -1 1 0	-1 -1 -1 -1 1 0
-1 -1 -1 -1 -1 1	-1 -1 1 -1 -1 1
5-34- 1	5-39- 2
-1 1 0 0 0 0	-1 1 0 0 0 0
-1 -1 1 0 0 0	-1 -1 1 0 0 0
-1 -1 -1 1 0 0	-1 -1 -1 1 0 0
-1 1 -1 -1 1 0	-1 -1 -1 -1 1 0
-1 1 1 1 -1 1	1 1 -1 -1 -1 1
5-35- 1	5-40- 1
-1 1 0 0 0 0	-1 1 0 0 0 0
-1 -1 1 0 0 0	-1 -1 1 0 0 0
-1 -1 -1 1 0 0	-1 -1 -1 1 0 0
-1 -1 -1 -1 1 0	-1 -1 -1 -1 1 0
-1 -1 1 1 -1 1	-1 1 -1 -1 -1 1
5-35- 2	5-41- 1
-1 1 0 0 0 0	-1 1 0 0 0 0
-1 -1 1 0 0 0	-1 -1 1 0 0 0
-1 -1 -1 1 0 0	-1 -1 -1 1 0 0
-1 -1 -1 -1 1 0	-1 -1 -1 -1 1 0
1 1 -1 1 -1 1	-1 -1 -1 -1 -1 1
5-36- 1	
-1 1 0 0 0 0	
-1 -1 1 0 0 0	
-1 -1 -1 1 0 0	
-1 -1 -1 -1 1 0	
-1 1 -1 1 -1 1	
5-37- 1	
-1 1 0 0 0 0	
-1 -1 1 0 0 0	
-1 -1 -1 1 0 0	
-1 -1 -1 -1 1 0	
-1 -1 -1 1 -1 1	
5-37- 2	

Fig. 3.7 continued

DOF= 6		total number=3905							
category		homogeneous solution							no. of structures
6-	1	1	1	2	2	2	2	2	180
6-	2	1	1	2	2	2	2	4	144
6-	3	1	1	2	2	2	2	6	90
6-	4	1	1	2	2	2	2	8	36
6-	5	1	1	2	2	2	2	10	18
6-	6	1	1	2	2	2	4	2	96
6-	7	1	1	2	2	2	4	4	84
6-	8	1	1	2	2	2	4	6	72
6-	9	1	1	2	2	2	4	8	48
6-	10	1	1	2	2	2	4	10	24
6-	11	1	1	2	2	2	4	12	12
6-	12	1	1	2	2	2	6	2	30
6-	13	1	1	2	2	2	6	4	36
6-	14	1	1	2	2	2	6	6	36
6-	15	1	1	2	2	2	6	8	36
6-	16	1	1	2	2	2	6	10	24
6-	17	1	1	2	2	2	6	12	12
6-	18	1	1	2	2	2	6	14	6
6-	19	1	1	2	2	2	8	2	6
6-	20	1	1	2	2	2	8	4	12
6-	21	1	1	2	2	2	8	6	18
6-	22	1	1	2	2	2	8	8	18
6-	23	1	1	2	2	2	8	10	18
6-	24	1	1	2	2	2	8	12	12
6-	25	1	1	2	2	2	8	14	6
6-	26	1	1	2	2	2	8	16	3
6-	27	1	1	2	2	4	2	2	64
6-	28	1	1	2	2	4	2	4	56
6-	29	1	1	2	2	4	2	6	48
6-	30	1	1	2	2	4	2	8	32
6-	31	1	1	2	2	4	2	10	16
6-	32	1	1	2	2	4	2	12	8
6-	33	1	1	2	2	4	4	2	56
6-	34	1	1	2	2	4	4	4	48
6-	35	1	1	2	2	4	4	6	40
6-	36	1	1	2	2	4	4	8	32
6-	37	1	1	2	2	4	4	10	24
6-	38	1	1	2	2	4	4	12	16
6-	39	1	1	2	2	4	4	14	8
6-	40	1	1	2	2	4	6	2	36
6-	41	1	1	2	2	4	6	4	30
6-	42	1	1	2	2	4	6	6	24
6-	43	1	1	2	2	4	6	8	24
6-	44	1	1	2	2	4	6	10	24
6-	45	1	1	2	2	4	6	12	18
6-	46	1	1	2	2	4	6	14	12
6-	47	1	1	2	2	4	6	16	6
6-	48	1	1	2	2	4	8	2	16

Table 3.3 Homogeneous solutions for six-DOF tendon-driven manipulators having pseudo-triangular structure matrix

6-	49	1	1	2	2	4	8	4	16
6-	50	1	1	2	2	4	8	6	16
6-	51	1	1	2	2	4	8	8	16
6-	52	1	1	2	2	4	8	10	16
6-	53	1	1	2	2	4	8	12	16
6-	54	1	1	2	2	4	8	14	12
6-	55	1	1	2	2	4	8	16	8
6-	56	1	1	2	2	4	8	18	4
6-	57	1	1	2	2	4	10	2	4
6-	58	1	1	2	2	4	10	4	6
6-	59	1	1	2	2	4	10	6	8
6-	60	1	1	2	2	4	10	8	8
6-	61	1	1	2	2	4	10	10	8
6-	62	1	1	2	2	4	10	12	8
6-	63	1	1	2	2	4	10	14	8
6-	64	1	1	2	2	4	10	16	6
6-	65	1	1	2	2	4	10	18	4
6-	66	1	1	2	2	4	10	20	2
6-	67	1	1	2	2	6	2	2	10
6-	68	1	1	2	2	6	2	4	12
6-	69	1	1	2	2	6	2	6	12
6-	70	1	1	2	2	6	2	8	12
6-	71	1	1	2	2	6	2	10	8
6-	72	1	1	2	2	6	2	12	4
6-	73	1	1	2	2	6	2	14	2
6-	74	1	1	2	2	6	4	2	18
6-	75	1	1	2	2	6	4	4	15
6-	76	1	1	2	2	6	4	6	12
6-	77	1	1	2	2	6	4	8	12
6-	78	1	1	2	2	6	4	10	12
6-	79	1	1	2	2	6	4	12	9
6-	80	1	1	2	2	6	4	14	6
6-	81	1	1	2	2	6	4	16	3
6-	82	1	1	2	2	6	6	2	24
6-	83	1	1	2	2	6	6	4	16
6-	84	1	1	2	2	6	6	6	12
6-	85	1	1	2	2	6	6	8	8
6-	86	1	1	2	2	6	6	10	12
6-	87	1	1	2	2	6	6	12	16
6-	88	1	1	2	2	6	6	14	12
6-	89	1	1	2	2	6	6	16	8
6-	90	1	1	2	2	6	6	18	4
6-	91	1	1	2	2	6	8	2	18
6-	92	1	1	2	2	6	8	4	12
6-	93	1	1	2	2	6	8	6	6
6-	94	1	1	2	2	6	8	8	6
6-	95	1	1	2	2	6	8	10	6
6-	96	1	1	2	2	6	8	12	9
6-	97	1	1	2	2	6	8	14	12
6-	98	1	1	2	2	6	8	16	9
6-	99	1	1	2	2	6	8	18	6
6-	100	1	1	2	2	6	8	20	3

Table 3.3 continued

6- 101	1	1	2	2	6	10	2	8
6- 102	1	1	2	2	6	10	4	8
6- 103	1	1	2	2	6	10	6	6
6- 104	1	1	2	2	6	10	8	4
6- 105	1	1	2	2	6	10	10	4
6- 106	1	1	2	2	6	10	12	4
6- 107	1	1	2	2	6	10	14	6
6- 108	1	1	2	2	6	10	16	8
6- 109	1	1	2	2	6	10	18	6
6- 110	1	1	2	2	6	10	20	4
6- 111	1	1	2	2	6	10	22	2
6- 112	1	1	2	2	6	12	2	2
6- 113	1	1	2	2	6	12	4	3
6- 114	1	1	2	2	6	12	6	4
6- 115	1	1	2	2	6	12	8	3
6- 116	1	1	2	2	6	12	10	2
6- 117	1	1	2	2	6	12	12	2
6- 118	1	1	2	2	6	12	14	2
6- 119	1	1	2	2	6	12	16	3
6- 120	1	1	2	2	6	12	18	4
6- 121	1	1	2	2	6	12	20	3
6- 122	1	1	2	2	6	12	22	2
6- 123	1	1	2	2	6	12	24	1
6- 124	1	1	2	4	2	2	2	32
6- 125	1	1	2	4	2	2	4	28
6- 126	1	1	2	4	2	2	6	24
6- 127	1	1	2	4	2	2	8	16
6- 128	1	1	2	4	2	2	10	8
6- 129	1	1	2	4	2	2	12	4
6- 130	1	1	2	4	2	4	2	28
6- 131	1	1	2	4	2	4	4	24
6- 132	1	1	2	4	2	4	6	20
6- 133	1	1	2	4	2	4	8	16
6- 134	1	1	2	4	2	4	10	12
6- 135	1	1	2	4	2	4	12	8
6- 136	1	1	2	4	2	4	14	4
6- 137	1	1	2	4	2	6	2	18
6- 138	1	1	2	4	2	6	4	15
6- 139	1	1	2	4	2	6	6	12
6- 140	1	1	2	4	2	6	8	12
6- 141	1	1	2	4	2	6	10	12
6- 142	1	1	2	4	2	6	12	9
6- 143	1	1	2	4	2	6	14	6
6- 144	1	1	2	4	2	6	16	3
6- 145	1	1	2	4	2	8	2	8
6- 146	1	1	2	4	2	8	4	8
6- 147	1	1	2	4	2	8	6	8
6- 148	1	1	2	4	2	8	8	8
6- 149	1	1	2	4	2	8	10	8
6- 150	1	1	2	4	2	8	12	8
6- 151	1	1	2	4	2	8	14	6
6- 152	1	1	2	4	2	8	16	4

Table 3.3 continued

6- 153	1	1	2	4	2	8	18	2
6- 154	1	1	2	4	2	10	2	2
6- 155	1	1	2	4	2	10	4	3
6- 156	1	1	2	4	2	10	6	4
6- 157	1	1	2	4	2	10	8	4
6- 158	1	1	2	4	2	10	10	4
6- 159	1	1	2	4	2	10	12	4
6- 160	1	1	2	4	2	10	14	4
6- 161	1	1	2	4	2	10	16	3
6- 162	1	1	2	4	2	10	18	2
6- 163	1	1	2	4	2	10	20	1
6- 164	1	1	2	4	4	2	2	28
6- 165	1	1	2	4	4	2	4	24
6- 166	1	1	2	4	4	2	6	20
6- 167	1	1	2	4	4	2	8	16
6- 168	1	1	2	4	4	2	10	12
6- 169	1	1	2	4	4	2	12	8
6- 170	1	1	2	4	4	2	14	4
6- 171	1	1	2	4	4	4	2	18
6- 172	1	1	2	4	4	4	4	36
6- 173	1	1	2	4	4	4	6	18
6- 174	1	1	2	4	4	4	8	24
6- 175	1	1	2	4	4	4	10	6
6- 176	1	1	2	4	4	4	12	12
6- 177	1	1	2	4	4	4	14	6
6- 178	1	1	2	4	4	4	16	6
6- 179	1	1	2	4	4	6	2	10
6- 180	1	1	2	4	4	6	4	12
6- 181	1	1	2	4	4	6	6	10
6- 182	1	1	2	4	4	6	8	8
6- 183	1	1	2	4	4	6	10	6
6- 184	1	1	2	4	4	6	12	4
6- 185	1	1	2	4	4	6	14	4
6- 186	1	1	2	4	4	6	16	4
6- 187	1	1	2	4	4	6	18	2
6- 188	1	1	2	4	4	8	2	8
6- 189	1	1	2	4	4	8	4	16
6- 190	1	1	2	4	4	8	6	8
6- 191	1	1	2	4	4	8	8	16
6- 192	1	1	2	4	4	8	10	8
6- 193	1	1	2	4	4	8	12	12
6- 194	1	1	2	4	4	8	14	4
6- 195	1	1	2	4	4	8	16	8
6- 196	1	1	2	4	4	8	18	4
6- 197	1	1	2	4	4	8	20	4
6- 198	1	1	2	4	4	10	2	6
6- 199	1	1	2	4	4	10	4	4
6- 200	1	1	2	4	4	10	6	6
6- 201	1	1	2	4	4	10	8	8
6- 202	1	1	2	4	4	10	10	8
6- 203	1	1	2	4	4	10	12	8
6- 204	1	1	2	4	4	10	14	6

Table 3.3 continued

6- 205	1	1	2	4	4	10	16	4
6- 206	1	1	2	4	4	10	18	4
6- 207	1	1	2	4	4	10	20	4
6- 208	1	1	2	4	4	10	22	2
6- 209	1	1	2	4	4	12	2	2
6- 210	1	1	2	4	4	12	4	4
6- 211	1	1	2	4	4	12	6	2
6- 212	1	1	2	4	4	12	8	6
6- 213	1	1	2	4	4	12	10	4
6- 214	1	1	2	4	4	12	12	8
6- 215	1	1	2	4	4	12	14	4
6- 216	1	1	2	4	4	12	16	6
6- 217	1	1	2	4	4	12	18	2
6- 218	1	1	2	4	4	12	20	4
6- 219	1	1	2	4	4	12	22	2
6- 220	1	1	2	4	4	12	24	2
6- 221	1	1	2	4	6	2	2	18
6- 222	1	1	2	4	6	2	4	15
6- 223	1	1	2	4	6	2	6	12
6- 224	1	1	2	4	6	2	8	12
6- 225	1	1	2	4	6	2	10	12
6- 226	1	1	2	4	6	2	12	9
6- 227	1	1	2	4	6	2	14	6
6- 228	1	1	2	4	6	2	16	3
6- 229	1	1	2	4	6	4	2	10
6- 230	1	1	2	4	6	4	4	12
6- 231	1	1	2	4	6	4	6	10
6- 232	1	1	2	4	6	4	8	8
6- 233	1	1	2	4	6	4	10	6
6- 234	1	1	2	4	6	4	12	4
6- 235	1	1	2	4	6	4	14	4
6- 236	1	1	2	4	6	4	16	4
6- 237	1	1	2	4	6	4	18	2
6- 238	1	1	2	4	6	6	2	8
6- 239	1	1	2	4	6	6	4	10
6- 240	1	1	2	4	6	6	6	12
6- 241	1	1	2	4	6	6	8	8
6- 242	1	1	2	4	6	6	10	4
6- 243	1	1	2	4	6	6	12	4
6- 244	1	1	2	4	6	6	14	4
6- 245	1	1	2	4	6	6	16	4
6- 246	1	1	2	4	6	6	18	4
6- 247	1	1	2	4	6	6	20	2
6- 248	1	1	2	4	6	8	2	8
6- 249	1	1	2	4	6	8	4	8
6- 250	1	1	2	4	6	8	6	8
6- 251	1	1	2	4	6	8	8	8
6- 252	1	1	2	4	6	8	10	6
6- 253	1	1	2	4	6	8	12	4
6- 254	1	1	2	4	6	8	14	4
6- 255	1	1	2	4	6	8	16	4
6- 256	1	1	2	4	6	8	18	4

Table 3.3 continued

6- 257	1	1	2	4	6	8	20	4
6- 258	1	1	2	4	6	8	22	2
6- 259	1	1	2	4	6	10	2	8
6- 260	1	1	2	4	6	10	4	6
6- 261	1	1	2	4	6	10	6	4
6- 262	1	1	2	4	6	10	8	6
6- 263	1	1	2	4	6	10	10	8
6- 264	1	1	2	4	6	10	12	6
6- 265	1	1	2	4	6	10	14	4
6- 266	1	1	2	4	6	10	16	4
6- 267	1	1	2	4	6	10	18	4
6- 268	1	1	2	4	6	10	20	4
6- 269	1	1	2	4	6	10	22	4
6- 270	1	1	2	4	6	10	24	2
6- 271	1	1	2	4	6	12	2	6
6- 272	1	1	2	4	6	12	4	4
6- 273	1	1	2	4	6	12	6	4
6- 274	1	1	2	4	6	12	8	4
6- 275	1	1	2	4	6	12	10	6
6- 276	1	1	2	4	6	12	12	8
6- 277	1	1	2	4	6	12	14	6
6- 278	1	1	2	4	6	12	16	4
6- 279	1	1	2	4	6	12	18	4
6- 280	1	1	2	4	6	12	20	4
6- 281	1	1	2	4	6	12	22	4
6- 282	1	1	2	4	6	12	24	4
6- 283	1	1	2	4	6	12	26	2
6- 284	1	1	2	4	6	14	2	2
6- 285	1	1	2	4	6	14	4	2
6- 286	1	1	2	4	6	14	6	2
6- 287	1	1	2	4	6	14	8	2
6- 288	1	1	2	4	6	14	10	2
6- 289	1	1	2	4	6	14	12	3
6- 290	1	1	2	4	6	14	14	4
6- 291	1	1	2	4	6	14	16	3
6- 292	1	1	2	4	6	14	18	2
6- 293	1	1	2	4	6	14	20	2
6- 294	1	1	2	4	6	14	22	2
6- 295	1	1	2	4	6	14	24	2
6- 296	1	1	2	4	6	14	26	2
6- 297	1	1	2	4	6	14	28	1
6- 298	1	1	2	4	8	2	2	4
6- 299	1	1	2	4	8	2	4	4
6- 300	1	1	2	4	8	2	6	4
6- 301	1	1	2	4	8	2	8	4
6- 302	1	1	2	4	8	2	10	4
6- 303	1	1	2	4	8	2	12	4
6- 304	1	1	2	4	8	2	14	3
6- 305	1	1	2	4	8	2	16	2
6- 306	1	1	2	4	8	2	18	1
6- 307	1	1	2	4	8	4	2	4
6- 308	1	1	2	4	8	4	4	8

Table 3.3 continued

6- 309	1	1	2	4	8	4	6	4
6- 310	1	1	2	4	8	4	8	8
6- 311	1	1	2	4	8	4	10	4
6- 312	1	1	2	4	8	4	12	6
6- 313	1	1	2	4	8	4	14	2
6- 314	1	1	2	4	8	4	16	4
6- 315	1	1	2	4	8	4	18	2
6- 316	1	1	2	4	8	4	20	2
6- 317	1	1	2	4	8	6	2	4
6- 318	1	1	2	4	8	6	4	4
6- 319	1	1	2	4	8	6	6	4
6- 320	1	1	2	4	8	6	8	4
6- 321	1	1	2	4	8	6	10	3
6- 322	1	1	2	4	8	6	12	2
6- 323	1	1	2	4	8	6	14	2
6- 324	1	1	2	4	8	6	16	2
6- 325	1	1	2	4	8	6	18	2
6- 326	1	1	2	4	8	6	20	2
6- 327	1	1	2	4	8	6	22	1
6- 328	1	1	2	4	8	8	2	4
6- 329	1	1	2	4	8	8	4	8
6- 330	1	1	2	4	8	8	6	4
6- 331	1	1	2	4	8	8	8	6
6- 332	1	1	2	4	8	8	10	2
6- 333	1	1	2	4	8	8	12	4
6- 334	1	1	2	4	8	8	14	2
6- 335	1	1	2	4	8	8	16	4
6- 336	1	1	2	4	8	8	18	2
6- 337	1	1	2	4	8	8	20	4
6- 338	1	1	2	4	8	8	22	2
6- 339	1	1	2	4	8	8	24	2
6- 340	1	1	2	4	8	10	2	4
6- 341	1	1	2	4	8	10	4	4
6- 342	1	1	2	4	8	10	6	3
6- 343	1	1	2	4	8	10	8	2
6- 344	1	1	2	4	8	10	10	2
6- 345	1	1	2	4	8	10	12	2
6- 346	1	1	2	4	8	10	14	2
6- 347	1	1	2	4	8	10	16	2
6- 348	1	1	2	4	8	10	18	2
6- 349	1	1	2	4	8	10	20	2
6- 350	1	1	2	4	8	10	22	2
6- 351	1	1	2	4	8	10	24	2
6- 352	1	1	2	4	8	10	26	1
6- 353	1	1	2	4	8	12	2	4
6- 354	1	1	2	4	8	12	4	6
6- 355	1	1	2	4	8	12	6	2
6- 356	1	1	2	4	8	12	8	4
6- 357	1	1	2	4	8	12	10	2
6- 358	1	1	2	4	8	12	12	4
6- 359	1	1	2	4	8	12	14	2
6- 360	1	1	2	4	8	12	16	4

Table 3.3 continued

6- 361	1	1	2	4	8	12	18	2
6- 362	1	1	2	4	8	12	20	4
6- 363	1	1	2	4	8	12	22	2
6- 364	1	1	2	4	8	12	24	4
6- 365	1	1	2	4	8	12	26	2
6- 366	1	1	2	4	8	12	28	2
6- 367	1	1	2	4	8	14	2	3
6- 368	1	1	2	4	8	14	4	2
6- 369	1	1	2	4	8	14	6	2
6- 370	1	1	2	4	8	14	8	2
6- 371	1	1	2	4	8	14	10	2
6- 372	1	1	2	4	8	14	12	2
6- 373	1	1	2	4	8	14	14	2
6- 374	1	1	2	4	8	14	16	2
6- 375	1	1	2	4	8	14	18	2
6- 376	1	1	2	4	8	14	20	2
6- 377	1	1	2	4	8	14	22	2
6- 378	1	1	2	4	8	14	24	2
6- 379	1	1	2	4	8	14	26	2
6- 380	1	1	2	4	8	14	28	2
6- 381	1	1	2	4	8	14	30	1
6- 382	1	1	2	4	8	16	2	1
6- 383	1	1	2	4	8	16	4	2
6- 384	1	1	2	4	8	16	6	1
6- 385	1	1	2	4	8	16	8	2
6- 386	1	1	2	4	8	16	10	1
6- 387	1	1	2	4	8	16	12	2
6- 388	1	1	2	4	8	16	14	1
6- 389	1	1	2	4	8	16	16	2
6- 390	1	1	2	4	8	16	18	1
6- 391	1	1	2	4	8	16	20	2
6- 392	1	1	2	4	8	16	22	1
6- 393	1	1	2	4	8	16	24	2
6- 394	1	1	2	4	8	16	26	1
6- 395	1	1	2	4	8	16	28	2
6- 396	1	1	2	4	8	16	30	1
6- 397	1	1	2	4	8	16	32	1

Table 3.3 continued

Chapter 4

Topological Analysis and Performance Evaluation

4.1 Introduction

Once various design alternatives have been generated, the following procedure in mechanical design is to assess their performance. The designer may set several suitable criteria for the performance assessment, for example, structural versus functional, or kinematic versus dynamic, and so on. By comparing the performance requirements, the number of potentially useful mechanisms may be reduced, or an optimum configuration may be identified. Following this rationale, we may ask ourselves the following questions. For a given number of degrees of freedom in a tendon-driven manipulator, how many different tendon routings are admissible? And if we know the solution, what type of routing is the optimal? In the previous chapter, a methodology for the enumeration of admissible tendon routings for manipulators having pseudo-triangular structure matrix has been developed. All the admissible kinematic structures with up to six-DOF have been enumerated. In this chapter, the kinematic and static force transmission characteristics associated with tendon-driven manipulators will be investigated and the structural differences among various tendon routings will be compared.

Various performance indices have been devised for assessing kinematic performance of robotic manipulators. Among these, the theory of differential geometry has been most frequently used by researchers to define various performance

indices, such as the velocity/force ellipsoid (Asada and Cro Granito, 1985; and Ghosal and Roth, 1987), the condition number (Salisbury and Craig, 1982) and the manipulability measure of a robotic manipulator (Yoshikawa, 1985). However, most of the performance measures are based on the evaluation of the transformation between the end-effector space and the joint space. In what follows, the theory of differential geometry will be used for the analysis of force and/or motion transformation between the actuator space and joint space in tendon-driven manipulators. First, it will be shown that a tendon-driven manipulator can be characterized by the condition number, defined as the ratio of the maximum singular-value to the minimum singular-value of the structure matrix, and the direction of its homogeneous solution. Then, an index for measuring the goodness of tendon routing will be defined and it will be shown that an isotropic transformation between the actuator space and joint space can be achieved for certain type of routings. Finally, a method for resolving the maximum tension required to produce a set of desired joint torques will be described.

4.2 Basic Equations

It has been shown in Section 3.2 that the kinematic and force relationships between the joint space and tendon space can be expressed by Eqs. (3.1) and (3.3). Taking the derivative of Eq. (3.1), yields

$$\underline{\dot{S}} = B R \underline{\dot{\Theta}} \quad (4.1)$$

Equation (3.3) can be written as

$$\underline{\tau} = R^T B^T \underline{F} \quad (4.2)$$

provided that all pulleys pivoted about one joint axis have the same radius. More specifically, if the number of tendons is greater than the number of DOF by one, then the solution of \underline{F} can be generally expressed as the summation of a particular solution and a homogeneous solution as shown below

$$\underline{F} = (R^T B^T)^+ \underline{\tau} + \lambda \underline{f}_h \quad (4.3)$$

where $(\#)^+ = \{(\#)^T[(\#)(\#)^T]^{-1}\}$ represents the pseudo-inverse of $(\#)$ (Strang, 1980), \underline{f}_h lies in the null space of structure matrix B^T , and λ is an arbitrary constant. The homogeneous solution vector \underline{f}_h represents a set of tendon forces which results in no net joint torques. The components of \underline{f}_h must be of the same sign. Thus by adjusting the constant λ , positive tension can be maintained in every tendon.

The structure matrix B^T is of primary importance in determining the characteristics of a manipulator, since the radius matrix R is a non-singular square matrix which does not affect the generic property of a manipulator. For the sake of clarity, it is assumed that R is an identity matrix so that manipulators are normalized to unity. A two-DOF system will be used as an example to develop the concept throughout this Chapter.

4.3 Transmission Ellipsoids

The planar schematic of a two-DOF tendon-driven manipulator with three control tendons is shown in Fig. 4.1. Defining the positive axes of rotation about the joints to be pointing out of the paper, Eq. (4.2) can be written as:

$$\underline{\tau} = B^T \underline{F} \quad (4.4)$$

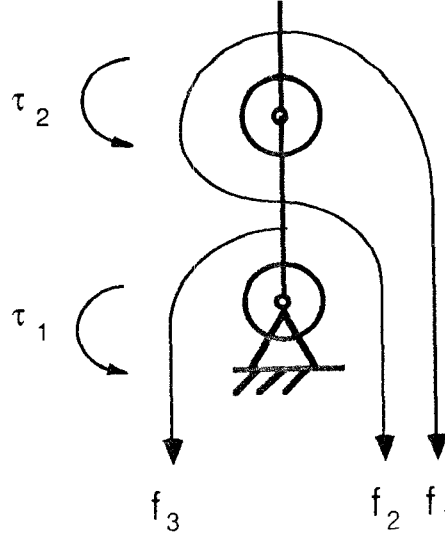


Fig. 4.1 A two-DOF tendon-driven manipulator

where $\underline{\tau} = [\tau_2 \quad \tau_1]^T$, $\underline{F} = [f_1 \quad f_2 \quad f_3]^T$ and $B^T = \begin{bmatrix} -1 & 1 & 0 \\ -1 & -1 & 1 \end{bmatrix}$.

When there is no joint torque requirement, tendon forces are given by the homogeneous solution, $\underline{f}_h = \lambda \cdot [1 \quad 1 \quad 2]^T$ and not much more can be said about it. One effective method is to compare tendon forces required to achieve a unity joint torque

$$\underline{\tau}^T \cdot \underline{\tau} = 1, \quad (4.5)$$

in all directions. For a two-DOF system, Equation (4.5) represents a circle in the joint torque space as shown in Fig. 4.2.

Substituting Eq. (4.4) into (4.5), yields:

$$\underline{F}^T B B^T \underline{F} = 1 \quad (4.6)$$

Since matrix B^T is of rank two, the quantity $(B B^T)$ is a symmetric 3×3 matrix of rank two. Therefore, Eq. (4.6) describes a cylinder with its elements

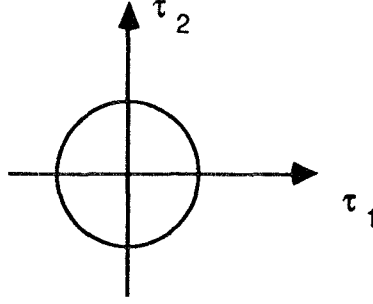


Fig. 4.2 Quadratic joint torque constraint

oblique to the coordinate axes in the tendon force space as shown in Fig. 4.3. The principal axes of this force ellipsoid coincide with the eigenvectors of (BB^T) and the lengths of its principal axes are equal to the reciprocals of the square roots of the eigenvalues. Since (BB^T) is a symmetric 3×3 matrix of rank two, this quantity always has an eigenvalue of zero magnitude which results in a principal axis of infinite length. This axis defines the direction of the homogeneous solution of Eq. (4.4).

4.3.1 Force Ellipsoid

The force ellipsoid shown in Fig. 4.3 is a useful tool for visualizing the force transmission characteristics. From geometric point of view, each element of the cylindrical surface in the tendon force space maps onto a point in the joint torque space. This implies that tendon forces can be proportionally increased along the direction of its homogeneous solution without affecting the resultant joint torques. If the direction of the homogeneous solution is not contained in the first quadrant, then increasing tendon forces along the longitudinal direction of the cylindrical surface will result in some negative tensions. Hence, all components of the homogeneous solution must be positive.

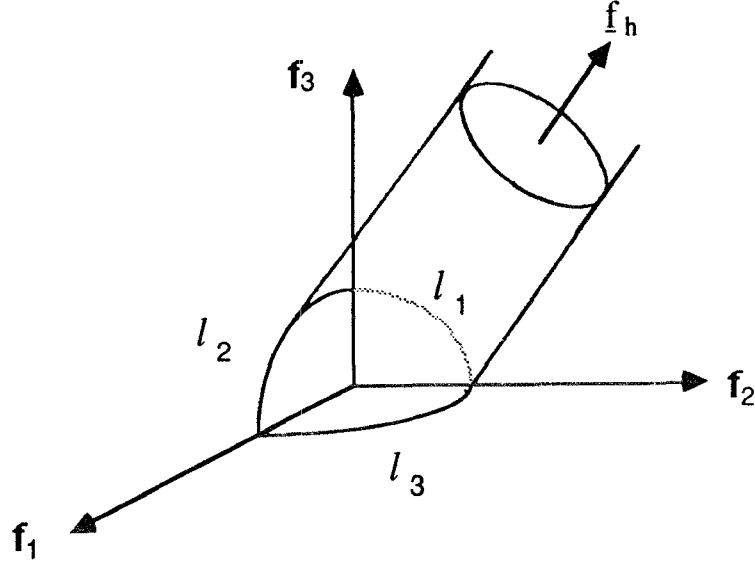


Fig. 4.3 Tendon force ellipsoid

4.3.2 Velocity Ellipsoid

Similar to the force ellipsoid, a velocity ellipsoid can be constructed to visualize the velocity transmission characteristics. Velocity in the joint space can be mapped into tendon space via Eq. (4.1). For a unity matrix R , Eq. (4.1) can be written as follows:

$$\underline{\dot{S}} = B \underline{\dot{\Theta}} \quad (4.7)$$

Given $\underline{\dot{S}}$, the least squares solution of $\underline{\dot{\Theta}}$ to the above equation can be obtained as follows (Strang, 1980). Taking the left general inverse of B , Eq. (4.7) yields:

$$\underline{\dot{\Theta}} = {}^l B^+ \underline{\dot{S}} \quad (4.8)$$

where ${}^l B^+$ is defined as $[(B^T B)^{-1} B^T]$. Restraining $\underline{\dot{\Theta}}$ with unit speed condition, one obtains:

$$\underline{\dot{\Theta}}^T \underline{\dot{\Theta}} = \underline{\dot{S}}^T ({}^l B^+)^T {}^l B^+ \underline{\dot{S}} = 1 \quad (4.9)$$

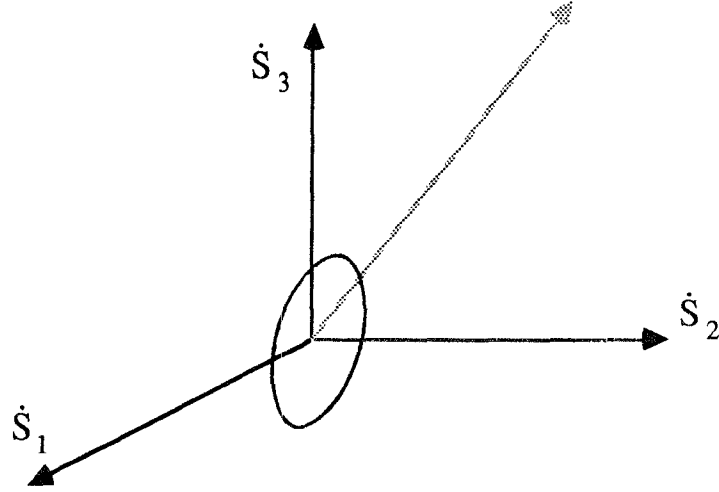


Fig. 4.4 Tendon velocity ellipsoid

The quantity $[(^l B^+)^T \ ^l B^+]$ is a symmetric 3×3 matrix of rank two, therefore, the velocity vector $\underline{\dot{S}}$ depicts an ellipse as shown in Fig. 4.4.

Another quick way to depict the velocity ellipsoid is to apply the duality property of force and velocity. The principal axes of the velocity and force ellipsoids coincide, while the lengths of the principal axes are inversely proportional to one another. Hence, principal axes of the velocity ellipsoid shown in Fig. 4.4 are oriented in the same direction as those of force ellipsoid shown in Fig. 4.3, and its lengths are the reciprocals of those of the force ellipsoid. Notice that one of the axes (corresponding to the homogeneous solution) in the force ellipsoid is infinite long; therefore, the length of the corresponding axis in the velocity ellipsoid is zero. Also, note that although $\underline{\dot{S}}$ has one fewer DOF than \underline{E} , $\underline{\dot{S}}$ still implicitly describes an ellipsoid with a degenerate axis of zero length.

4.4 Isotropy of the Transmission Ellipsoid

It is well known that the velocity transformation between the joint space

and end-effector space of a manipulator can be characterized by the Jacobian matrix J . The condition number of the Jacobian matrix has been used as a quality index for measuring the performance of a manipulator. The condition number is defined as the product of norms of J and J^{-1} (Strang, 1980). It can also be used as an indicator for measuring the shape of the transmission ellipsoid. When the condition number is equal to one, we call the mapping *isotropic*. Isotropic transmission has advantageous properties as discussed by Salisbury and Craig (1982), and Gosselin and Angeles (1988). For tendon-driven manipulators, the force transmission ellipsoid formed by the structure matrix B^T has an axis of infinite length. Therefore, traditional definition for the condition number can no longer be used. In this work, the condition number of the structure matrix is defined as:

$$cond(B^T) = \frac{\text{maximum singular value of } B^T}{\text{minimum singular value of } B^T} \quad (4.10)$$

This condition number measures the shape of the cross section perpendicular to the longitudinal axis of the cylinder. When the value is close to 1, the shape of the cross section approaches a circle. The physical meaning of this measure is given as follows. It can be shown that matrix B^T can be factored into

$$B^T = Q_1 \Sigma (Q_2)^T \quad (4.11)$$

where Q_1 is a 2×2 orthogonal matrix, Q_2 is a 3×3 orthogonal matrix, and Σ has a special diagonal form as shown below:

$$\Sigma = \begin{bmatrix} \sigma_1 & 0 & 0 \\ 0 & \sigma_2 & 0 \end{bmatrix} \quad (4.12)$$

with $\sigma_1 \geq \sigma_2 > 0$.

This is known as the singular value decomposition and, σ_1 and σ_2 are called the singular values of B^T . From Eq. (4.10), it follows that $\text{cond}(B^T) = \sigma_1/\sigma_2$. The shape of the cross section is an ellipse for which the ratio of the major axis to the minor axis is equal to the value of the condition number σ_1/σ_2 . The application of this index can be explained in the following. The cylinder intersects with the $f_2 - f_3$, $f_3 - f_1$, and $f_1 - f_2$ planes in three curves l_1 , l_2 , and l_3 , respectively, as shown in Fig. 4.3. Physically, these intersecting curves are the loci of minimum tendon forces required to produce a unity joint torque in all directions as shown in Fig. 4.2. Therefore, we can readily see that the shape of the cross section as well as the direction of the longitudinal axis has some dominant effect on the location of the curves. An ideal condition would be for the intersecting curves l_1 , l_2 , and l_3 to be located symmetrically with respect to the origin. For the ideal condition to happen, the cylinder must have a circular cross section and the longitudinal axis must intersect all the coordinate axes at equal angles.

From the above discussion, it can be concluded that the direction of the longitudinal axis plays an important role in the distribution of tendon forces. The more the longitudinal axis is skewed, i.e, the components of the vector are in an odd proportion, the larger the difference in tensions will occur. This will result in a severe antagonism among the tendons and greatly reduce the efficiency of the system. Therefore, it is desirable to have the longitudinal axis of the cylinder pointed as closely toward the direction which makes equal angles with all the coordinate axes as possible. We shall call the vector which makes equal angles with all the coordinate axes as the *isotropic vector*. Define:

$$\theta^* = \cos^{-1}(\underline{U} \cdot \underline{I}_s) \quad (4.13)$$

where \underline{U} is a unit vector defined along the longitudinal axis of the cylinder and \underline{I}_s is the unit isotropic vector. Then, the angle θ^* can be used to indicate the closeness of the longitudinal axis to the isotropic vector. The smaller the angle θ^* is, the closer the longitudinal axis is to the isotropic vector. In the three-dimensional space, the unit isotropic vector is given by $[1/\sqrt{3} \ 1/\sqrt{3} \ 1/\sqrt{3}]^T$. In an n -dimensional space, it is given by $[1/\sqrt{n} \ 1/\sqrt{n} \ \dots \ 1/\sqrt{n}]^T$.

Isotropic Transmission Ellipsoid. An *isotropic transmission ellipsoid* is defined as one which has a unit condition number of the structure matrix and has the isotropic vector as the direction of the homogeneous solution.

4.5 Maximum Tendon Force

To compute tendon forces, we first obtain a particular solution to Eq. (4.2), then the homogeneous solution multiplied by a constant λ is added onto the particular solution, see Eq.(4.3). The constant λ must be chosen such that all the tendons are under tension. The result is exactly the same as finding the intersection of the force ellipsoid with its coordinate planes, i.e., solving l_1 , l_2 , and l_3 in terms of joint torques. This procedure can be accomplished by substituting the equations of the coordinate planes $f_i = 0$ ($i=1,2,3$) into Eq. (4.4), and then solving for f_j ($j=1,2,3; j \neq i$).

Consider the two-DOF manipulator for example. Substituting $f_1 = 0$ into Eq. (4.4), and solving f_2 and f_3 , yields l_1 in parametric form as:

$$\begin{cases} f_2 = \tau_2 \\ f_3 = \tau_2 + \tau_1 \end{cases} \quad (4.14a)$$

where τ_1 and τ_2 are subject to the constraint imposed by Eq. (4.5).

Similarly, substituting $f_2 = 0$ into Eq. (4.4), yields l_2 as

$$\begin{cases} f_1 = -\tau_2 \\ f_3 = -\tau_2 + \tau_1 \end{cases} \quad (4.14b)$$

Substituting $f_3 = 0$ into Eq. (4.4), yields l_3 as

$$\begin{cases} f_1 = (-\tau_1 - \tau_2)/2 \\ f_2 = (\tau_2 - \tau_1)/2 \end{cases} \quad (4.14c)$$

The maximum value of f_j can be found using Cauchy-Schwarz inequality formula.

$$(ax + by)^2 \leq (a^2 + b^2)(x^2 + y^2) \quad (4.15)$$

Applying Cauchy-Schwarz inequality to the first equation of Eq. (4.14a), yields,

$$f_2^2 = \tau_2^2 \leq (0^2 + 1^2)(\tau_1^2 + \tau_2^2) \quad (4.16a)$$

or

$$f_2 \leq 1 \quad (4.16b)$$

Applying Cauchy-Schwarz inequality to the second equation of Eq. (4.14c), yields,

$$f_2^2 = (\tau_2/2 - \tau_1/2)^2 \leq (1/2^2 + 1/2^2)(\tau_1^2 + \tau_2^2) \quad (4.17a)$$

or

$$f_2 \leq 1/\sqrt{2} \quad (4.17b)$$

Hence, tendon f_2 has an extreme value of 1. Similarly, extreme values of f_1 and f_3 can be found.

The above procedure can be extended to n -DOF manipulators. For an n -DOF manipulator, there are $n + 1$ hyperplanes with which the $(n + 1)$ -dimensional force ellipsoid may intersect. The equations of the hyperplanes can be represented as

$$f_i = 0, \quad i = 1, 2, \dots, n + 1 \quad (4.18)$$

Substituting Eq. (4.18) into (4.2), yields:

$$\underline{\tau} = B_i^T \underline{F}^i \quad (4.19)$$

where B_i^T is the matrix obtained by deleting the i^{th} column from B^T and \underline{F}^i is the column matrix obtained by deleting the i^{th} element of \underline{F} .

For each i , Eq. (4.19) denotes n linear equations in n unknowns. Hence, \underline{F}^i can be obtained by inverting B_i^T , or by using Crammer's rule. The j^{th} element f_j can then be represented as:

$$f_j = \frac{(-1)^s |\underline{\tau} \ B_{ij}^T|}{|B_i^T|} \quad (4.20)$$

where

$$\begin{cases} s = j - 1 & \text{if } i > j \\ s = j & \text{if } i < j \end{cases} ;$$

and where $i=1,2, \dots, n+1$; $j=1,2,\dots, n+1$; and $j \neq i$; and where B_{ij}^T represents the matrix obtained by deleting the i^{th} and j^{th} column of B^T ; and $|(\#)|$ represents the determinant of $(\#)$.

There are $n(n+1)$ such equations. For each equation, an extreme value of the tendon force can be obtained using Cauchy-Schwarz inequality formula. Therefore, the maximum tension in each tendon can be derived. Comparing the extreme values, the static performance among various tendon routings can be distinguished.

4.6 Application to Three-DOF Systems

In this section, the foregoing concepts will be applied to analyzing three-DOF systems. A three-DOF manipulator requires four tendons. Therefore,

to achieve a unit joint torque in all directions, joint torques describe a three-dimensional sphere while tendon forces describe a four-dimensional cylinder with an axis of infinite length. Similar to the two-DOF manipulator, the condition number of the structure matrix measures the shape of the directrix of the cylinder. Figure 4.5 shows five nonisomorphic tendon routings derived from the previous chapter, Table 3.1.

Table 4.1 (on page 78) lists the structure matrix B^T , homogeneous solution \underline{f}_h of the B^T , condition number C , and the angle θ^* for each of the kinematic structures shown in Fig. 4.5.

Note that Fig. 4.5(c) represents the kinematic structure of a finger used in the Stanford/JPL Hand. The homogeneous solution of the Stanford/JPL finger points in the isotropic direction, $\theta^*=0$. However, its condition number is not equal to one, but $C=2.618$. On the other hand, the tendon routing as shown in Fig. 4.5(d) results in an isotropic transmission. All other kinematic structures show different extent of nonisotropy in terms of the condition number and the angle θ^* .

Table 4.2 (on page 79) lists the maximum tendon forces for the structures shown in Fig. 4.5. To differentiate the performance among various structures, we can define an optimality criterion as follows:

$$\begin{aligned} \text{Objective function } & \min_{(B^T)_i} [\max_{\underline{F}} (f_j)], \\ \text{subject to } & \underline{\tau}^T \cdot \underline{\tau} = 1, \end{aligned} \tag{4.21}$$

where $\max(f_j)$ denotes the maximum tendon force in a given kinematic structure, and $\min[]$ denotes the least maximum tendon force among a set of different structures.

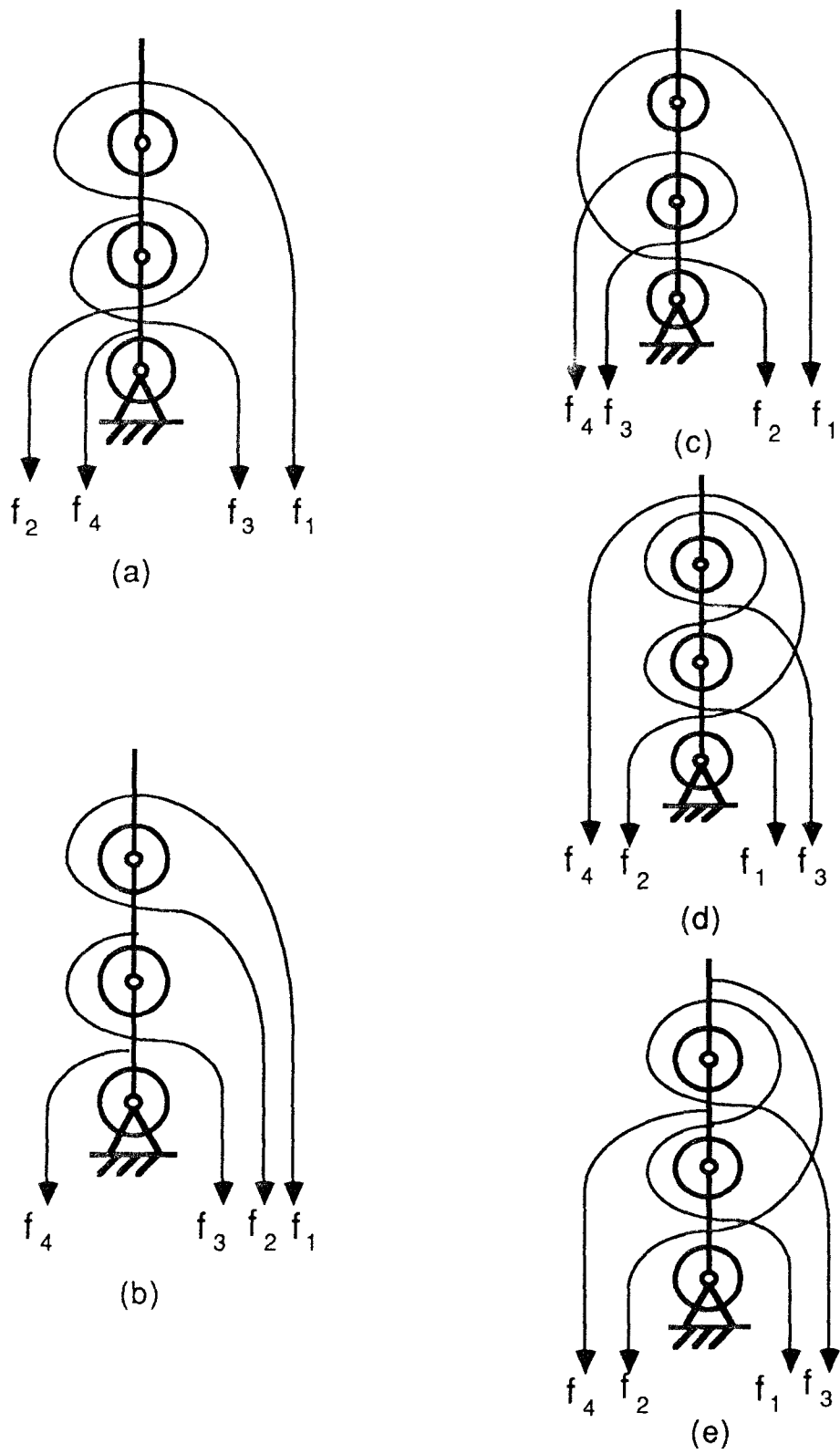


Fig. 4.5 Non-isomorphic kinematic structures having three-DOF

Fig. 4.5	B^T	\underline{f}_h	C	θ^*
(a)	$\begin{bmatrix} -1 & 1 & 0 & 0 \\ -1 & -1 & 1 & 0 \\ -1 & 1 & -1 & 1 \end{bmatrix}$	$\begin{bmatrix} 1 \\ 1 \\ 2 \\ 2 \end{bmatrix}$	2.943	18.43°
(b)	$\begin{bmatrix} -1 & 1 & 0 & 0 \\ -1 & -1 & 1 & 0 \\ -1 & -1 & -1 & 1 \end{bmatrix}$	$\begin{bmatrix} 1 \\ 1 \\ 2 \\ 4 \end{bmatrix}$	1.520	31.48°
(c)	$\begin{bmatrix} -1 & 1 & 0 & 0 \\ -1 & 1 & -1 & 1 \\ -1 & -1 & 1 & 1 \end{bmatrix}$	$\begin{bmatrix} 1 \\ 1 \\ 1 \\ 1 \end{bmatrix}$	2.618	0
(d)	$\begin{bmatrix} -1 & -1 & 1 & 1 \\ 1 & -1 & -1 & 1 \\ -1 & 1 & -1 & 1 \end{bmatrix}$	$\begin{bmatrix} 1 \\ 1 \\ 1 \\ 1 \end{bmatrix}$	1	0
(e)	$\begin{bmatrix} -1 & -1 & 1 & 0 \\ 1 & -1 & -1 & 1 \\ -1 & 1 & -1 & 1 \end{bmatrix}$	$\begin{bmatrix} 1 \\ 1 \\ 2 \\ 2 \end{bmatrix}$	1.581	18.43°

Table 4.1 List of B^T , \underline{f}_h , C , and θ^*

Fig. 4.5	(a)	(b)	(c)	(d)	(e)
$\begin{bmatrix} \max(f_1) \\ \max(f_2) \\ \max(f_3) \\ \max(f_4) \end{bmatrix}$	$\begin{bmatrix} 1 \\ \sqrt{3/2} \\ \sqrt{2} \\ \sqrt{6} \end{bmatrix}$	$\begin{bmatrix} 1 \\ 1 \\ \sqrt{2} \\ \sqrt{6} \end{bmatrix}$	$\begin{bmatrix} \sqrt{3/2} \\ \sqrt{3/2} \\ \sqrt{2} \\ \sqrt{2} \end{bmatrix}$	$\begin{bmatrix} 1/\sqrt{2} \\ 1/\sqrt{2} \\ 1/\sqrt{2} \\ 1/\sqrt{2} \end{bmatrix}$	$\begin{bmatrix} 1/\sqrt{2} \\ 1/\sqrt{2} \\ \sqrt{3/2} \\ \sqrt{2} \end{bmatrix}$
$\max(f_j)$	f_4	f_4	$f_3 = f_4$	$f_1 = f_2 = f_3 = f_4$	f_4

Table 4.2 A comparison of maximum tendon forces

It can be seen that the structure shown in Fig. 4.5(d) requires the least maximum tendon force, which is two times smaller than that of the structure of Stanford finger shown in Fig. 4.5(c). An additional merit of the structure shown in Fig. 4.5(d) is that it requires equal strength actuators and tendons. This characteristic can simplify the selection and design of the actuating system.

4.7 Summary

The force and velocity transmissions for tendon-driven manipulators have been analyzed. It has been shown that the effect of routing on force/velocity transmission can be characterized by both the condition number and the direction of the homogeneous solution. Isotropic transmission of tendon-driven manipulators has been defined and several three-DOF kinematic structures have

been used to illustrate the concept. In addition, a criterion for differentiating force transmission characteristics has been defined and a procedure for identifying the least maximum-tendon-force has been presented. It is found that the kinematic structure of the three-DOF manipulator shown in Fig. 4.5(d) satisfies the isotropic transmission as well as the least maximum-tendon-force conditions. The results may be of great help for the design of new generation of tendon-driven manipulator systems.

The performance of force transmission can also be affected by the pulley radii of the manipulator. We feel that it is a topic worth further research on the optimization of the pulley radii in a kinematic structure to achieve the optimal performance.

Chapter 5

Control and Simulation

5.1 Introduction

Based on the material developed in Chapters 2 through 4, the control problem of tendon-driven manipulators can now be studied. Although the control of tendon-driven manipulators has been investigated by a few researchers (Salisbury, 1984; Jacobsen, et al. 1989), the problem is still relatively unexplored. It can be further complicated by friction, compliance, and the coupling of the displacements and forces in tendons. In general, the control problem consists of: 1) kinematic and dynamic modelling of the system, and 2) design of control strategies to achieve desired system performance. The objective of this chapter is to study the dynamic characteristics, investigate relevant control issues, and suggest appropriate control strategies for tendon-driven manipulators.

First, a dynamic model for tendon-driven manipulators will be established under the assumption that friction and compliance effects in tendons can be neglected. Following the derivation, a control algorithm based on computed torque method will be described. This algorithm assumes that feedback signals from the sensors at each joint can be used to compute torques required for the motors. Then, an efficient method for transforming joint feedback signals to motor torques will be developed. Finally, based on the developed model, simulation results for the realization of dynamic characteristics of a sample tendon-driven manipulator will be presented.

5.2 Dynamic Modelling

We now proceed to the dynamic modelling of a tendon-driven manipulator. A three-DOF system will be used to demonstrate the concept throughout this chapter. The dynamics of a tendon-driven manipulator can be divided into three parts: 1) dynamics of the open-loop chain, 2) transformation between the joint space and the tendon space, and 3) rotor dynamics.

5.2.1 Dynamics of the Open-Loop Chain

The generalized dynamic equations of motion for an open-loop chain can be obtained using Lagrangian Mechanics. The equations of motion without gravity term for a three-DOF manipulator can be expressed as (Paul, 1981):

$$M(\theta) \ddot{\underline{\theta}} + \underline{h}(\theta, \dot{\theta}) = \underline{\tau} \quad (5.1)$$

where $M(\theta)$ is a 3×3 inertia matrix, $\underline{\theta}$ a 3×1 vector representing the joint angles θ , $\underline{h}(\theta, \dot{\theta})$ a 3×1 vector representing the Centrifugal and Coriolis terms, and $\underline{\tau}$ a joint torque vector for the open-loop chain.

5.2.2 Kinematic Relationship Between Joint Space and Tendon Space

The force and displacement transformations between the joint space and the tendon space have been developed in Section 3.2. They are

$$\underline{\tau} = R^T B^T \underline{F} \quad (5.2a)$$

and

$$\underline{S} = BR\underline{\theta} \quad (5.2b)$$

The definitions of the parameters are given in Section 3.2.

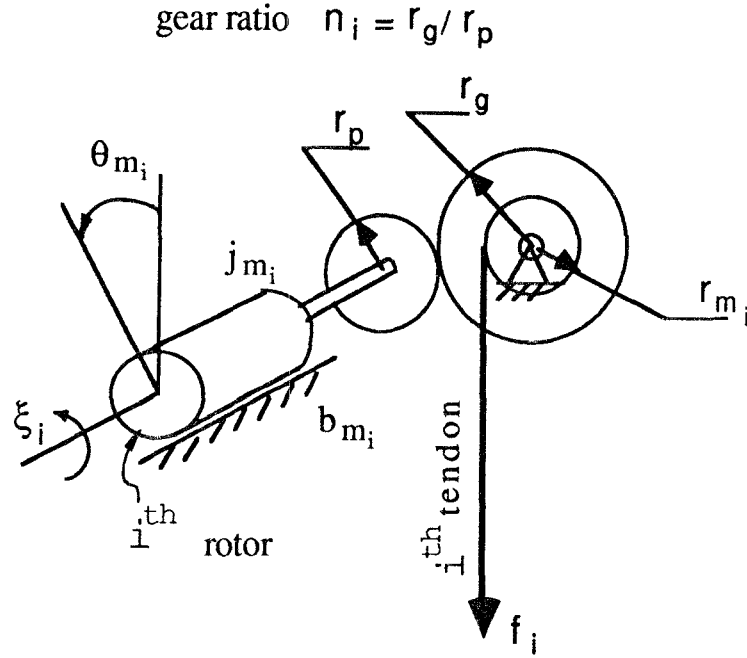


Fig. 5.1 Schematic of the motor-tendon spooling system

5.2.3 Rotor Dynamics

The motor rotor dynamics can be approximated by a second-order system. Consider the i th motor-tendon spooling system as shown in Fig. 5.1. If the i th tendon is wound around the i th pulley of radius r_{m_i} , and the pulley is coupled to a gear reducer having a gear ratio of $n_i = r_g / r_p$ ($n_i \geq 1$), then the torque developed by the i th motor is equal to the sum of the inertia torque, friction torque, and the torque reflected at the motor shaft due to tension in the tendon. Specifically, the equation can be written as

$$j_{m_i} \ddot{\theta}_{m_i} + b_{m_i} \dot{\theta}_{m_i} + \frac{r_{m_i}}{n_i} f_i = \xi_i \quad (5.3a)$$

where j_{m_i} , b_{m_i} , θ_{m_i} , f_i , and ξ_i denote motor rotor inertia, viscous-friction coefficient, motor-rotor angular displacement, tension in the i th tendon, and torque developed by the i th motor, respectively.

Since there are four motors for a three-DOF tendon-driven manipulator, Equation (5.3a) can be written four times, once for each motor. These four dynamic equations can be compiled into a matrix form as:

$$J_m \ddot{\underline{\Theta}}_m + B_m \dot{\underline{\Theta}}_m + R_m \underline{F} = \underline{\xi} \quad (5.3b)$$

where J_m , B_m , and R_m are 4×4 diagonal matrices whose diagonal elements are j_{m_i} , b_{m_i} , and $\frac{r_{m_i}}{n_i}$, respectively; and $\underline{\Theta}_m$ and $\underline{\xi}$ are 4×1 vectors whose elements are the motor-rotor angular displacements and motor torques, respectively.

5.2.4 Overall System Dynamics

The motor-rotor angular displacements can be related to the manipulator joint angles by $R_m \underline{\Theta}_m = BR \underline{\Theta}$. Substituting this relationship into Eq. (5.3b), one can solve tendon forces in terms of motor torques and joint angles as:

$$\underline{F} = R_m^{-1} [\underline{\xi} - J_m R_m^{-1} BR \ddot{\underline{\Theta}} - B_m R_m^{-1} BR \dot{\underline{\Theta}}] \quad (5.4)$$

Substituting Eqs. (5.4) and (5.2a) into (5.1), yields

$$(M + \tilde{M}) \ddot{\underline{\Theta}} + \tilde{B}_m \dot{\underline{\Theta}} + \underline{h}(\underline{\theta}, \dot{\underline{\theta}}) = R^T B^T R_m^{-1} \underline{\xi} \quad (5.5)$$

where $\tilde{M} = R^T B^T R_m^{-1} J_m R_m^{-1} BR$

and $\tilde{B}_m = R^T B^T R_m^{-1} B_m R_m^{-1} BR$.

Equation (5.5) completely describes the dynamics of the tendon-driven manipulator. The term \tilde{M} gives the effect of rotor inertia to the dynamics of the system and the term \tilde{B}_m gives the effect of damping to the system. It should be noted that tendon tensions given by Eq.(5.4) must be positive at all times for the dynamic model to be valid. This will be described in more detail in Section 5.3.

5.3 Computed Torque Controller

The purpose of a controller is to servo the motors so that the end-effector will trace a desired path. In this work, the “computed torque” technique will be implemented for controlling the manipulator. The technique assumes that one can accurately compute the configuration dependent variables, $M(\theta)$, and $\underline{h}(\theta, \dot{\theta})$, in the equations of motion to minimize their nonlinear effect. It uses a proportional plus derivative feedback to servo the motors. Therefore, the proposed control law consists of two terms:

- (i) Compensation of the Centrifugal/Coriolis force and the viscous friction terms:

$$\tilde{B}_m \dot{\underline{\Theta}} + \underline{h}(\theta, \dot{\theta}) \quad (5.6)$$

- (ii) Proportional and derivative feedback terms:

$$(M + \tilde{M})[\ddot{\underline{\Theta}}_d + K_v \dot{\underline{e}} + K_p \underline{e}] \quad (5.7)$$

where K_v and K_p are respectively 3×3 derivative and position feedback gain matrices, $\underline{\Theta}_d$ is the desired joint angular displacement vector, and $\underline{e} \equiv \underline{\Theta}_d - \underline{\Theta}$ is the error vector.

If the structure of the control law contains the above two terms, then the tracking error $\underline{e}(t)$ will approach zero asymptotically. This can be explained as follows. Let the computed torque τ_{cm} be related to the motor torques by

$$\tau_{cm} = R^T B^T R_m^{-1} \underline{\xi} \quad (5.8a)$$

and let the value of τ_{cm} be computed from joint feedback signals as

$$\tau_{cm} = (M + \tilde{M})[\ddot{\underline{\Theta}}_d + K_v \dot{\underline{e}} + K_p \underline{e}] + \tilde{B}_m \dot{\underline{\Theta}} + \underline{h}(\theta, \dot{\theta}) \quad (5.8b)$$

Substituting Eq.(5.8a) and Eq. (5.8b) into (5.5), yields

$$\begin{aligned}
& (M + \tilde{M})\ddot{\underline{\theta}} + \tilde{B}_m\dot{\underline{\theta}} + \underline{h}(\theta, \dot{\theta}) \\
& = R^T B^T R_m^{-1} \underline{\xi} \\
& = (M + \tilde{M})[\ddot{\underline{\theta}}_d + K_v\dot{\underline{e}} + K_p\underline{e}] + \tilde{B}_m\dot{\underline{\theta}} + \underline{h}(\theta, \dot{\theta}) \tag{5.9a}
\end{aligned}$$

After some simplification, Eq. (5.9a) becomes

$$(M + \tilde{M})(\ddot{\underline{e}} + K_v\dot{\underline{e}} + K_p\underline{e}) = 0 \tag{5.9b}$$

Since $(M + \tilde{M})$ is always nonsingular, one can choose K_v and K_p appropriately so that the characteristic roots of Eq. (5.9b) have negative real parts and the tracking error $\underline{e}(t)$ approaches zero asymptotically.

Note that since the vector spaces of $\underline{\tau}_{cm}$ and $\underline{\xi}$ do not have the same dimensions, the mapping between these two spaces is not one to one. Therefore, it is necessary to devise a “torque resolver” to convert the computed torque $\underline{\tau}_{cm}$ to the motor torque $\underline{\xi}$. This will be explained in the following section.

5.4 Torque Resolver

As mentioned in Section 3.2, given desired joint torques, the determination of tendon forces is an indeterminate problem. For an $n \times (n + 1)$ system, the pseudo-inverse technique can be used to solve for tendon forces as shown in Eq. (4.3). In Eq. (4.3), the constant λ must be chosen properly such that all the tendons are under tension. To achieve this, the largest ratio of all the negative tendon forces in the particular solution to their corresponding components in the homogeneous solution must be identified. This process will inevitably increase the computation time and reduce the probability for real time control of the system.

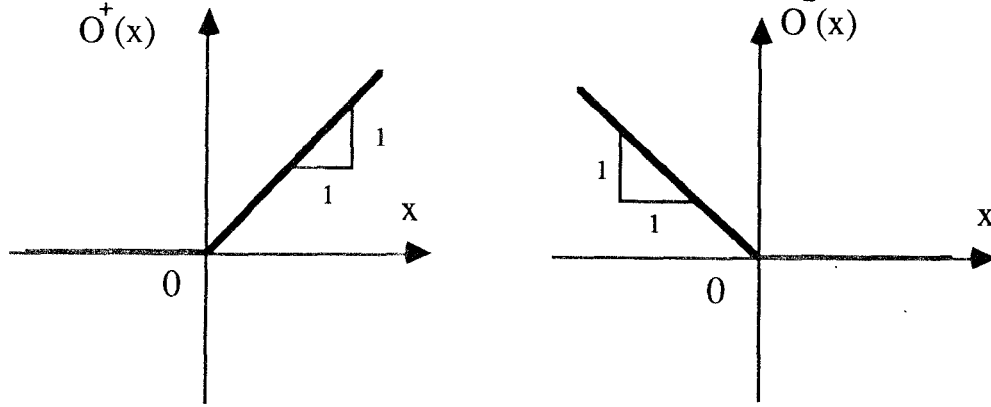


Fig. 5.2 Characteristics of $O^+(x)$ and $O^-(x)$

Another method proposed by Jacobsen et al.(1985, 1989) is to use the “rectifier” concept to determine the appropriate tendon tension. This method, without going through the pseudo-inverse formulation, uses circuit-like operators to convert joint torque signals to tendon tension (or motor torque) signals. It provides a closed-form-like solution to determine the necessary tendon tensions and can be implemented by analog circuits. Nonetheless, the result developed by Jacobsen, et al. is solely applicable to the Utah/MIT hand for which the tendon forces is less coupled than that of the $n \times (n + 1)$ system. In what follows, this method will be refined for the $n \times (n + 1)$ system. It will be shown that this concept can be systematized.

First, let the operators O^+ and O^- be defined as

$$O^+(x) = \begin{cases} x, & x \geq 0; \\ 0, & x < 0 \end{cases} \quad (5.10a)$$

and

$$O^-(x) = \begin{cases} 0, & x \geq 0; \\ -x, & x < 0 \end{cases} \quad (5.10b)$$

where x is a dummy variable. Figure 5.2 shows the characteristics of $O^+(x)$

and $O^-(x)$. From Fig. 5.2, the mathematical forms for $O^+(x)$ and $O^-(x)$ can be written as

$$O^+(x) = [x + |x|]/2 \quad (5.10c)$$

and

$$O^-(x) = [-x + |x|]/2 \quad (5.10d)$$

Note that $O^+(x) + O^-(x) = |x|$, and $O^+(x) - O^-(x) = x$.

For convenience, Equation (5.2a) can be rewritten as

$$B^T \underline{F} = (R^T)^{-1} \underline{\tau} \quad (5.11)$$

The application of operators $O^+(x)$ and $O^-(x)$ to Eq. (5.11) leads to a general approach for the determination of tendon forces without using the pseudo-inverse technique. In general, the system of equations shown in Eq. (5.11) will be reduced to such an extent that every equation contains only two unknown variables. Until then, the solution for the unknown forces can be obtained by applying the operators $O^+(x)$ and $O^-(x)$. The following three examples are designed to illustrate the principle.

Example 1. Structure Matrix in Pseudo-Triangular Form

Take the structure shown in Fig. 5.3(a) (on page 90) for example. The structure matrix B^T is given by

$$B^T = \begin{bmatrix} -1 & 1 & 0 & 0 \\ -1 & -1 & 1 & 0 \\ -1 & -1 & -1 & 1 \end{bmatrix}.$$

The homogeneous solution is given by $[1 \ 1 \ 2 \ 4]^T$. Substituting the structure matrix into Eq. (5.11), yields

$$-f_1 + f_2 = \tau_3/r_3 \quad (5.12a)$$

$$-f_1 - f_2 + f_3 = \tau_2/r_2 \quad (5.12b)$$

$$-f_1 - f_2 - f_3 + f_4 = \tau_1/r_1 \quad (5.12c)$$

In view of the fact that Eq. (5.12a) contains only two unknowns and the condition that f_1 and f_2 must be positive, we conclude that if τ_3 is a positive value, the minimum forces required will be τ_3/r_3 for f_2 and zero for f_1 . On the other hand, if τ_3 is negative, the minimum force will be $-\tau_3/r_3$ for f_1 and zero for f_2 . This can be expressed mathematically as,

$$\begin{cases} f_1 = \delta_1 \\ f_2 = \tau_3/r_3 + \delta_1, \end{cases} \quad \text{if } \tau_3 \geq 0 \quad (5.13a)$$

and

$$\begin{cases} f_1 = -\tau_3/r_3 + \delta_1 \\ f_2 = \delta_1, \end{cases} \quad \text{if } \tau_3 < 0 \quad (5.13b)$$

where δ_1 is a positive biased force which has no effect on the joint torque τ_3 .

Writing Eq. (5.13) in terms of operators O^+ and O^- , yields

$$\begin{cases} f_1 = O^-(\tau_3/r_3) + \delta_1 \\ f_2 = O^+(\tau_3/r_3) + \delta_1 \end{cases} \quad (5.14)$$

The physical meaning of Eq. (5.14) can be readily seen from Fig. 5.3(b). If the torque required in joint 3 is positive (counterclockwise), then tendon f_2 must have a minimum pull of magnitude τ_3/r_3 while f_1 remains zero. On the other hand, if the torque required is negative (clockwise), then tendon f_1 must have a pull of magnitude $-\tau_3/r_3$ while f_2 remains zero. Adding δ_1 to both f_1 and f_2 has no influence on τ_3 .

To determine f_3 , we substitute Eq. (5.14) into Eq. (5.12b) and apply the fact that $O^-(x) + O^+(x) = |x|$. This yields

$$-2\delta_1 + f_3 = \tau_2/r_2 + |\tau_3/r_3| \quad (5.15a)$$

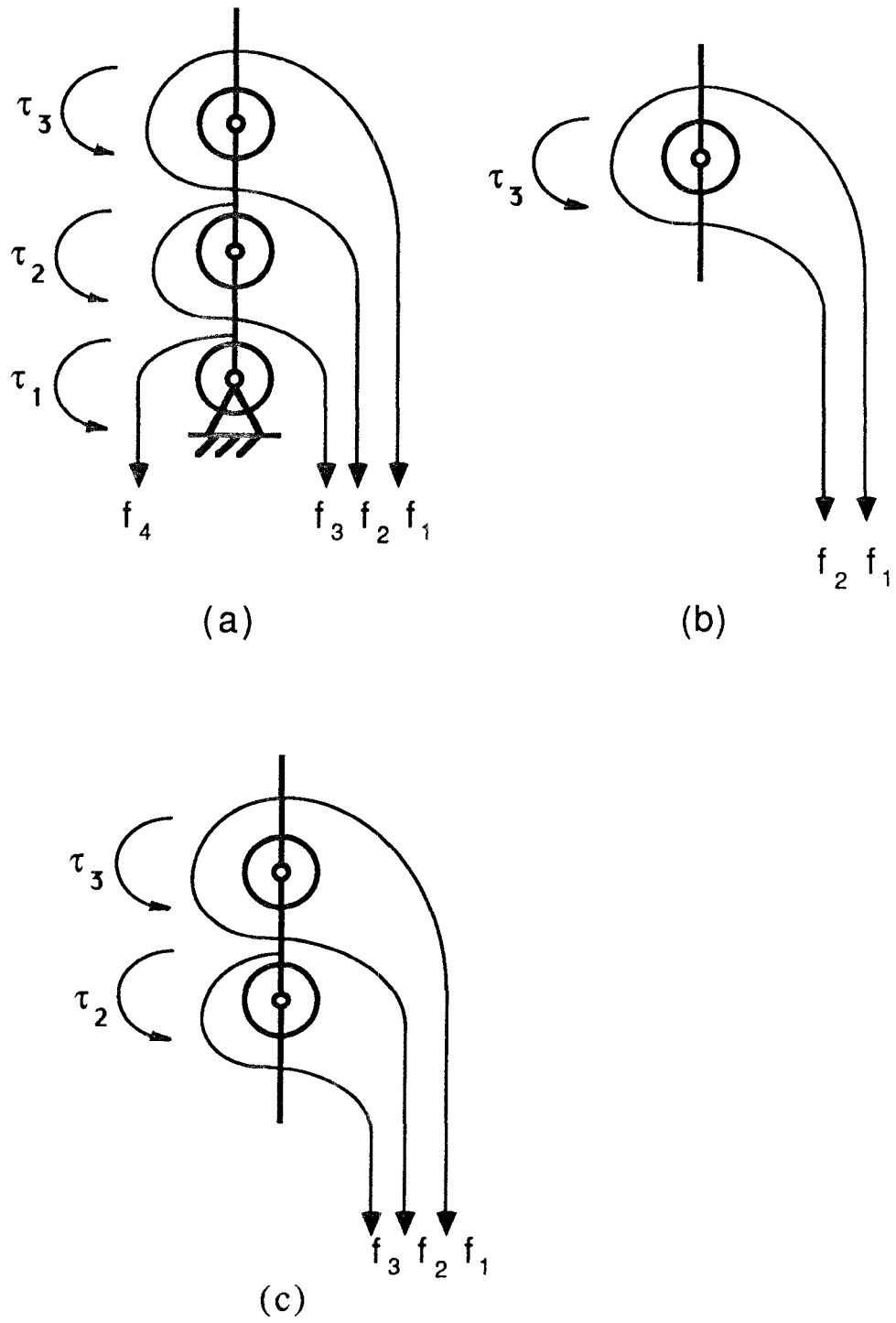


Fig. 5.3 Free-body diagrams of a three-DOF manipulator

Following the same reasoning, one can conclude that if the value of $(\tau_2/r_2 + |\tau_3/r_3|)$ is positive, then the minimum force will be $(\tau_2/r_2 + |\tau_3/r_3|)$ for f_3 and zero for δ_1 . On the other hand, if $(\tau_2/r_2 + |\tau_3/r_3|)$ is negative, then the minimum forces will be zero for f_3 and $(-\tau_2/r_2 - |\tau_3/r_3|)$ for $2\delta_1$. This can be mathematically expressed as:

For $(\tau_2/r_2 + |\tau_3/r_3|) \geq 0$, then

$$\begin{cases} 2\delta_1 = \delta_2 \\ f_3 = \tau_2/r_2 + |\tau_3/r_3| + \delta_2, \end{cases} \quad (5.15b)$$

else

$$\begin{cases} 2\delta_1 = -\tau_2/r_2 - |\tau_3/r_3| + \delta_2 \\ f_3 = \delta_2 \end{cases} \quad (5.15c)$$

where δ_2 is a positive biased force which will result in no net joint torque about joint 2.

Combining Eqs. (5.14), (5.15b), and (5.15c), yields

$$f_1 = O^-(\tau_3/r_3) + O^-(\tau_2/r_2 + |\tau_3/r_3|)/2 + \delta_2/2 \quad (5.16a)$$

$$f_2 = O^+(\tau_3/r_3) + O^-(\tau_2/r_2 + |\tau_3/r_3|)/2 + \delta_2/2 \quad (5.16b)$$

$$f_3 = O^+(\tau_2/r_2 + |\tau_3/r_3|) + \delta_2 \quad (5.16c)$$

The physical meaning of Eqs (5.15) can also be explained from the tendon routing shown in Fig. 5.3(c). Both f_1 and f_2 pull to the right while f_3 pulls to the left of the pulley at joint 2. The two tendons f_1 and f_2 always produce a net force of $|\tau_3/r_3|$. Hence, to generate a desired torque of τ_2 at joint 2, the force difference between f_3 and that from the biased force $2\delta_1$ must be equal to $(\tau_2/r_2 + |\tau_3/r_3|)$. If it is positive, then the minimum forces will be $(\tau_2/r_2 + |\tau_3/r_3|)$ for f_3 and zero for δ_1 . If it is negative, then the minimum forces will be zero for f_3 and one-half of $(\tau_2/r_2 + |\tau_3/r_3|)$ for δ_1 . The biased

force δ_2 is added to adjust torque about the first joint axis. Note that adding $\delta_2/2$, $\delta_2/2$, and δ_2 to f_1 , f_2 , and f_3 , respectively has no effect on the net joint torques τ_3 and τ_2 .

Likewise, substituting Eq. (5.16) into Eq. (5.12c), yields

$$-2\delta_2 + f_4 = \tau_1/r_1 + |\tau_2/r_2 + |\tau_3/r_3|| + |\tau_3/r_3| \quad (5.17a)$$

Following the same reasoning, one concludes that

if $(\tau_1/r_1 + |\tau_2/r_2 + |\tau_3/r_3|| + |\tau_3/r_3|) \geq 0$, then

$$\begin{cases} 2\delta_2 = \delta_3 \\ f_4 = \tau_1/r_1 + |\tau_2/r_2 + |\tau_3/r_3|| + |\tau_3/r_3| + \delta_3, \end{cases} \quad (5.17b)$$

else

$$\begin{cases} 2\delta_2 = -(\tau_1/r_1 + |\tau_2/r_2 + |\tau_3/r_3|| + |\tau_3/r_3|) + \delta_3 \\ f_4 = \delta_3 \end{cases} \quad (5.17c)$$

where δ_3 is a positive biased force.

Combining Eqs. (5.17b,c) and (5.16), yields

$$\begin{cases} f_1 = O^-(\tau_3/r_3) + O^-(\tau_2/r_2 + |\tau_3/r_3|)/2 \\ \quad + O^-(\tau_1/r_1 + |\tau_2/r_2 + |\tau_3/r_3|| + |\tau_3/r_3|)/4 + \delta_3/4 \\ f_2 = O^+(\tau_3/r_3) + O^-(\tau_2/r_2 + |\tau_3/r_3|)/2 \\ \quad + O^-(\tau_1/r_1 + |\tau_2/r_2 + |\tau_3/r_3|| + |\tau_3/r_3|)/4 + \delta_3/4 \\ f_3 = O^+(\tau_2/r_2 + |\tau_3/r_3|) + O^-(\tau_1/r_1 + |\tau_2/r_2 + |\tau_3/r_3|| + |\tau_3/r_3|)/2 + \delta_3/2 \\ f_4 = O^+(\tau_1/r_1 + |\tau_2/r_2 + |\tau_3/r_3|| + |\tau_3/r_3|) + \delta_3 \end{cases} \quad (5.18)$$

Equation (5.18) provides an alternative method for the transformation of joint torques to tendon forces other than the pseudo-inverse formulation. The result guarantees that each tendon force is greater than or equal to zero. It can be seen that the computation is more straight forward than that of the

pseudo-inverse technique. It should be noticed that the biased force δ_3 can be chosen arbitrarily beforehand and its effect on the joint torques is in accordance with that of the homogeneous solution.

Example 2. The Stanford/JPL Finger

The kinematic structure of the Stanford/JPL finger is shown in Fig. 4.5(c) (on page 77) and its corresponding structure matrix is listed in Table 4.1. The homogeneous solution is given by $[1 \ 1 \ 1 \ 1]^T$. Substituting B^T into Eq. (5.11), yields

$$-f_1 + f_2 = \tau_3/r_3 \quad (5.19a)$$

$$-f_1 + f_2 - f_3 + f_4 = \tau_2/r_2 \quad (5.19b)$$

$$-f_1 - f_2 + f_3 + f_4 = \tau_1/r_1 \quad (5.19c)$$

Since Eq. (5.19a) contains only two unknowns, f_1 and f_2 can be written in terms of O^+ and O^- as,

$$\begin{cases} f_1 = O^-(\tau_3/r_3) + \delta_1 \\ f_2 = O^+(\tau_3/r_3) + \delta_1 \end{cases} \quad (5.20)$$

where δ_1 is a positive biased force which has no influence on joint torques τ_2 and τ_3 .

Substituting above equations into Eq. (5.19b), yields

$$-f_3 + f_4 = \tau_2/r_2 - \tau_3/r_3 \quad (5.21)$$

Hence, f_3 and f_4 can be written as

$$\begin{cases} f_3 = O^-(\tau_2/r_2 - \tau_3/r_3) + \delta_2 \\ f_4 = O^+(\tau_2/r_2 - \tau_3/r_3) + \delta_2 \end{cases} \quad (5.22)$$

where δ_2 is a positive biased force which has no influence on torque τ_2 .

Substituting Eqs. (5.20) and (5.22) into (5.19c), yields

$$-2\delta_1 + 2\delta_2 = \tau_1/r_1 + |\tau_3/r_3| - |\tau_2/r_2 - \tau_3/r_3| \quad (5.23)$$

If the value on the right-hand-side of Eq. (5.23) is positive, the minimum value will be equal to that value for $2\delta_2$ and zero for $2\delta_1$. On the other side, if the value is negative, then the minimum value will be zero for $2\delta_2$ and equal to that value for $2\delta_1$. Writing this in terms of the O^+ and O^- operators gives

$$\delta_2 = O^+(\tau_1/r_1 + |\tau_3/r_3| - |\tau_2/r_2 - \tau_3/r_3|)/2 + \delta_3 \quad (5.24a)$$

and

$$\delta_1 = O^-(\tau_1/r_1 + |\tau_3/r_3| - |\tau_2/r_2 - \tau_3/r_3|)/2 + \delta_3 \quad (5.24b)$$

where δ_3 is a positive biased force which has no effect on joint torques τ_1 , τ_2 , and τ_3 .

Substituting Eqs. (5.24b) and (5.24a) into (5.20) and (5.22), respectively, yields

$$\begin{cases} f_1 = O^-(\tau_3/r_3) + O^-(\tau_1/r_1 + |\tau_3/r_3| - |\tau_2/r_2 - \tau_3/r_3|)/2 + \delta_3 \\ f_2 = O^+(\tau_3/r_3) + O^-(\tau_1/r_1 + |\tau_3/r_3| - |\tau_2/r_2 - \tau_3/r_3|)/2 + \delta_3 \\ f_3 = O^-(\tau_2/r_2 - \tau_3/r_3) + O^+(\tau_1/r_1 + |\tau_3/r_3| - |\tau_2/r_2 - \tau_3/r_3|)/2 + \delta_3 \\ f_4 = O^+(\tau_2/r_2 - \tau_3/r_3) + O^+(\tau_1/r_1 + |\tau_3/r_3| - |\tau_2/r_2 - \tau_3/r_3|)/2 + \delta_3 \end{cases} \quad (5.25)$$

Note that the value δ_3 can be used as a pretensioning force for the tendons.

Example 3. Fully Coupled Kinematic Structure

The kinematic structure shown in Fig. 4.5(d) is a fully coupled kinematic structure. The B^T for the structure is given by $\begin{bmatrix} -1 & -1 & 1 & 1 \\ 1 & -1 & -1 & 1 \\ -1 & 1 & -1 & 1 \end{bmatrix}$.

The homogeneous solution is given by $[1 \ 1 \ 1 \ 1]^T$.

Substituting the structure matrix into Eq. (5.11), yields

$$-f_1 - f_2 + f_3 + f_4 = \tau_3/r_3 \quad (5.26a)$$

$$f_1 - f_2 - f_3 + f_4 = \tau_2/r_2 \quad (5.26b)$$

$$-f_1 + f_2 - f_3 + f_4 = \tau_1/r_1 \quad (5.26c)$$

In this case, none of the f_1 , f_2 , f_3 , and f_4 can be determined by using just one of the above equations. Thus, some algebraic manipulations are necessary. Adding Eq. (5.26a) to (5.26b), yields

$$f_4 - f_2 = (\tau_3/r_3 + \tau_2/r_2)/2 \quad (5.27)$$

Therefore, f_2 and f_4 can be written in terms of the operators O^+ and O^- ,

$$\begin{cases} f_2 = O^-(\tau_3/r_3 + \tau_2/r_2)/2 + \delta_1 \\ f_4 = O^+(\tau_3/r_3 + \tau_2/r_2)/2 + \delta_1 \end{cases} \quad (5.28)$$

where δ_1 is a positive biased force which produces no net torques about joints 2 and 3.

Substituting Eq. (5.28) back into (5.26b), yields

$$f_1 - f_3 = (\tau_2/r_2 - \tau_3/r_3)/2 \quad (5.29)$$

Therefore, f_1 and f_3 can be obtained in terms of the operators O^+ and O^- as,

$$\begin{cases} f_1 = O^+(\tau_2/r_2 - \tau_3/r_3)/2 + \delta_2 \\ f_3 = O^-(\tau_2/r_2 - \tau_3/r_3)/2 + \delta_2 \end{cases} \quad (5.30)$$

where δ_2 is a positive biased force which produces no net torque about joints 2 and 3.

Substituting Eqs. (5.28) and (5.30) into (5.26c), yields

$$\begin{aligned} 2\delta_1 - 2\delta_2 &= \tau_1/r_1 + |\tau_2/r_2 - \tau_3/r_3|/2 - |\tau_3/r_3 + \tau_2/r_2|/2 \\ &= b \end{aligned} \quad (5.31)$$

Hence, $\delta_1 = O^+(b)/2 + \delta_3$ and $\delta_2 = O^-(b)/2 + \delta_3$, where δ_3 is a biased force which has no effect on joint torques τ_1 , τ_2 , and τ_3 . Substituting δ_1 and δ_2 into Eqs. (5.28) and (5.30), yields

$$\begin{cases} f_1 = O^+(\tau_2/r_2 - \tau_3/r_3)/2 + O^-(b)/2 + \delta_3 \\ f_2 = O^-(\tau_3/r_3 + \tau_2/r_2)/2 + O^+(b)/2 + \delta_3 \\ f_3 = O^-(\tau_2/r_2 - \tau_3/r_3)/2 + O^-(b)/2 + \delta_3 \\ f_4 = O^+(\tau_3/r_3 + \tau_2/r_2)/2 + O^+(b)/2 + \delta_3 \end{cases} \quad (5.32)$$

It can be seen that the above procedure is general and can be applied to any kind of $n \times (n + 1)$ systems.

5.5 Implementation and Simulation Results

In this section the simulation results of a three-DOF tendon-driven manipulator using the control algorithm developed in Sections 5.2 and 5.3 are presented. The kinematic structure shown in Fig. 4.5(d) is used for illustration. Figure 5.4 shows the control block diagram for the system. The detailed dimensions of the manipulator used for the simulation are given in the Appendix B.

5.5.1 Controller and Torque Resolver Design

The controller is designed according to Eq. (5.8b). Figure 5.5(a) (on page 98) shows the detailed diagram of the controller shown in Fig. 5.4, where k_{p_i} , k_{v_i} , and m_{ij} are the elements of matrices K_p , K_v , and $(M + \tilde{M})$, respectively.

As mentioned in Section 5.2, it is necessary to keep tendon forces positive at all times in order for the dynamic simulation to be valid. The following heuristic has been implemented to assure positive tendon force. In view of Eq. 5.4, to compensate for the uncertainty due to motor inertia torques and viscous

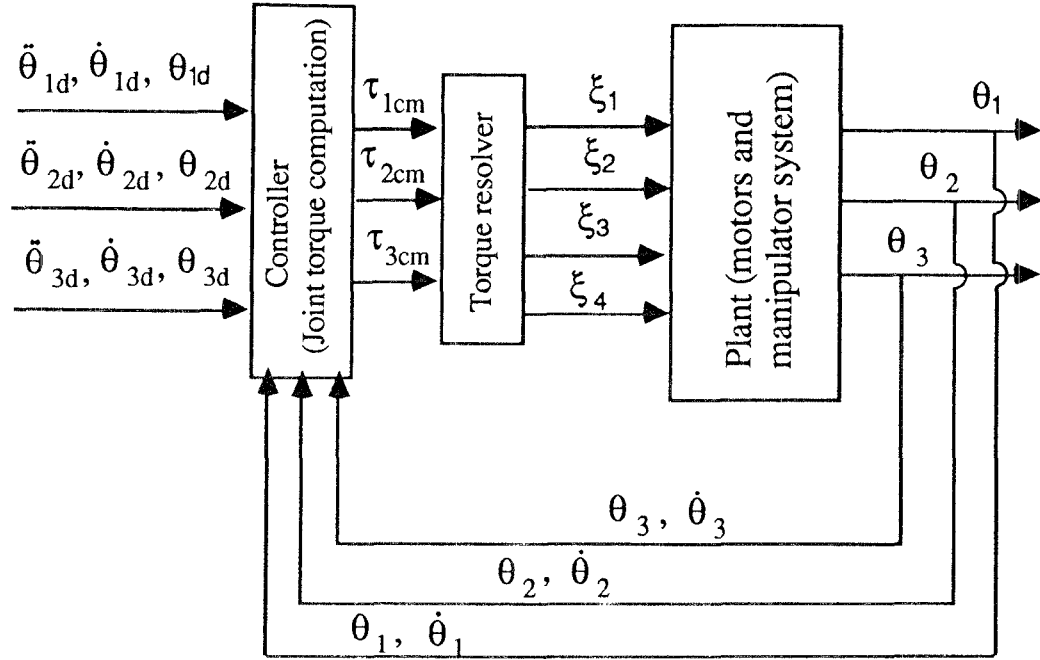


Fig. 5.4 Control block diagram of a three-DOF tendon-driven manipulator

friction torques, the computed joint torques are first rectified through a “torque resolver”, then the maximum desirable manipulator acceleration and velocity, $\ddot{\theta}_m$ and $\dot{\theta}_m$, are used to estimate additional motor torques, $J_m(\ddot{\theta}_m)_{max}$ and $B_m(\dot{\theta}_m)_{max}$, needed for pretensioning the tendons. These added values can be thought as the biased force δ_3 shown in Eq. (5.32). Derived from Eq. (5.32), Figure 5.5(b) (on page 99) shows the detailed design of the resolver shown in Fig. 5.4. It can be seen that the transformation from joint signals to motor signals has been replaced by a circuit-like procedure which can be easily programmed on a digital computer or implemented into an analog circuit.

5.5.2 Feedback Gains Design

The performance of a nonlinear system can be realized or compared if uniform criteria are used for the design of feedback system. That is, the gain

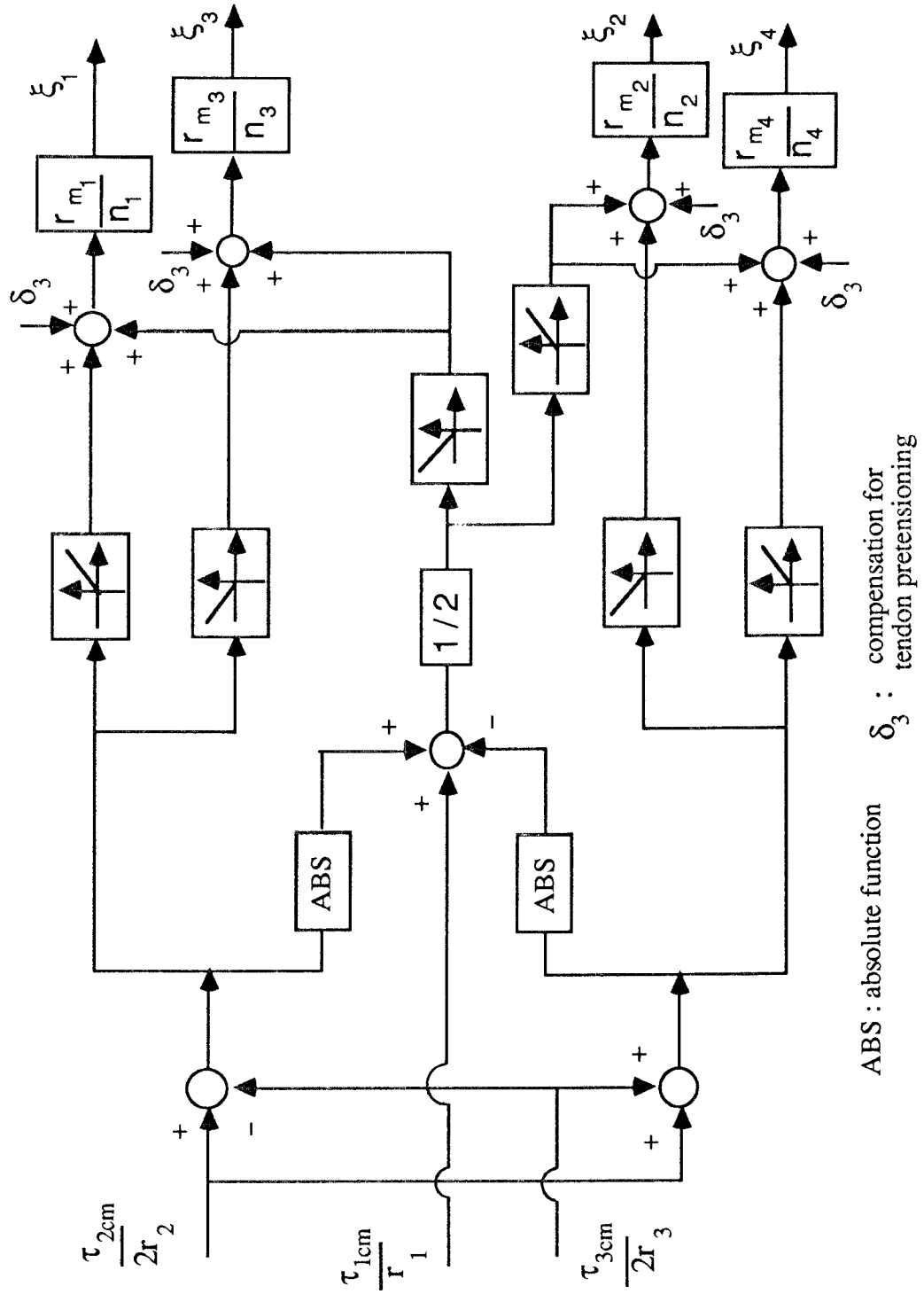


Fig. 5.5(b) Design details of the torque resolver shown in Fig. 5.4

matrices are chosen to satisfy a specified output response criterion. To do this, first the influence of feedback gains K_p and K_v on the positional response of the system is investigated. Figure 5.6 shows the response of joint angle 3 to the simultaneous execution of step inputs to all the three joints for various damping ratios. The initial conditions for the simulations are given as $\theta_i = 0$ and $\dot{\theta}_i = 0$, ($i=1,2,3$) and the step function for each joint is applied at $t=0.1$ sec and has a step value of 0.2618 radian. Three sets of gain values are chosen for comparison, they are $(K_p, K_v)=(225, 23)$, $(225, 30)$, and $(225, 35)$, respectively. The system is underdamped for the value $(K_p, K_v)=(225, 23)$; overdamped for the value of $(225, 35)$; and critically damped for the value of $(225, 30)$. Since critical damping yields better system response, in what follows the gain matrices will be chosen such that the system is critically damped, i.e.,

$$k_{v_i} = 2\sqrt{k_{p_i}}, \quad i = 1, 2, 3 \quad (5.33)$$

In practice, one method for improving the response time is to increase the gains k_{p_i} and k_{v_i} . However, increasing the gains also increases torque requirement on motors, hence resulting in an unstable situation. Figure 5.7 shows the response of the system to simultaneous step inputs of three joints for two different gain values. Both gains are chosen to satisfy the critically damped condition. It can be seen that the higher the gains are, the stiffer the system is. The demand of motor torques for these two gain values are plotted in Fig. 5.8(a) and (b) (on page 103), respectively. To achieve high system response and stability, the gain value $(225, 30)$ which demands about one third of the available motor torque will be used for the following studies. Note that a biased motor torque of 2045 dyne-cm has been added to all motors in order to obtain proper pretension of the tendons. The velocity and acceleration responses of the

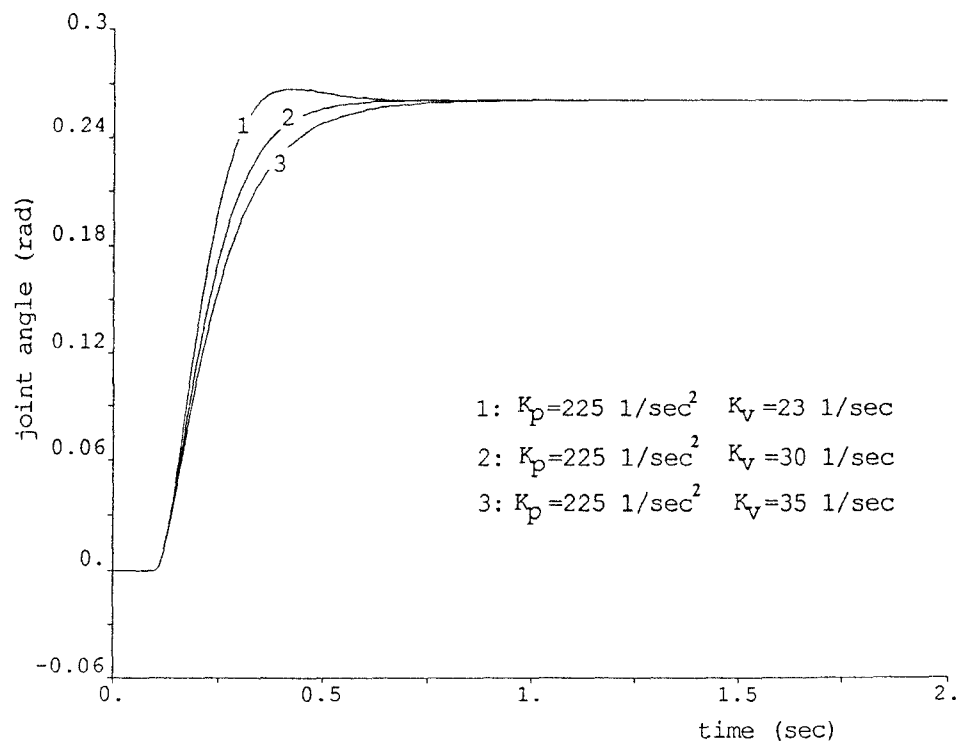


Fig. 5.6 Joint angle response vs. various damping ratios

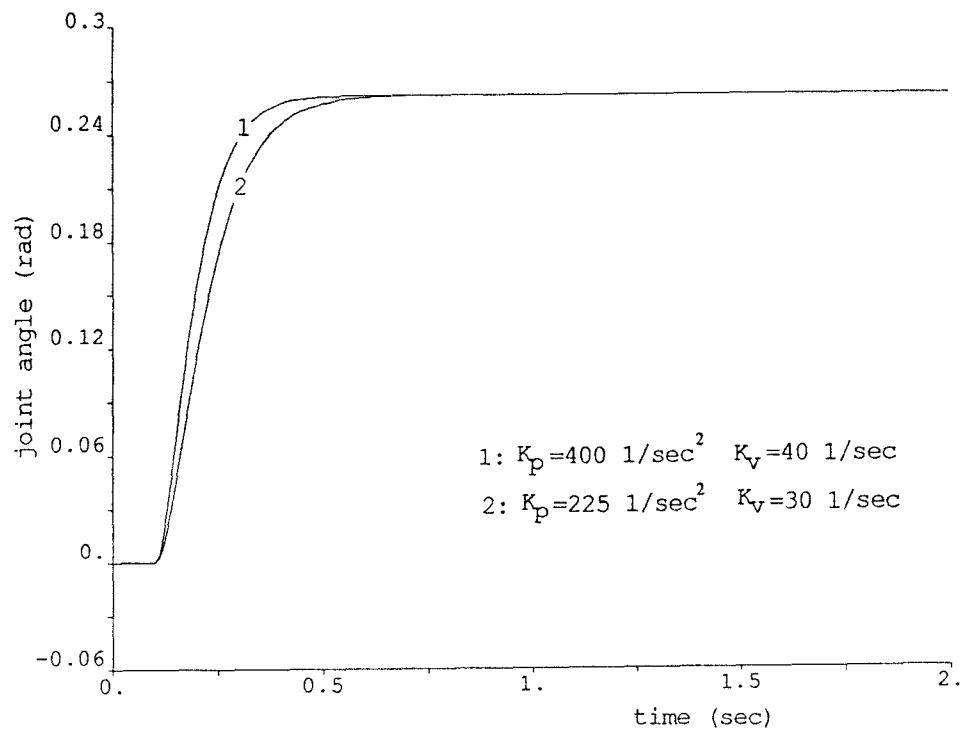


Fig. 5.7 The effect of feedback gain on system stiffness

motors are also shown in Figs. 5.9 and 5.10 (on page 104), respectively. Note that the negative velocities of motors 1, 2, and 3 shown in Fig. 5.9 denote that the motors are under “back driving” condition, i.e., the direction of rotation is in the opposite direction of the motor torque applied.

5.5.3 Motor Inertia and Viscous Friction Effects on Tendon Force

Figures 5.11 and 5.12 (on page 106) show the response of tendon forces for two different gains. In Fig. 5.11, the gain is (225, 30) and the lowest tendon tension occurs at the point B where the force magnitude is 1.67×10^4 dyne (45.5 % below the pretensioning force). On the other hand, in Fig. 5.12, the gain is (400, 40) and the point B has dropped to a value of 1.22×10^4 dyne (60.2 % below the pretensioning force). This is due to the effect of motor inertia and viscous friction. Figures 5.13 and 5.14 (on page 107) respectively show motor torque and tendon force responses without considering the motor inertias and viscous frictions. Comparing the tendon force curves shown in Figs. 5.11 and 5.14, it can be seen that if pretensioning is not well managed, system modelling without considering motor inertia and viscous friction terms may cause slackness in tendons and result in errors. It should also be noted that the magnitude of pretension may play an important role in the dynamic response of tendon-driven manipulators.

5.5.4 Maximum Motor Torque

To compare the motor torque requirement among different kinematic structures, motor torque response for various combinations of simultaneous step inputs to a kinematic structure has been investigated. A step input can be applied either in the positive or negative direction of a joint. For a three-jointed ma-

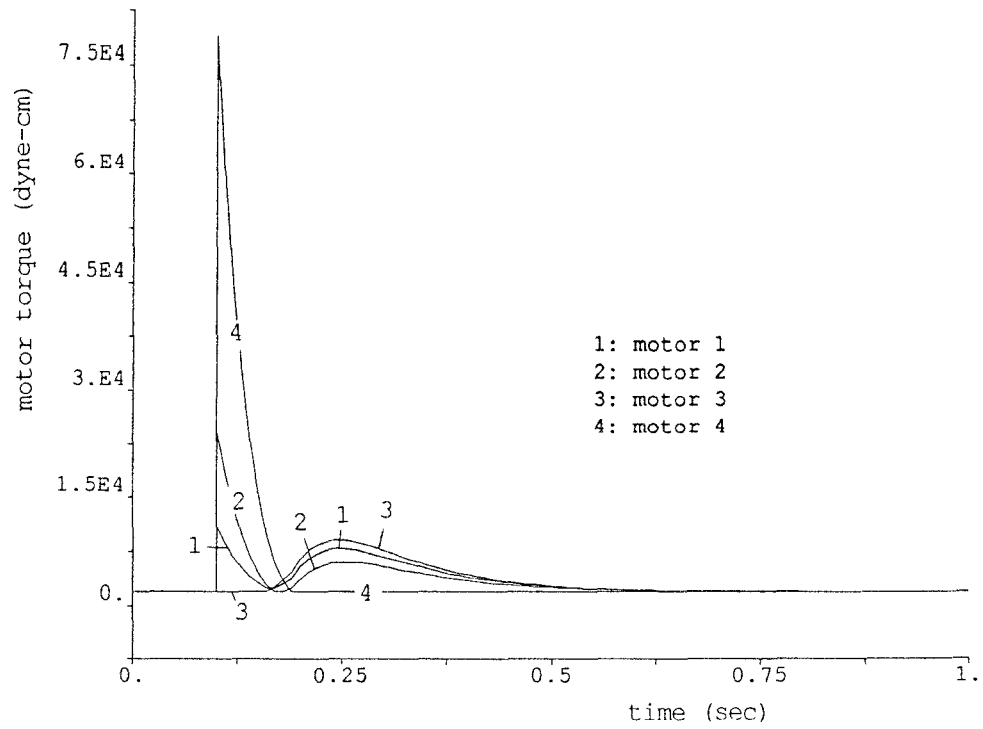


Fig. 5.8(a) Motor torque response with $K_p=225$ and $K_v=30$, peak value= 7.64×10^4 dyne - cm

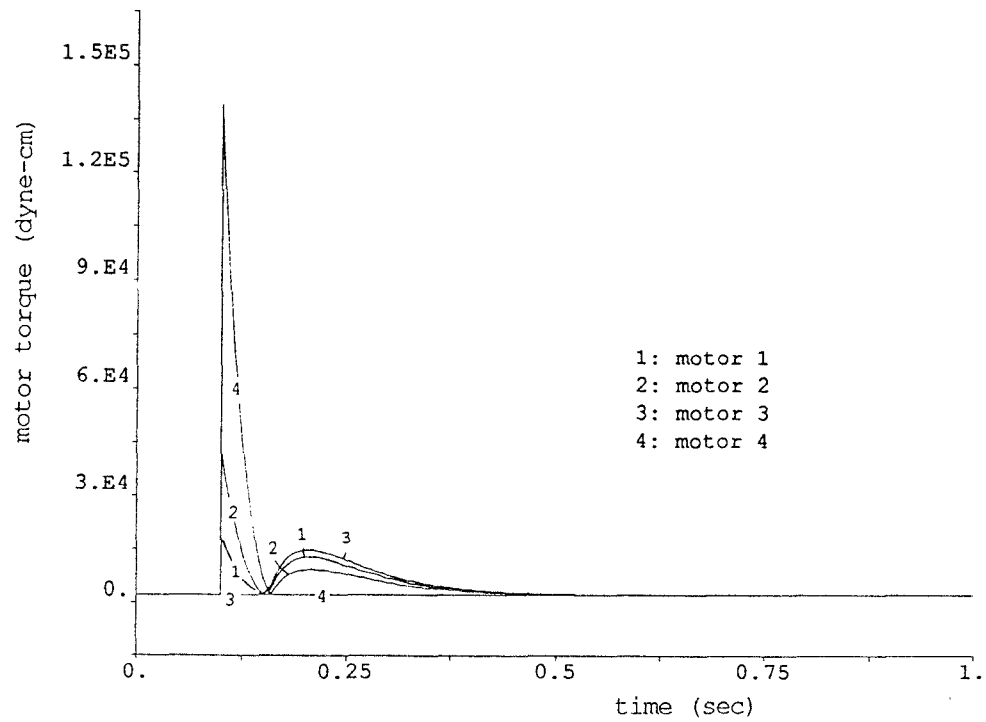


Fig. 5.8(b) Motor torque response with $K_p=400$ and $K_v=40$, peak value= 1.34×10^5 dyne - cm

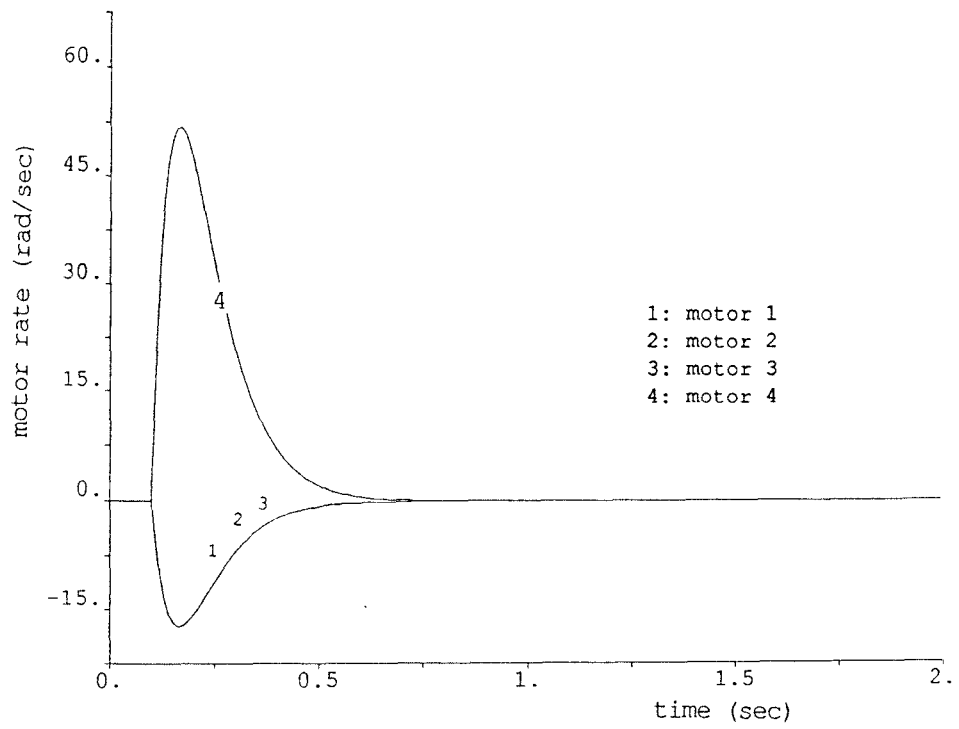


Fig. 5.9 Motor rates with $K_p=225$ and $K_v=30$

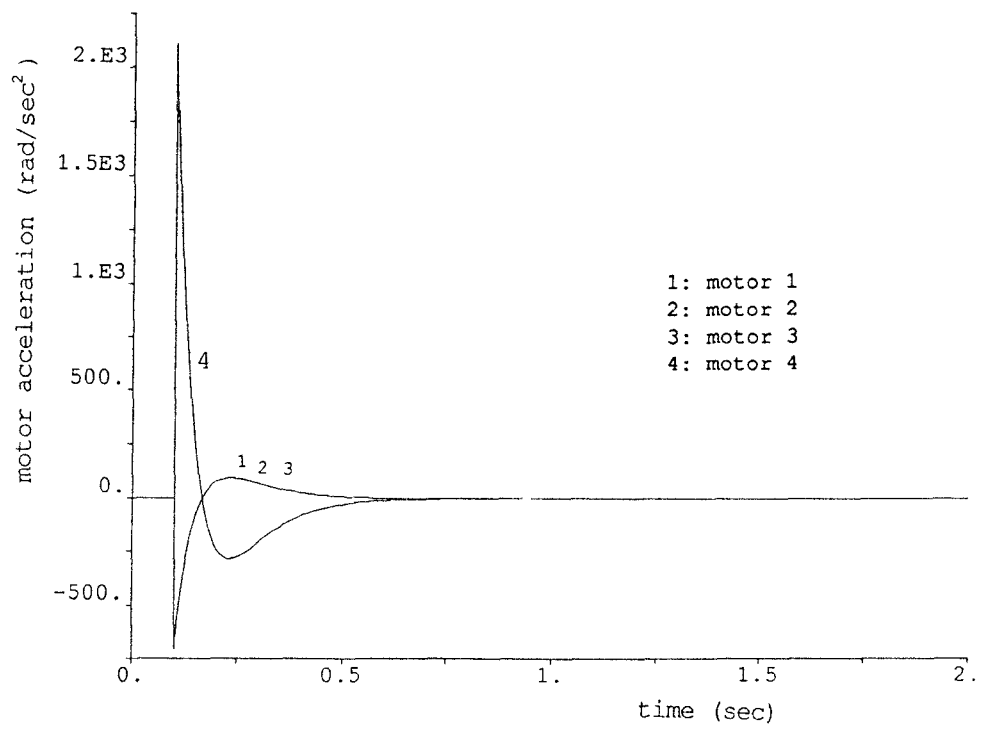


Fig. 5.10 Motor accelerations with $K_p=225$ and $K_v=30$

nipulator, there are eight combinations of step inputs that can be applied to each kinematic structure. Due to directional sensitivity in the manipulator, all the combinations of the simultaneous step inputs are executed and the worst condition which requires maximum motor torque for each kinematic structure is recorded. For the kinematic structures shown in Fig. 4.5(a,b,c, and d), the maximum motor torque occurs at the step input of $\theta_{1d} = \theta_{2d} = \theta_{3d} = 0.2618$ radian, while the maximum motor torque for the structure shown in Fig. 4.5(e) occurs at the step input of $\theta_{1d} = \theta_{3d} = 0.2618$ radian and $\theta_{2d} = -0.2618$ radian. Figures 5.15 through 5.18 (on page 108,109) show the simulation results. It can be observed that for the kinematic structure as shown in Fig. 4.5(d), the peak motor torque as shown in Fig. 5.8(a) has the least value among all the kinematic structures.

5.6 Summary

The formulation of the dynamic equations of motion and the control algorithm for a general class of tendon-driven manipulators have been developed. The computed torque method has been used to illustrate the principle of the control algorithm and a technique for transforming joint-torque signals to motor-torque signals has been developed. The integral of the control method in the simulation is demonstrated through a three-DOF tendon-driven manipulator. Several system characteristics have been investigated through the simulation. It is hoped that this study will lead to a better understanding of tendon-driven manipulators.

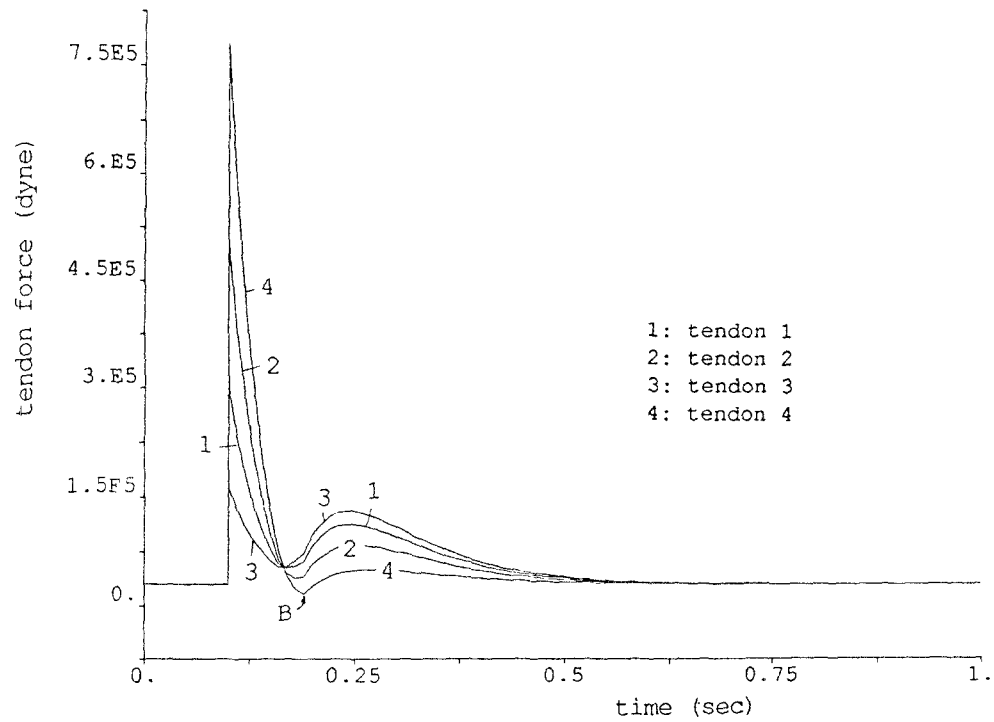


Fig. 5.11 Tendon force response with $K_p=225$ and $K_v=30$, $B=1.67 \times 10^4$ dyne

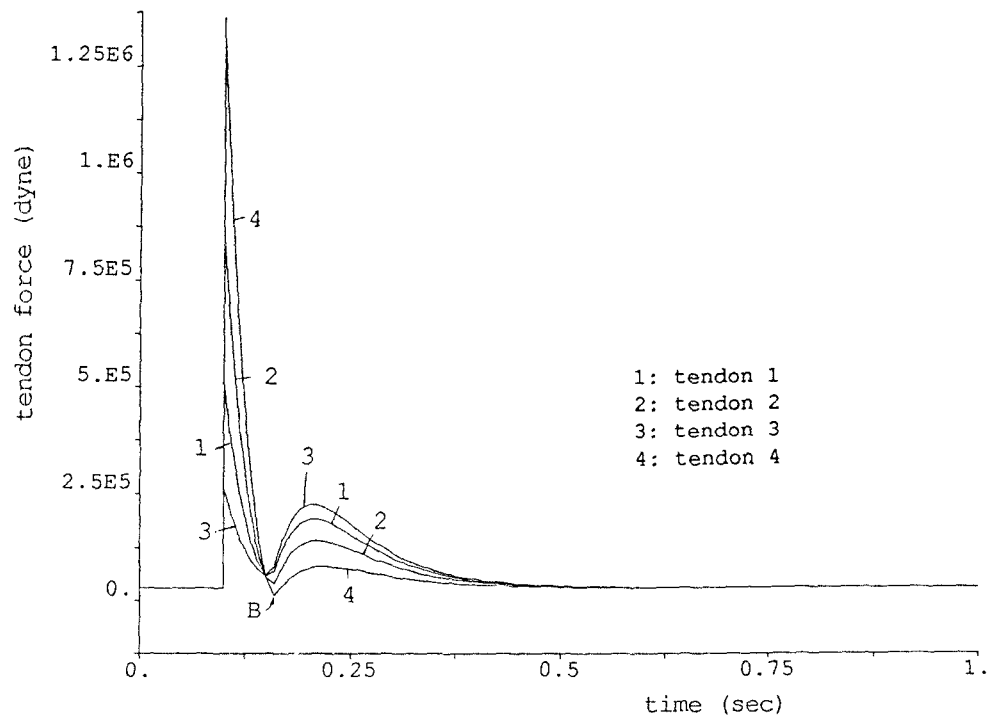


Fig. 5.12 Tendon force response with $K_p=400$ and $K_v=40$, $B=1.22 \times 10^4$ dyne

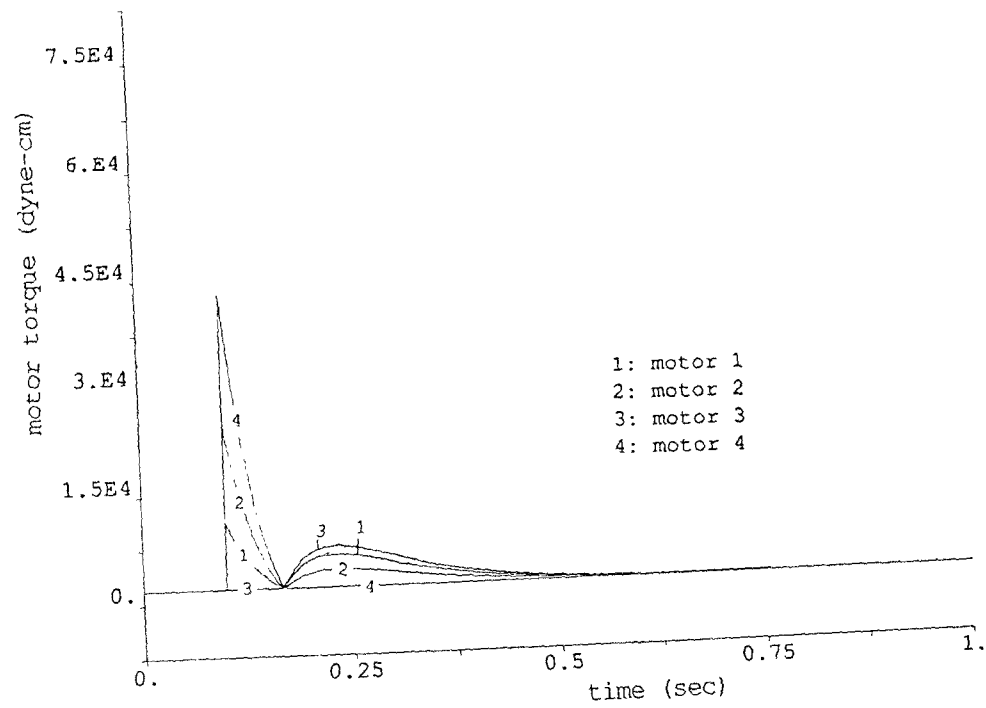


Fig. 5.13 Motor torque response without considering motor inertia and viscous friction ($K_p=225$ and $K_v=30$)

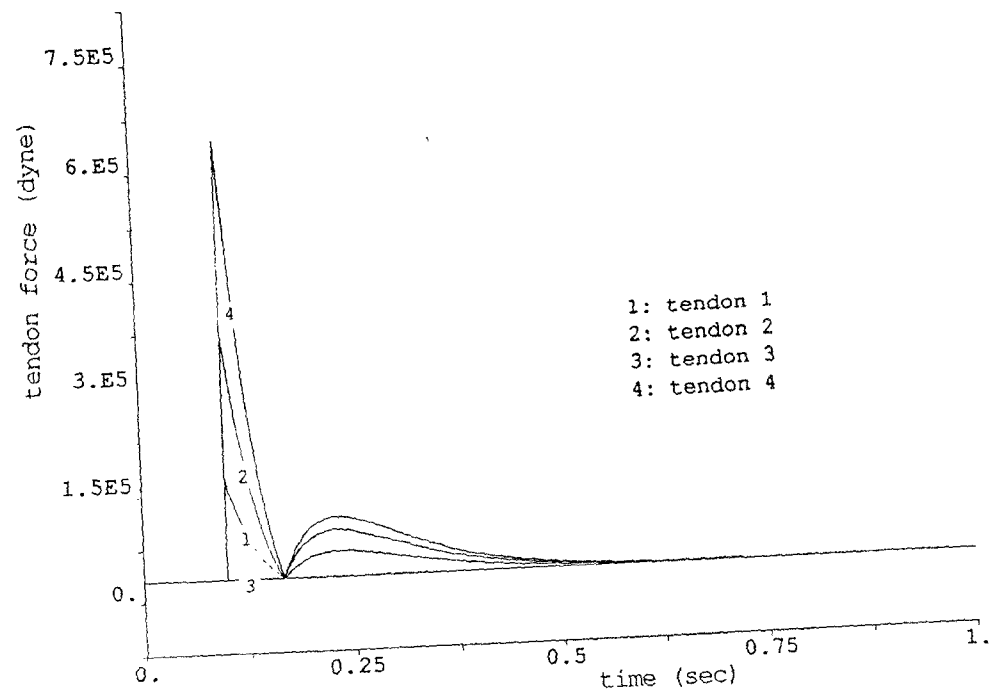


Fig. 5.14 Tendon force response without considering motor inertia and viscous friction ($K_p=225$ and $K_v=30$)

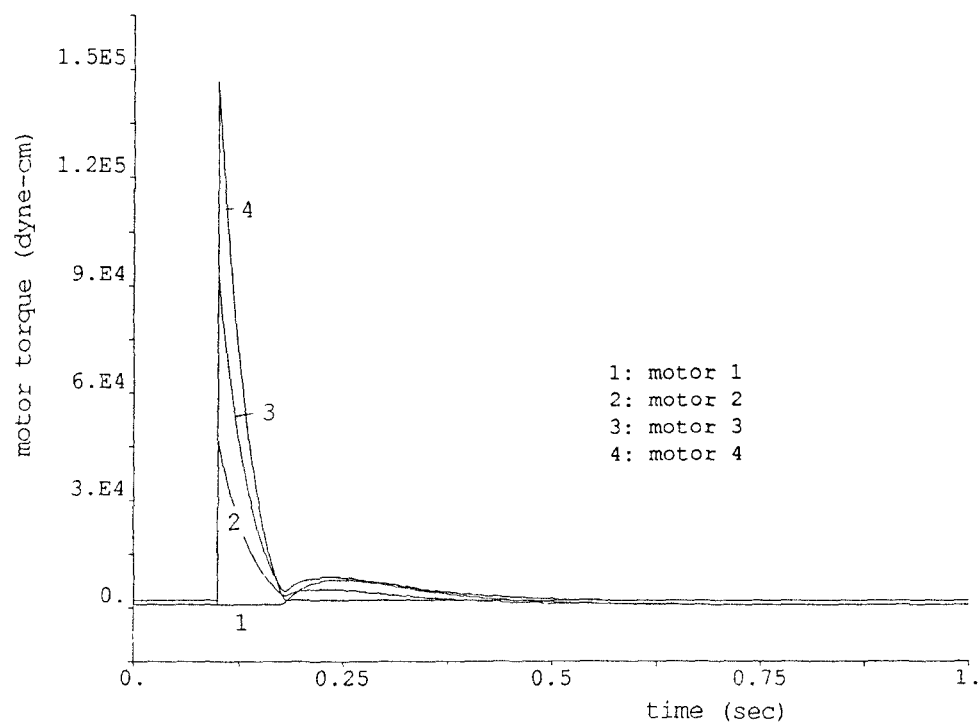


Fig. 5.15 Motor torque response for the structure shown in Fig. 4.5(a), peak value= 1.47×10^5 dyne - cm

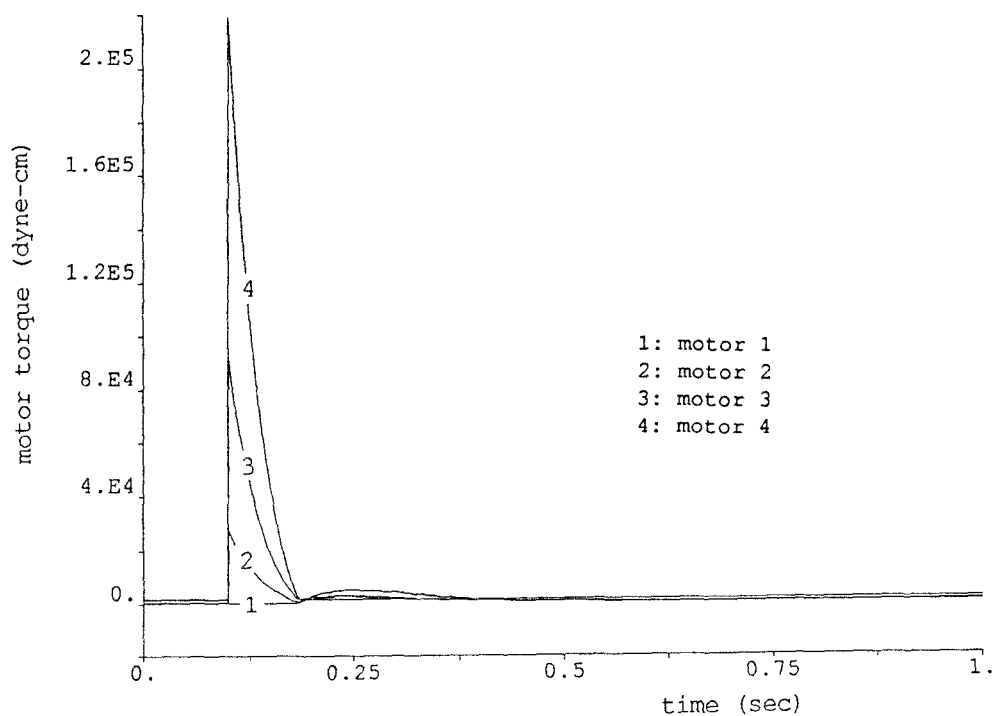


Fig. 5.16 Motor torque response for the structure shown in Fig. 4.5(b), peak value= 2.19×10^5 dyne - cm

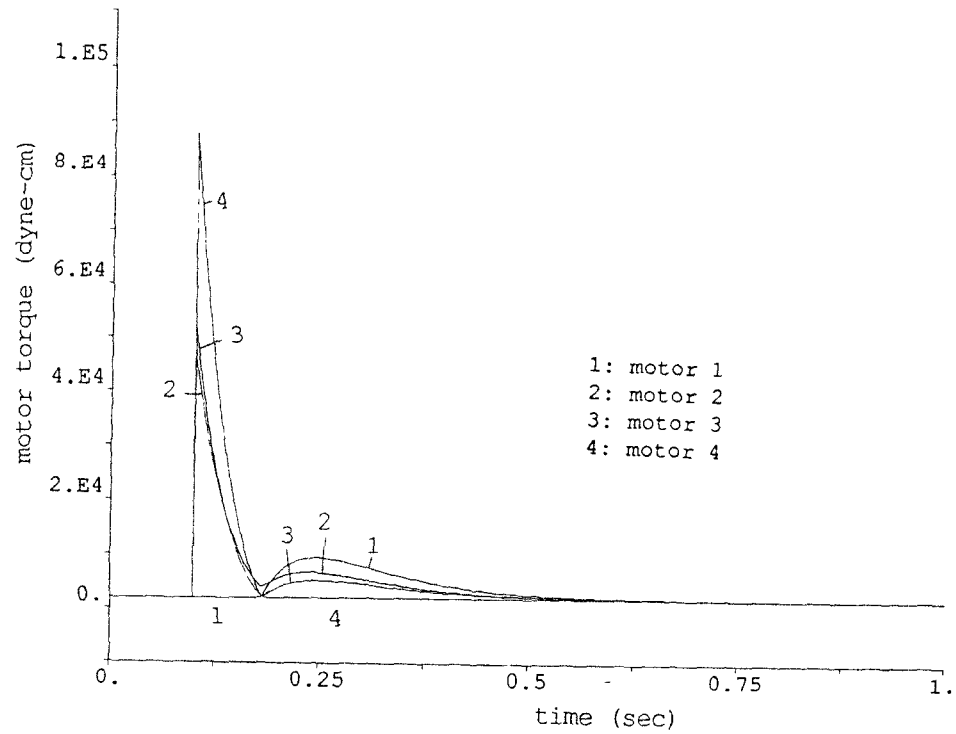


Fig. 5.17 Motor torque response for the structure shown in Fig. 4.5(c), peak value= 8.88×10^4 dyne - cm

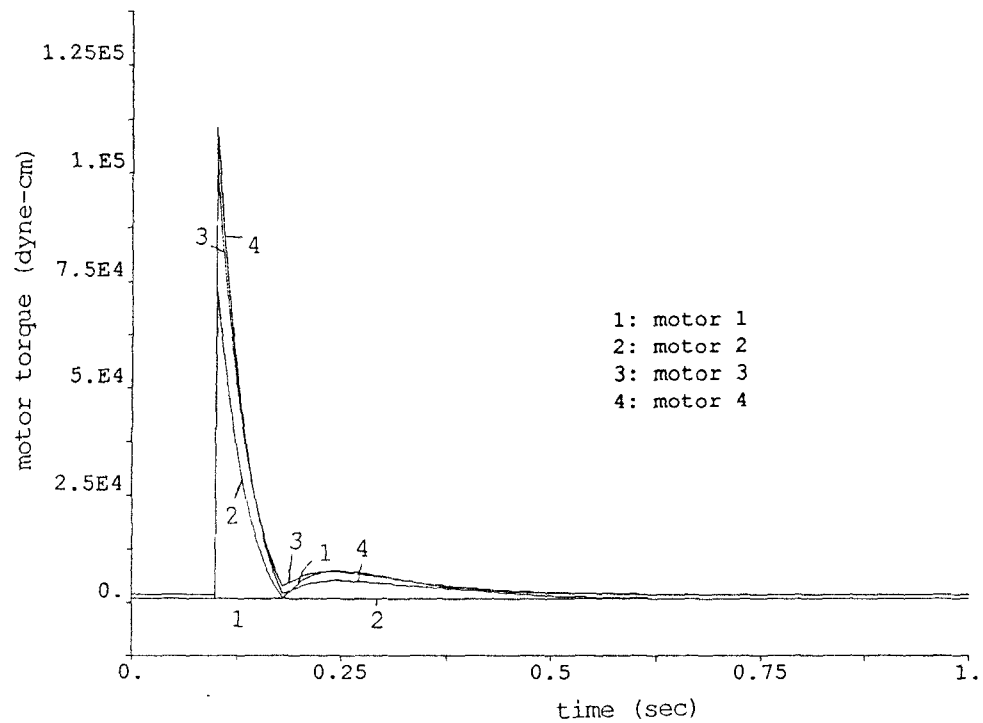


Fig. 5.18 Motor torque response for the structure shown in Fig. 4.5(e), peak value= 1.11×10^5 dyne - cm

Chapter 6

Summary and Conclusions

6.1 Review

This research has addressed four aspects of tendon-driven manipulators: 1) kinematic analysis, 2) structural synthesis, 3) transmission assessment, and 4) control issues.

In Chapter 2 a systematic methodology for the kinematic analysis of tendon-driven manipulators was presented. Using graph representation, it has been shown that the kinematic structure of tendon-driven mechanisms is similar to that of epicyclic gear trains. Thus, the graph theory established for the kinematic analysis of epicyclic gear trains can be applied to this type of mechanism. It has also been shown that the relationship between joint angular displacement and tendon linear displacement can be easily obtained by an inspection of the kinematic structure without going through the graph representation.

In Chapter 3 the topological structure of a tendon-driven manipulator was separated from its functional consideration by using a structure matrix representation. The characteristics of the structure matrix were investigated and a criterion for identifying structure isomorphism was established. Applying these structure characteristics, a methodology was developed for the enumeration of tendon-driven manipulators having pseudo-triangular structure matrix. All the admissible structure matrices with up to six-DOF were enumerated.

In Chapter 4 the effect of tendon routing on kinematic and static force

transmission associated with tendon-driven manipulators was investigated. The transmission characteristics can be described by the velocity and/or force ellipsoid. It has been shown that the effect of tendon routing can be characterized by a condition number and the direction of a homogeneous solution. The condition number is defined as the ratio of the maximum to the minimum singular value of the structure matrix and the homogeneous solution is the set of tendon forces that results in no net joint torques. A methodology for calculating maximum tension in a tendon-driven manipulator was developed. It has also been shown that among the various tendon routings in three-DOF manipulators, the routing with an isotropic transmission ellipsoid possesses least maximum-tendon-force.

In Chapter 5 the dynamic equation of a model of $n \times (n+1)$ class of tendon-driven manipulators was formulated. A control algorithm based on the computed torqued method of such a model was developed and a technique for transforming joint feedback signals to motor torque signals was established. This technique uses a circuit-like form to serve as the transformation between two different vector spaces and can be implemented into an analog-circuit system to simplify the calculation. The integral of the control algorithm in the simulation was demonstrated by a three-DOF tendon-driven manipulator. Through the results of simulation, several dynamic characteristics of the system were identified .

We believe that the contributions of this dissertation are the development of a:

- 1) Systematic procedure for the kinematic analysis of tendon-driven manipulators,
- 2) Methodology for the structural synthesis of tendon-driven manipulators,

3) Method for assessing the transmission quality of tendon-driven manipulators, and

4) Model of a control algorithm governing the manipulation and force control of this type of manipulator.

6.2 Suggestions for Future Research

We suggest the following research directions to extend our understanding of tendon-driven manipulators:

- Research on the structures with combinations of rigid-elastic assemblies. These may include rigid-link assemblies and elastic transmission elements, such as belts, springs, and bellows, and so on.

- a systematic methodology for deriving the kinematic equations of such structures,

- generation of the varieties of kinematic structures with combined rigid/flexible elements,

- performance assessment, and

- the dynamic characteristics of such rigid-elastic combined models.

References

Asada, H., and Cro Granito, J. A., 1985, "Kinematic and Static Characterization of Wrist Joints and Their Optimal Design," IEEE Proceedings of Int'l Conference on Robotics and Automation, pp. 244-250.

Åström, K. J., 1985, *A SIMNON Tutorial*, Report of Dept. of Automatic Control, Lund Institute of Technology, Lund, Sweden.

Buchsbaum, F., and Freudenstein, F., 1970, "Synthesis of Kinematic Structure of Geared Kinematic Chains and Other Mechanisms," J. of Mechanisms, Vol. 5, pp. 357-392.

Day, C. P., Akeel, H. A., and Gutkowski, L. J., 1983, "Kinematic Design and Analysis of Coupled Planetary Bevel-Gear Trains," ASME J. of Mechanisms, Transmissions, and Automation in Design, Vol. 105, No. 3, pp. 441-445.

Denavit, J., and Hartenberg, R. S., 1955, "A Kinematic Notation for Lower Pair Mechanisms Based on Matrices," ASME J. of Applied Mechanics, Vol. 77, pp. 215-211.

Faires, V. M., 1959, *Kinematics*, Chp. 13, McGraw-Hill Book Co., New York.

Freudenstein, F., 1971, "An Application of Boolean Algebra to the Motion of Epicyclic Drives," ASME J. of Engineering for Industry, Vol. 93, pp. 176-182.

Freudenstein, F., Longman, R. W., and Chen, C. K., 1984, "Kinematic Analysis of Robotic Bevel-Gear Trains," ASME J. of Mechanisms, Transmissions, and Automation in Design, Vol. 106, No. 3, pp. 371-375.

Freudenstein, F., and Yang, A. T., 1972, "Kinematics and Statics of a Coupled Epicyclic Spur-Gear Train," J. of Mechanisms and Machine Theory, Vol. 7, pp. 263-275.

Ghosal, A., and Roth, B., 1987, "Instantaneous Properties of Multi-Degrees-of-Freedom Motions—Point Trajectories," ASME J. of Mechanisms, Transmissions, and Automation in Design, Vol. 109, No. 1, pp. 107-115.

Gosselin, C., and Angeles J., 1988, "The Optimum Kinematic Design of a Planar Three-Degree-of-Freedom Parallel Manipulator," ASME J. of Mechanisms, Transmissions, and Automation in Design, Vol. 110, No. 1, pp. 35-41.

Jacobsen, S. C., Wood, J. E., Knutti, D. F., and Biggers, K. B., 1985, "The Utah/MIT Dextrous Hand: Work in Progress," The Inte'l Journal of Robotics Research, Vol. 3, No. 4, pp. 21-50.

Jacobsen, S.C., Ko, H., Iversen, E. K., and Davis, C. C., 1989, "Antagonistic Control of a Tendon Driven Manipulator," IEEE Proceedings of Inte'l Conference on Robotics and Automation, pp. 1334-1339.

Leaver, S. O., and McCarthy, J. M., 1987, "The Design of Three Jointed Two-Degree-of-Freedom Robot Fingers," ASME Advances in Design Automation, Volume Two: Robotics, Mechanisms, and Machine System, DE-Vol. 10-2, pp. 127-134, presented at the 1987 ASME Design Technology Conference.

Mason, M.T., and Salisbury, J.K., 1985, *Robot Hands and the Mechanics of Manipulation*, The MIT Press, Cambridge, MA.

Morecki, A., Busko, Z., Gasztold, H., and Jaworek, K., 1980, "Synthesis and Control of the Anthropomorphic Two-Handed Manipulator," Proceedings of the 10th Inte'l Symposium on Industrial Robots, Milan, Italy, pp. 461-474.

Morecki, A., Ekiel, J., and Fidelus, K., 1984, *Cybernetic Systems of Limb Movements in Man, Animals and Robots*, Ellis Horwood Limited, Warszawa, Poland, PWN-Polish Scientific Publishers.

Okada, T., 1977, "On a Versatile Finger System," Proceedings of the 7th Inte'l Symposium on Industrial Robots, Tokyo, Japan, pp. 345-352.

Paul, R. P., 1981, *Robot Manipulator: Mathematics, Programming and Control*, MIT Press, Cambridge, MA.

Pham, D. T., and Heginbotham, W. B., 1986, *Robot Grippers*, IFS (Publications) Ltd., UK., Springer-Verlag.

Rovetta, A., 1977, "On Specific Problems of Design of Multipurpose of Mechanical Hands in Industrial Robots," Proceedings of the 7th Inte'l Symposium on Industrial Robots, Tokyo, Japan, pp. 337-343.

Salisbury, J. K., 1982, "Kinematic and Force Analysis of Articulated Hands," Ph.D. Dissertation, Dept. of Mechanical Engineering, Stanford University, Stanford, CA.

Salisbury, J. K., 1984, "Design And Control of an Articulated Hand," Proceedings of the 1th Inte'l Symposium on Design and Synthesis, Tokyo, Japan.

Salisbury, J. K., and Craig, J. J., 1982, "Articulated Hands: Force Control and Kinematic Issues," The Inte'l J. of Robotics Research, Vol. 1, No. 1, pp. 4-17.

Shigley, J. E., and Mitchell, L. D., 1983, *Mechanical Engineering Design*, 4th ed., Chp. 17, McGraw-Hill Book Co., New York.

Strang, G., 1980, *Linear Algebra and Its Applications*, Academic Press, Inc., Orlando, Florida.

Tsai, L. W., 1987, "An Application of the Linkage Characteristic Polynomial to the Topological Synthesis of Epicyclic Gear Trains," ASME J. of Mechanisms, Transmissions, and Automation in Design, Vol. 109, No. 3, pp. 329-336.

Tsai, L. W., 1988, "The Kinematics of Spatial Robotic Bevel-Gear Trains," IEEE J. of Robotics and Automation, Vol. 4, No. 2, pp. 150-156.

Tsai, L. W., and Lin, C. C., 1989, "The Creation of Non-Fractionated Two-Degree-of-Freedom Epicyclic Gear Trains," ASME J. of Mechanisms, Transmissions, and Automation in Design, Vol. 111, No. 4, pp. 524-529.

Yoshikawa, T., 1985, "Manipulability and Redundancy Control of Robotic Mechanisms," IEEE Proceedings of Inte'l Conference on Robotics and Automation, pp.1004-1009.

systems

$$\begin{array}{ccccccc} -1 & 1 & 0 & 0 & 0 & 0 & 0 \\ -1 & -1 & 1 & 0 & 0 & 0 & 0 \\ -1 & 1 & -1 & 1 & 0 & 0 & 0 \\ 1 & 1 & -1 & -1 & 1 & 0 & 0 \\ 1 & 1 & -1 & -1 & -1 & 1 & 0 \\ 1 & 1 & 1 & -1 & -1 & -1 & 1 \end{array}$$
$$\begin{array}{rrrrrrr} -1 & 1 & 0 & 0 & 0 & 0 & 0 \\ -1 & -1 & 1 & 0 & 0 & 0 & 0 \\ -1 & 1 & -1 & 1 & 0 & 0 & 0 \\ 1 & 1 & -1 & -1 & 1 & 0 & 0 \\ 1 & -1 & -1 & -1 & -1 & 1 & 0 \\ 1 & 1 & 1 & -1 & -1 & -1 & 1 \end{array}$$
$$\begin{array}{rrrrrrr} -1 & 1 & 0 & 0 & 0 & 0 & 0 \\ -1 & -1 & 1 & 0 & 0 & 0 & 0 \\ -1 & 1 & -1 & 1 & 0 & 0 & 0 \\ 1 & 1 & -1 & -1 & 1 & 0 & 0 \\ -1 & -1 & -1 & -1 & -1 & 1 & 0 \\ 1 & -1 & 1 & 1 & -1 & -1 & 1 \end{array}$$

-1 1 0 0 0 0 0
-1 -1 1 0 0 0 0
-1 1 -1 1 0 0 0
1 1 -1 -1 1 0 0
-1 -1 -1 -1 -1 1 0
1 1 1 -1 -1 -1 1
6- 22

-1 1 0 0 0 0 0
-1 -1 1 0 0 0 0
-1 1 -1 1 0 0 0
1 -1 -1 -1 1 0 0
1 1 1 -1 -1 1 0
1 -1 1 -1 -1 -1 1
6- 29

-1 1 0 0 0 0 0
-1 -1 1 0 0 0 0
-1 1 -1 1 0 0 0
1 -1 -1 -1 1 0 0
1 -1 1 -1 -1 1 0
1 -1 1 -1 -1 -1 1
6- 36

-1 1 0 0 0 0 0
-1 -1 1 0 0 0 0
-1 1 -1 1 0 0 0
1 1 -1 -1 1 0 0
-1 -1 -1 -1 -1 1 0
1 -1 1 -1 -1 -1 1
6- 23

-1 1 0 0 0 0 0
-1 -1 1 0 0 0 0
-1 1 -1 1 0 0 0
1 -1 -1 -1 1 0 0
1 1 1 -1 -1 1 0
1 1 -1 -1 -1 -1 1
6- 30

-1 1 0 0 0 0 0
-1 -1 1 0 0 0 0
-1 1 -1 1 0 0 0
1 -1 -1 -1 1 0 0
1 -1 1 -1 -1 1 0
1 1 -1 -1 -1 -1 1
6- 37

-1 1 0 0 0 0 0
-1 -1 1 0 0 0 0
-1 1 -1 1 0 0 0
1 1 -1 -1 1 0 0
-1 -1 -1 -1 -1 1 0
1 1 -1 -1 -1 -1 1
6- 24

-1 1 0 0 0 0 0
-1 -1 1 0 0 0 0
-1 1 -1 1 0 0 0
1 -1 -1 -1 1 0 0
1 1 1 -1 -1 1 0
1 -1 -1 -1 -1 -1 1
6- 31

-1 1 0 0 0 0 0
-1 -1 1 0 0 0 0
-1 1 -1 1 0 0 0
1 -1 -1 -1 1 0 0
1 -1 1 -1 -1 1 0
1 -1 -1 -1 -1 -1 1
6- 38

-1 1 0 0 0 0 0
-1 -1 1 0 0 0 0
-1 1 -1 1 0 0 0
1 1 -1 -1 1 0 0
-1 -1 -1 -1 -1 1 0
1 -1 -1 -1 -1 -1 1
6- 25

-1 1 0 0 0 0 0
-1 -1 1 0 0 0 0
-1 1 -1 1 0 0 0
1 -1 -1 -1 1 0 0
1 1 1 -1 -1 1 0
-1 -1 -1 -1 -1 -1 1
6- 32

-1 1 0 0 0 0 0
-1 -1 1 0 0 0 0
-1 1 -1 1 0 0 0
1 -1 -1 -1 1 0 0
1 -1 1 -1 -1 1 0
-1 -1 -1 -1 -1 -1 1
6- 39

-1 1 0 0 0 0 0
-1 -1 1 0 0 0 0
-1 1 -1 1 0 0 0
1 1 -1 -1 1 0 0
-1 -1 -1 -1 -1 1 0
-1 -1 -1 -1 -1 -1 1
6- 26

-1 1 0 0 0 0 0
-1 -1 1 0 0 0 0
-1 1 -1 1 0 0 0
1 -1 -1 -1 1 0 0
1 -1 1 -1 -1 1 0
1 1 1 1 -1 -1 1
6- 33

-1 1 0 0 0 0 0
-1 -1 1 0 0 0 0
-1 1 -1 1 0 0 0
1 -1 -1 -1 1 0 0
1 1 -1 -1 -1 1 0
1 -1 1 -1 1 -1 1
6- 40

-1 1 0 0 0 0 0
-1 -1 1 0 0 0 0
-1 1 -1 1 0 0 0
1 -1 -1 -1 1 0 0
1 1 1 -1 -1 1 0
1 -1 1 1 -1 -1 1
6- 27

-1 1 0 0 0 0 0
-1 -1 1 0 0 0 0
-1 1 -1 1 0 0 0
1 -1 -1 -1 1 0 0
1 -1 1 -1 -1 1 0
1 -1 1 1 -1 -1 1
6- 34

-1 1 0 0 0 0 0
-1 -1 1 0 0 0 0
-1 1 -1 1 0 0 0
1 -1 -1 -1 1 0 0
1 1 -1 -1 -1 1 0
1 1 1 1 -1 -1 1
6- 41

-1 1 0 0 0 0 0
-1 -1 1 0 0 0 0
-1 1 -1 1 0 0 0
1 -1 -1 -1 1 0 0
1 1 1 -1 -1 1 0
1 1 1 -1 -1 -1 1
6- 28

-1 1 0 0 0 0 0
-1 -1 1 0 0 0 0
-1 1 -1 1 0 0 0
1 -1 -1 -1 1 0 0
1 -1 1 -1 -1 1 0
1 1 1 -1 -1 -1 1
6- 35

-1 1 0 0 0 0 0
-1 -1 1 0 0 0 0
-1 1 -1 1 0 0 0
1 -1 -1 -1 1 0 0
1 1 -1 -1 -1 1 0
1 -1 1 1 -1 -1 1
6- 42

-1 1 0 0 0 0 0
 -1 -1 1 0 0 0 0
 -1 1 -1 1 0 0 0
 1 -1 -1 -1 1 0 0
 1 1 -1 -1 -1 1 0
 1 1 1 -1 -1 -1 1
 6- 43

-1 1 0 0 0 0 0
 -1 -1 1 0 0 0 0
 -1 1 -1 1 0 0 0
 1 -1 -1 -1 1 0 0
 1 -1 -1 -1 -1 1 0
 1 1 1 1 -1 -1 1
 6- 50

-1 1 0 0 0 0 0
 -1 -1 1 0 0 0 0
 -1 1 -1 1 0 0 0
 1 -1 -1 -1 1 0 0
 -1 -1 -1 -1 -1 1 0
 1 -1 1 1 1 -1 1
 6- 57

-1 1 0 0 0 0 0
 -1 -1 1 0 0 0 0
 -1 1 -1 1 0 0 0
 1 -1 -1 -1 1 0 0
 1 1 -1 -1 -1 1 0
 1 -1 1 -1 -1 -1 1
 6- 44

-1 1 0 0 0 0 0
 -1 -1 1 0 0 0 0
 -1 1 -1 1 0 0 0
 1 -1 -1 -1 1 0 0
 1 -1 -1 -1 -1 1 0
 1 -1 1 1 -1 -1 1
 6- 51

-1 1 0 0 0 0 0
 -1 -1 1 0 0 0 0
 -1 1 -1 1 0 0 0
 1 -1 -1 -1 1 0 0
 -1 -1 -1 -1 -1 1 0
 1 1 1 -1 1 -1 1
 6- 58

-1 1 0 0 0 0 0
 -1 -1 1 0 0 0 0
 -1 1 -1 1 0 0 0
 1 -1 -1 -1 1 0 0
 1 1 -1 -1 -1 1 0
 1 1 -1 -1 -1 -1 1
 6- 45

-1 1 0 0 0 0 0
 -1 -1 1 0 0 0 0
 -1 1 -1 1 0 0 0
 1 -1 -1 -1 1 0 0
 1 -1 -1 -1 -1 1 0
 1 1 1 -1 -1 -1 1
 6- 52

-1 1 0 0 0 0 0
 -1 -1 1 0 0 0 0
 -1 1 -1 1 0 0 0
 1 -1 -1 -1 1 0 0
 -1 -1 -1 -1 -1 1 0
 1 -1 1 -1 1 -1 1
 6- 59

-1 1 0 0 0 0 0
 -1 -1 1 0 0 0 0
 -1 1 -1 1 0 0 0
 1 -1 -1 -1 1 0 0
 1 1 -1 -1 -1 1 0
 1 -1 -1 -1 -1 -1 1
 6- 46

-1 1 0 0 0 0 0
 -1 -1 1 0 0 0 0
 -1 1 -1 1 0 0 0
 1 -1 -1 -1 1 0 0
 1 -1 -1 -1 -1 1 0
 1 -1 1 -1 -1 -1 1
 6- 53

-1 1 0 0 0 0 0
 -1 -1 1 0 0 0 0
 -1 1 -1 1 0 0 0
 1 -1 -1 -1 1 0 0
 -1 -1 -1 -1 -1 1 0
 1 1 1 1 -1 -1 1
 6- 60

-1 1 0 0 0 0 0
 -1 -1 1 0 0 0 0
 -1 1 -1 1 0 0 0
 1 -1 -1 -1 1 0 0
 1 1 -1 -1 -1 1 0
 -1 -1 -1 -1 -1 -1 1
 6- 47

-1 1 0 0 0 0 0
 -1 -1 1 0 0 0 0
 -1 1 -1 1 0 0 0
 1 -1 -1 -1 1 0 0
 1 -1 -1 -1 -1 1 0
 1 1 -1 -1 -1 -1 1
 6- 54

-1 1 0 0 0 0 0
 -1 -1 1 0 0 0 0
 -1 1 -1 1 0 0 0
 1 -1 -1 -1 1 0 0
 -1 -1 -1 -1 -1 1 0
 1 -1 1 1 -1 -1 1
 6- 61

-1 1 0 0 0 0 0
 -1 -1 1 0 0 0 0
 -1 1 -1 1 0 0 0
 1 -1 -1 -1 1 0 0
 1 -1 -1 -1 -1 1 0
 1 1 1 -1 1 -1 1
 6- 48

-1 1 0 0 0 0 0
 -1 -1 1 0 0 0 0
 -1 1 -1 1 0 0 0
 1 -1 -1 -1 1 0 0
 1 -1 -1 -1 -1 1 0
 1 -1 -1 -1 -1 -1 1
 6- 55

-1 1 0 0 0 0 0
 -1 -1 1 0 0 0 0
 -1 1 -1 1 0 0 0
 1 -1 -1 -1 1 0 0
 -1 -1 -1 -1 -1 1 0
 1 1 1 -1 -1 -1 1
 6- 62

-1 1 0 0 0 0 0
 -1 -1 1 0 0 0 0
 -1 1 -1 1 0 0 0
 1 -1 -1 -1 1 0 0
 1 -1 1 -1 -1 1 0
 1 -1 1 -1 1 -1 1
 6- 49

-1 1 0 0 0 0 0
 -1 -1 1 0 0 0 0
 -1 1 -1 1 0 0 0
 1 -1 -1 -1 1 0 0
 1 -1 -1 -1 -1 1 0
 -1 -1 -1 -1 -1 -1 1
 6- 56

-1 1 0 0 0 0 0
 -1 -1 1 0 0 0 0
 -1 1 -1 1 0 0 0
 1 -1 -1 -1 1 0 0
 -1 -1 -1 -1 -1 1 0
 1 -1 1 -1 -1 -1 1
 6- 63

-1 1 0 0 0 0 0 -1 -1 1 0 0 0 0 -1 1 -1 1 0 0 0 1 -1 -1 -1 1 0 0 -1 -1 -1 -1 -1 1 0 1 1 -1 -1 -1 -1 1 6- 64	-1 1 0 0 0 0 0 -1 -1 1 0 0 0 0 -1 1 -1 1 0 0 0 -1 -1 -1 -1 1 0 0 1 -1 1 1 -1 1 0 1 1 -1 -1 -1 -1 1 6- 71	-1 1 0 0 0 0 0 -1 -1 1 0 0 0 0 -1 1 -1 1 0 0 0 -1 -1 -1 -1 1 0 0 1 1 1 -1 -1 1 0 1 -1 1 -1 -1 -1 1 6- 78
-1 1 0 0 0 0 0 -1 -1 1 0 0 0 0 -1 1 -1 1 0 0 0 1 -1 -1 -1 1 0 0 -1 -1 -1 -1 -1 1 0 1 -1 -1 -1 -1 -1 1 6- 65	-1 1 0 0 0 0 0 -1 -1 1 0 0 0 0 -1 1 -1 1 0 0 0 -1 -1 -1 -1 1 0 0 1 -1 1 1 -1 1 0 1 -1 -1 -1 -1 -1 1 6- 72	-1 1 0 0 0 0 0 -1 -1 1 0 0 0 0 -1 1 -1 1 0 0 0 -1 -1 -1 -1 1 0 0 1 1 1 -1 -1 1 0 1 1 -1 -1 -1 -1 1 6- 79
-1 1 0 0 0 0 0 -1 -1 1 0 0 0 0 -1 1 -1 1 0 0 0 1 -1 -1 -1 1 0 0 -1 -1 -1 -1 -1 1 0 -1 -1 -1 -1 -1 -1 1 6- 66	-1 1 0 0 0 0 0 -1 -1 1 0 0 0 0 -1 1 -1 1 0 0 0 -1 -1 -1 -1 1 0 0 1 -1 1 1 -1 1 0 -1 -1 -1 -1 -1 -1 1 6- 73	-1 1 0 0 0 0 0 -1 -1 1 0 0 0 0 -1 1 -1 1 0 0 0 -1 -1 -1 -1 1 0 0 1 1 1 -1 -1 1 0 1 -1 -1 -1 -1 -1 1 6- 80
-1 1 0 0 0 0 0 -1 -1 1 0 0 0 0 -1 1 -1 1 0 0 0 -1 -1 -1 -1 1 0 0 1 -1 1 1 -1 1 0 1 1 1 1 -1 -1 1 6- 67	-1 1 0 0 0 0 0 -1 -1 1 0 0 0 0 -1 1 -1 1 0 0 0 -1 -1 -1 -1 1 0 0 1 1 1 -1 -1 1 0 1 -1 -1 -1 1 -1 1 6- 74	-1 1 0 0 0 0 0 -1 -1 1 0 0 0 0 -1 1 -1 1 0 0 0 -1 -1 -1 -1 1 0 0 1 1 1 -1 -1 1 0 -1 -1 -1 -1 -1 -1 1 6- 81
-1 1 0 0 0 0 0 -1 -1 1 0 0 0 0 -1 1 -1 1 0 0 0 -1 -1 -1 -1 1 0 0 1 -1 1 1 -1 1 0 1 -1 1 1 -1 -1 1 6- 68	-1 1 0 0 0 0 0 -1 -1 1 0 0 0 0 -1 1 -1 1 0 0 0 -1 -1 -1 -1 1 0 0 1 1 1 -1 -1 1 0 1 1 1 1 -1 -1 1 6- 75	-1 1 0 0 0 0 0 -1 -1 1 0 0 0 0 -1 1 -1 1 0 0 0 -1 -1 -1 -1 1 0 0 1 -1 1 -1 -1 1 0 1 1 -1 -1 1 -1 1 6- 82
-1 1 0 0 0 0 0 -1 -1 1 0 0 0 0 -1 1 -1 1 0 0 0 -1 -1 -1 -1 1 0 0 1 -1 1 1 -1 1 0 1 1 1 -1 -1 -1 1 6- 69	-1 1 0 0 0 0 0 -1 -1 1 0 0 0 0 -1 1 -1 1 0 0 0 -1 -1 -1 -1 1 0 0 1 1 1 -1 -1 1 0 1 -1 1 1 -1 -1 1 6- 76	-1 1 0 0 0 0 0 -1 -1 1 0 0 0 0 -1 1 -1 1 0 0 0 -1 -1 -1 -1 1 0 0 1 -1 1 -1 -1 1 0 1 -1 -1 -1 1 -1 1 6- 83
-1 1 0 0 0 0 0 -1 -1 1 0 0 0 0 -1 1 -1 1 0 0 0 -1 -1 -1 -1 1 0 0 1 -1 1 1 -1 1 0 1 -1 1 -1 -1 -1 1 6- 70	-1 1 0 0 0 0 0 -1 -1 1 0 0 0 0 -1 1 -1 1 0 0 0 -1 -1 -1 -1 1 0 0 1 1 1 -1 -1 1 0 1 1 1 -1 -1 -1 1 6- 77	-1 1 0 0 0 0 0 -1 -1 1 0 0 0 0 -1 1 -1 1 0 0 0 -1 -1 -1 -1 1 0 0 1 -1 1 -1 -1 1 0 1 1 1 1 -1 -1 1 6- 84

-1 1 0 0 0 0 0
-1 -1 1 0 0 0 0
-1 1 -1 1 0 0 0
-1 -1 -1 -1 1 0 0
1 -1 1 -1 -1 1 0
1 -1 1 1 -1 -1 1
6- 85

-1 1 0 0 0 0 0
-1 -1 1 0 0 0 0
-1 1 -1 1 0 0 0
-1 -1 -1 -1 1 0 0
1 1 -1 -1 -1 1 0
1 1 -1 -1 1 -1 1
6- 92

-1 1 0 0 0 0 0
-1 -1 1 0 0 0 0
-1 1 -1 1 0 0 0
-1 -1 -1 -1 1 0 0
1 1 -1 -1 -1 1 0
1 -1 -1 -1 -1 -1 1
6- 99

-1 1 0 0 0 0 0
-1 -1 1 0 0 0 0
-1 1 -1 1 0 0 0
-1 -1 -1 -1 1 0 0
1 -1 1 -1 -1 1 0
1 1 1 -1 -1 -1 1
6- 86

-1 1 0 0 0 0 0
-1 -1 1 0 0 0 0
-1 1 -1 1 0 0 0
-1 -1 -1 -1 1 0 0
1 1 -1 -1 -1 1 0
1 -1 -1 -1 1 -1 1
6- 93

-1 1 0 0 0 0 0
-1 -1 1 0 0 0 0
-1 1 -1 1 0 0 0
-1 -1 -1 -1 1 0 0
1 1 -1 -1 -1 1 0
-1 -1 -1 -1 -1 -1 1
6-100

-1 1 0 0 0 0 0
-1 -1 1 0 0 0 0
-1 1 -1 1 0 0 0
-1 -1 -1 -1 1 0 0
1 -1 1 -1 -1 1 0
1 -1 1 -1 -1 -1 1
6- 87

-1 1 0 0 0 0 0
-1 -1 1 0 0 0 0
-1 1 -1 1 0 0 0
-1 -1 -1 -1 1 0 0
1 1 -1 -1 -1 1 0
1 1 1 1 -1 -1 1
6- 94

-1 1 0 0 0 0 0
-1 -1 1 0 0 0 0
-1 1 -1 1 0 0 0
-1 -1 -1 -1 1 0 0
1 -1 -1 -1 -1 1 0
1 1 1 -1 1 -1 1
6-101

-1 1 0 0 0 0 0
-1 -1 1 0 0 0 0
-1 1 -1 1 0 0 0
-1 -1 -1 -1 1 0 0
1 -1 1 -1 -1 1 0
1 1 -1 -1 -1 -1 1
6- 88

-1 1 0 0 0 0 0
-1 -1 1 0 0 0 0
-1 1 -1 1 0 0 0
-1 -1 -1 -1 1 0 0
1 1 -1 -1 -1 1 0
1 -1 1 1 -1 -1 1
6- 95

-1 1 0 0 0 0 0
-1 -1 1 0 0 0 0
-1 1 -1 1 0 0 0
-1 -1 -1 -1 1 0 0
1 -1 -1 -1 -1 1 0
1 -1 1 -1 1 -1 1
6-102

-1 1 0 0 0 0 0
-1 -1 1 0 0 0 0
-1 1 -1 1 0 0 0
-1 -1 -1 -1 1 0 0
1 -1 1 -1 -1 1 0
1 -1 -1 -1 -1 -1 1
6- 89

-1 1 0 0 0 0 0
-1 -1 1 0 0 0 0
-1 1 -1 1 0 0 0
-1 -1 -1 -1 1 0 0
1 1 -1 -1 -1 1 0
1 1 1 -1 -1 -1 1
6- 96

-1 1 0 0 0 0 0
-1 -1 1 0 0 0 0
-1 1 -1 1 0 0 0
-1 -1 -1 -1 1 0 0
1 -1 -1 -1 -1 1 0
1 1 -1 -1 1 -1 1
6-103

-1 1 0 0 0 0 0
-1 -1 1 0 0 0 0
-1 1 -1 1 0 0 0
-1 -1 -1 -1 1 0 0
1 -1 1 -1 -1 1 0
-1 -1 -1 -1 -1 -1 1
6- 90

-1 1 0 0 0 0 0
-1 -1 1 0 0 0 0
-1 1 -1 1 0 0 0
-1 -1 -1 -1 1 0 0
1 1 -1 -1 -1 1 0
1 -1 1 -1 -1 -1 1
6- 97

-1 1 0 0 0 0 0
-1 -1 1 0 0 0 0
-1 1 -1 1 0 0 0
-1 -1 -1 -1 1 0 0
1 -1 -1 -1 -1 1 0
1 -1 -1 -1 1 -1 1
6-104

-1 1 0 0 0 0 0
-1 -1 1 0 0 0 0
-1 1 -1 1 0 0 0
-1 -1 -1 -1 1 0 0
1 1 -1 -1 -1 1 0
1 -1 1 -1 1 -1 1
6- 91

-1 1 0 0 0 0 0
-1 -1 1 0 0 0 0
-1 1 -1 1 0 0 0
-1 -1 -1 -1 1 0 0
1 1 -1 -1 -1 1 0
1 1 -1 -1 -1 -1 1
6- 98

-1 1 0 0 0 0 0
-1 -1 1 0 0 0 0
-1 1 -1 1 0 0 0
-1 -1 -1 -1 1 0 0
1 -1 -1 -1 -1 1 0
1 1 1 1 -1 -1 1
6-105

-1 1 0 0 0 0 0 -1 -1 1 0 0 0 0 -1 1 -1 1 0 0 0 -1 -1 -1 -1 1 0 0 1 -1 -1 -1 -1 1 0 1 -1 1 1 -1 -1 1 6-106	-1 1 0 0 0 0 0 -1 -1 1 0 0 0 0 -1 1 -1 1 0 0 0 -1 -1 -1 -1 1 0 0 -1 -1 -1 -1 -1 1 0 1 1 1 -1 1 -1 1 6-113	-1 1 0 0 0 0 0 -1 -1 1 0 0 0 0 -1 1 -1 1 0 0 0 -1 -1 -1 -1 1 0 0 -1 -1 -1 -1 -1 1 0 1 -1 1 -1 -1 -1 1 6-120
-1 1 0 0 0 0 0 -1 -1 1 0 0 0 0 -1 1 -1 1 0 0 0 -1 -1 -1 -1 1 0 0 1 -1 -1 -1 -1 1 0 1 1 1 -1 -1 -1 1 6-107	-1 1 0 0 0 0 0 -1 -1 1 0 0 0 0 -1 1 -1 1 0 0 0 -1 -1 -1 -1 1 0 0 -1 -1 -1 -1 -1 1 0 1 -1 1 -1 1 -1 1 6-114	-1 1 0 0 0 0 0 -1 -1 1 0 0 0 0 -1 1 -1 1 0 0 0 -1 -1 -1 -1 1 0 0 -1 -1 -1 -1 -1 1 0 1 1 -1 -1 -1 -1 1 6-121
-1 1 0 0 0 0 0 -1 -1 1 0 0 0 0 -1 1 -1 1 0 0 0 -1 -1 -1 -1 1 0 0 1 -1 -1 -1 -1 1 0 1 -1 1 -1 -1 -1 1 6-108	-1 1 0 0 0 0 0 -1 -1 1 0 0 0 0 -1 1 -1 1 0 0 0 -1 -1 -1 -1 1 0 0 -1 -1 -1 -1 -1 1 0 1 1 -1 -1 1 -1 1 6-115	-1 1 0 0 0 0 0 -1 -1 1 0 0 0 0 -1 1 -1 1 0 0 0 -1 -1 -1 -1 1 0 0 -1 -1 -1 -1 -1 1 0 1 -1 -1 -1 -1 -1 1 6-122
-1 1 0 0 0 0 0 -1 -1 1 0 0 0 0 -1 1 -1 1 0 0 0 -1 -1 -1 -1 1 0 0 1 -1 -1 -1 -1 1 0 1 1 -1 -1 -1 -1 1 6-109	-1 1 0 0 0 0 0 -1 -1 1 0 0 0 0 -1 1 -1 1 0 0 0 -1 -1 -1 -1 1 0 0 -1 -1 -1 -1 -1 1 0 1 -1 -1 -1 1 -1 1 6-116	-1 1 0 0 0 0 0 -1 -1 1 0 0 0 0 -1 1 -1 1 0 0 0 -1 -1 -1 -1 1 0 0 -1 -1 -1 -1 -1 1 0 -1 -1 -1 -1 -1 -1 1 6-123
-1 1 0 0 0 0 0 -1 -1 1 0 0 0 0 -1 1 -1 1 0 0 0 -1 -1 -1 -1 1 0 0 1 -1 -1 -1 -1 1 0 1 -1 -1 -1 -1 -1 1 6-110	-1 1 0 0 0 0 0 -1 -1 1 0 0 0 0 -1 1 -1 1 0 0 0 -1 -1 -1 -1 1 0 0 -1 -1 -1 -1 -1 1 0 1 1 1 1 -1 -1 1 6-117	-1 1 0 0 0 0 0 -1 -1 1 0 0 0 0 -1 -1 -1 1 0 0 0 -1 1 1 -1 1 0 0 1 1 1 -1 -1 1 0 1 -1 -1 1 -1 -1 1 6-124
-1 1 0 0 0 0 0 -1 -1 1 0 0 0 0 -1 1 -1 1 0 0 0 -1 -1 -1 -1 1 0 0 1 -1 -1 -1 -1 1 0 -1 -1 -1 -1 -1 -1 1 6-111	-1 1 0 0 0 0 0 -1 -1 1 0 0 0 0 -1 1 -1 1 0 0 0 -1 -1 -1 -1 1 0 0 -1 -1 -1 -1 -1 1 0 1 -1 1 1 -1 -1 1 6-118	-1 1 0 0 0 0 0 -1 -1 1 0 0 0 0 -1 -1 -1 1 0 0 0 -1 1 1 -1 1 0 0 1 1 1 -1 -1 1 0 1 1 1 -1 -1 -1 1 6-125
-1 1 0 0 0 0 0 -1 -1 1 0 0 0 0 -1 1 -1 1 0 0 0 -1 -1 -1 -1 1 0 0 -1 -1 -1 -1 -1 1 0 1 -1 1 1 1 -1 1 6-112	-1 1 0 0 0 0 0 -1 -1 1 0 0 0 0 -1 1 -1 1 0 0 0 -1 -1 -1 -1 1 0 0 -1 -1 -1 -1 -1 1 0 1 1 1 -1 -1 -1 1 6-119	-1 1 0 0 0 0 0 -1 -1 1 0 0 0 0 -1 -1 -1 1 0 0 0 -1 1 1 -1 1 0 0 1 1 1 -1 -1 1 0 1 -1 1 -1 -1 -1 1 6-126

-1 1 0 0 0 0 0
 -1 -1 1 0 0 0 0
 -1 -1 -1 1 0 0 0
 -1 1 1 -1 1 0 0
 1 1 1 -1 -1 1 0
 1 1 -1 -1 -1 -1 1
 6-127

-1 1 0 0 0 0 0
 -1 -1 1 0 0 0 0
 -1 -1 -1 1 0 0 0
 -1 1 1 -1 1 0 0
 1 -1 1 -1 -1 1 0
 1 1 -1 -1 -1 -1 1
 6-134

-1 1 0 0 0 0 0
 -1 -1 1 0 0 0 0
 -1 -1 -1 1 0 0 0
 -1 1 1 -1 1 0 0
 1 1 -1 -1 -1 1 0
 1 -1 1 -1 -1 -1 1
 6-141

-1 1 0 0 0 0 0
 -1 -1 1 0 0 0 0
 -1 -1 -1 1 0 0 0
 -1 1 1 -1 1 0 0
 1 1 1 -1 -1 1 0
 1 -1 -1 -1 -1 -1 1
 6-128

-1 1 0 0 0 0 0
 -1 -1 1 0 0 0 0
 -1 -1 -1 1 0 0 0
 -1 1 1 -1 1 0 0
 1 -1 1 -1 -1 1 0
 1 -1 -1 -1 -1 -1 1
 6-135

-1 1 0 0 0 0 0
 -1 -1 1 0 0 0 0
 -1 -1 -1 1 0 0 0
 -1 1 1 -1 1 0 0
 1 1 -1 -1 -1 1 0
 1 1 -1 -1 -1 -1 1
 6-142

-1 1 0 0 0 0 0
 -1 -1 1 0 0 0 0
 -1 -1 -1 1 0 0 0
 -1 1 1 -1 1 0 0
 1 1 1 -1 -1 1 0
 -1 -1 -1 -1 -1 -1 1
 6-129

-1 1 0 0 0 0 0
 -1 -1 1 0 0 0 0
 -1 -1 -1 1 0 0 0
 -1 1 1 -1 1 0 0
 1 -1 1 -1 -1 1 0
 -1 -1 -1 -1 -1 -1 1
 6-136

-1 1 0 0 0 0 0
 -1 -1 1 0 0 0 0
 -1 -1 -1 1 0 0 0
 -1 1 1 -1 1 0 0
 1 1 -1 -1 -1 1 0
 1 -1 -1 -1 -1 -1 1
 6-143

-1 1 0 0 0 0 0
 -1 -1 1 0 0 0 0
 -1 -1 -1 1 0 0 0
 -1 1 1 -1 1 0 0
 1 -1 1 -1 -1 1 0
 1 1 -1 1 -1 -1 1
 6-130

-1 1 0 0 0 0 0
 -1 -1 1 0 0 0 0
 -1 -1 -1 1 0 0 0
 -1 1 1 -1 1 0 0
 1 1 -1 -1 -1 1 0
 1 -1 1 1 -1 -1 1
 6-137

-1 1 0 0 0 0 0
 -1 -1 1 0 0 0 0
 -1 -1 -1 1 0 0 0
 -1 1 1 -1 1 0 0
 1 1 -1 -1 -1 1 0
 -1 -1 -1 -1 -1 -1 1
 6-144

-1 1 0 0 0 0 0
 -1 -1 1 0 0 0 0
 -1 -1 -1 1 0 0 0
 -1 1 1 -1 1 0 0
 1 -1 1 -1 -1 1 0
 1 -1 -1 1 -1 -1 1
 6-131

-1 1 0 0 0 0 0
 -1 -1 1 0 0 0 0
 -1 -1 -1 1 0 0 0
 -1 1 1 -1 1 0 0
 1 1 -1 -1 -1 1 0
 1 1 -1 1 -1 -1 1
 6-138

-1 1 0 0 0 0 0
 -1 -1 1 0 0 0 0
 -1 -1 -1 1 0 0 0
 -1 1 1 -1 1 0 0
 1 -1 -1 -1 -1 1 0
 1 1 1 1 -1 -1 1
 6-145

-1 1 0 0 0 0 0
 -1 -1 1 0 0 0 0
 -1 -1 -1 1 0 0 0
 -1 1 1 -1 1 0 0
 1 -1 1 -1 -1 1 0
 1 1 1 -1 -1 -1 1
 6-132

-1 1 0 0 0 0 0
 -1 -1 1 0 0 0 0
 -1 -1 -1 1 0 0 0
 -1 1 1 -1 1 0 0
 1 1 -1 -1 -1 1 0
 1 -1 -1 1 -1 -1 1
 6-139

-1 1 0 0 0 0 0
 -1 -1 1 0 0 0 0
 -1 -1 -1 1 0 0 0
 -1 1 1 -1 1 0 0
 1 -1 -1 -1 -1 1 0
 1 -1 1 1 -1 -1 1
 6-146

-1 1 0 0 0 0 0
 -1 -1 1 0 0 0 0
 -1 -1 -1 1 0 0 0
 -1 1 1 -1 1 0 0
 1 -1 1 -1 -1 1 0
 1 -1 1 -1 -1 -1 1
 6-133

-1 1 0 0 0 0 0
 -1 -1 1 0 0 0 0
 -1 -1 -1 1 0 0 0
 -1 1 1 -1 1 0 0
 1 1 -1 -1 -1 1 0
 1 1 1 -1 -1 -1 1
 6-140

-1 1 0 0 0 0 0
 -1 -1 1 0 0 0 0
 -1 -1 -1 1 0 0 0
 -1 1 1 -1 1 0 0
 1 -1 -1 -1 -1 1 0
 1 1 -1 1 -1 -1 1
 6-147

-1 1 0 0 0 0 0
 -1 -1 1 0 0 0 0
 -1 -1 -1 1 0 0 0
 -1 1 1 -1 1 0 0
 1 -1 -1 -1 -1 1 0
 1 -1 -1 1 -1 -1 1
 6-148

-1 1 0 0 0 0 0
 -1 -1 1 0 0 0 0
 -1 -1 -1 1 0 0 0
 -1 1 1 -1 1 0 0
 -1 -1 -1 -1 -1 1 0
 1 1 1 1 -1 -1 1
 6-155

-1 1 0 0 0 0 0
 -1 -1 1 0 0 0 0
 -1 -1 -1 1 0 0 0
 -1 1 1 -1 1 0 0
 -1 -1 -1 -1 -1 1 0
 1 -1 -1 -1 -1 -1 1
 6-162

-1 1 0 0 0 0 0
 -1 -1 1 0 0 0 0
 -1 -1 -1 1 0 0 0
 -1 1 1 -1 1 0 0
 1 -1 -1 -1 -1 1 0
 1 1 1 -1 -1 -1 1
 6-149

-1 1 0 0 0 0 0
 -1 -1 1 0 0 0 0
 -1 -1 -1 1 0 0 0
 -1 1 1 -1 1 0 0
 -1 -1 -1 -1 -1 1 0
 1 -1 1 1 -1 -1 1
 6-156

-1 1 0 0 0 0 0
 -1 -1 1 0 0 0 0
 -1 -1 -1 1 0 0 0
 -1 1 1 -1 1 0 0
 -1 -1 -1 -1 -1 1 0
 -1 -1 -1 -1 -1 -1 1
 6-163

-1 1 0 0 0 0 0
 -1 -1 1 0 0 0 0
 -1 -1 -1 1 0 0 0
 -1 1 1 -1 1 0 0
 1 -1 -1 -1 -1 1 0
 1 -1 1 -1 -1 -1 1
 6-150

-1 1 0 0 0 0 0
 -1 -1 1 0 0 0 0
 -1 -1 -1 1 0 0 0
 -1 1 1 -1 1 0 0
 -1 -1 -1 -1 -1 1 0
 1 1 -1 1 -1 -1 1
 6-157

-1 1 0 0 0 0 0
 -1 -1 1 0 0 0 0
 -1 -1 -1 1 0 0 0
 1 1 -1 -1 1 0 0
 -1 1 -1 1 -1 1 0
 1 1 -1 1 -1 -1 1
 6-164

-1 1 0 0 0 0 0
 -1 -1 1 0 0 0 0
 -1 -1 -1 1 0 0 0
 -1 1 1 -1 1 0 0
 1 -1 -1 -1 -1 1 0
 1 1 -1 -1 -1 -1 1
 6-151

-1 1 0 0 0 0 0
 -1 -1 1 0 0 0 0
 -1 -1 -1 1 0 0 0
 -1 1 1 -1 1 0 0
 -1 -1 -1 -1 -1 1 0
 1 -1 -1 1 -1 -1 1
 6-158

-1 1 0 0 0 0 0
 -1 -1 1 0 0 0 0
 -1 -1 -1 1 0 0 0
 1 1 -1 -1 1 0 0
 -1 1 -1 1 -1 1 0
 1 -1 -1 1 -1 -1 1
 6-165

-1 1 0 0 0 0 0
 -1 -1 1 0 0 0 0
 -1 -1 -1 1 0 0 0
 -1 1 1 -1 1 0 0
 1 -1 -1 -1 -1 1 0
 1 -1 -1 -1 -1 -1 1
 6-152

-1 1 0 0 0 0 0
 -1 -1 1 0 0 0 0
 -1 -1 -1 1 0 0 0
 -1 1 1 -1 1 0 0
 -1 -1 -1 -1 -1 1 0
 1 1 1 -1 -1 -1 1
 6-159

-1 1 0 0 0 0 0
 -1 -1 1 0 0 0 0
 -1 -1 -1 1 0 0 0
 1 1 -1 -1 1 0 0
 -1 1 -1 1 -1 1 0
 1 1 1 -1 -1 -1 1
 6-166

-1 1 0 0 0 0 0
 -1 -1 1 0 0 0 0
 -1 -1 -1 1 0 0 0
 -1 1 1 -1 1 0 0
 1 -1 -1 -1 -1 1 0
 -1 -1 -1 -1 -1 -1 1
 6-153

-1 1 0 0 0 0 0
 -1 -1 1 0 0 0 0
 -1 -1 -1 1 0 0 0
 -1 1 1 -1 1 0 0
 -1 -1 -1 -1 -1 1 0
 1 -1 1 -1 -1 -1 1
 6-160

-1 1 0 0 0 0 0
 -1 -1 1 0 0 0 0
 -1 -1 -1 1 0 0 0
 1 1 -1 -1 1 0 0
 -1 1 -1 1 -1 1 0
 1 -1 1 -1 -1 -1 1
 6-167

-1 1 0 0 0 0 0
 -1 -1 1 0 0 0 0
 -1 -1 -1 1 0 0 0
 -1 1 1 -1 1 0 0
 -1 -1 -1 -1 -1 1 0
 1 -1 1 1 1 -1 1
 6-154

-1 1 0 0 0 0 0
 -1 -1 1 0 0 0 0
 -1 -1 -1 1 0 0 0
 -1 1 1 -1 1 0 0
 -1 -1 -1 -1 -1 1 0
 1 1 -1 -1 -1 -1 1
 6-161

-1 1 0 0 0 0 0
 -1 -1 1 0 0 0 0
 -1 -1 -1 1 0 0 0
 1 1 -1 -1 1 0 0
 -1 1 -1 1 -1 1 0
 1 1 -1 -1 -1 -1 1
 6-168

-1 1 0 0 0 0 0 -1 -1 1 0 0 0 0 -1 -1 -1 1 0 0 0 1 1 -1 -1 1 0 0 -1 1 -1 1 -1 1 0 1 -1 -1 -1 -1 -1 1 6-169	-1 1 0 0 0 0 0 -1 -1 1 0 0 0 0 -1 -1 -1 1 0 0 0 1 1 -1 -1 1 0 0 1 1 1 -1 -1 1 0 1 1 -1 -1 -1 -1 1 6-176	-1 1 0 0 0 0 0 -1 -1 1 0 0 0 0 -1 -1 -1 1 0 0 0 1 1 -1 -1 1 0 0 -1 1 1 -1 -1 1 0 1 1 1 -1 -1 -1 1 6-183
-1 1 0 0 0 0 0 -1 -1 1 0 0 0 0 -1 -1 -1 1 0 0 0 1 1 -1 -1 1 0 0 -1 1 -1 1 -1 1 0 -1 -1 -1 -1 -1 -1 1 6-170	-1 1 0 0 0 0 0 -1 -1 1 0 0 0 0 -1 -1 -1 1 0 0 0 1 1 -1 -1 1 0 0 1 1 1 -1 -1 1 0 -1 1 -1 -1 -1 -1 1 6-177	-1 1 0 0 0 0 0 -1 -1 1 0 0 0 0 -1 -1 -1 1 0 0 0 1 1 -1 -1 1 0 0 -1 1 1 -1 -1 1 0 1 -1 1 -1 -1 -1 1 6-184
-1 1 0 0 0 0 0 -1 -1 1 0 0 0 0 -1 -1 -1 1 0 0 0 1 1 -1 -1 1 0 0 1 1 1 -1 -1 1 0 -1 1 1 1 -1 -1 1 6-171	-1 1 0 0 0 0 0 -1 -1 1 0 0 0 0 -1 -1 -1 1 0 0 0 1 1 -1 -1 1 0 0 1 1 1 -1 -1 1 0 -1 -1 -1 -1 -1 -1 1 6-178	-1 1 0 0 0 0 0 -1 -1 1 0 0 0 0 -1 -1 -1 1 0 0 0 1 1 -1 -1 1 0 0 -1 1 1 -1 -1 1 0 1 1 -1 -1 -1 -1 1 6-185
-1 1 0 0 0 0 0 -1 -1 1 0 0 0 0 -1 -1 -1 1 0 0 0 1 1 -1 -1 1 0 0 1 1 1 -1 -1 1 0 1 1 -1 1 -1 -1 1 6-172	-1 1 0 0 0 0 0 -1 -1 1 0 0 0 0 -1 -1 -1 1 0 0 0 1 1 -1 -1 1 0 0 -1 1 1 -1 -1 1 0 1 1 1 1 -1 -1 1 6-179	-1 1 0 0 0 0 0 -1 -1 1 0 0 0 0 -1 -1 -1 1 0 0 0 1 1 -1 -1 1 0 0 -1 1 1 -1 -1 1 0 1 -1 -1 -1 -1 -1 1 6-186
-1 1 0 0 0 0 0 -1 -1 1 0 0 0 0 -1 -1 -1 1 0 0 0 1 1 -1 -1 1 0 0 1 1 1 -1 -1 1 0 -1 1 -1 1 -1 -1 1 6-173	-1 1 0 0 0 0 0 -1 -1 1 0 0 0 0 -1 -1 -1 1 0 0 0 1 1 -1 -1 1 0 0 -1 1 1 -1 -1 1 0 1 -1 1 1 -1 -1 1 6-180	-1 1 0 0 0 0 0 -1 -1 1 0 0 0 0 -1 -1 -1 1 0 0 0 1 1 -1 -1 1 0 0 -1 1 1 -1 -1 1 0 -1 -1 -1 -1 -1 -1 1 6-187
-1 1 0 0 0 0 0 -1 -1 1 0 0 0 0 -1 -1 -1 1 0 0 0 1 1 -1 -1 1 0 0 1 1 1 -1 -1 1 0 1 1 1 -1 -1 -1 1 6-174	-1 1 0 0 0 0 0 -1 -1 1 0 0 0 0 -1 -1 -1 1 0 0 0 1 1 -1 -1 1 0 0 -1 1 1 -1 -1 1 0 1 1 -1 1 -1 -1 1 6-181	-1 1 0 0 0 0 0 -1 -1 1 0 0 0 0 -1 -1 -1 1 0 0 0 1 1 -1 -1 1 0 0 1 1 -1 -1 -1 1 0 -1 1 -1 1 1 -1 1 6-188
-1 1 0 0 0 0 0 -1 -1 1 0 0 0 0 -1 -1 -1 1 0 0 0 1 1 -1 -1 1 0 0 1 1 1 -1 -1 1 0 -1 1 1 -1 -1 -1 1 6-175	-1 1 0 0 0 0 0 -1 -1 1 0 0 0 0 -1 -1 -1 1 0 0 0 1 1 -1 -1 1 0 0 -1 1 1 -1 -1 1 0 1 -1 -1 1 -1 -1 1 6-182	-1 1 0 0 0 0 0 -1 -1 1 0 0 0 0 -1 -1 -1 1 0 0 0 1 1 -1 -1 1 0 0 1 1 -1 -1 -1 1 0 1 1 1 1 -1 -1 1 6-189

-1 1 0 0 0 0 0
 -1 -1 1 0 0 0 0
 -1 -1 -1 1 0 0 0
 1 1 -1 -1 1 0 0
 1 1 -1 -1 -1 1 0
 -1 1 1 1 -1 -1 1
 6-190

-1 1 0 0 0 0 0
 -1 -1 1 0 0 0 0
 -1 -1 -1 1 0 0 0
 1 1 -1 -1 1 0 0
 1 1 -1 -1 -1 1 0
 -1 -1 -1 -1 -1 -1 1
 6-197

-1 1 0 0 0 0 0
 -1 -1 1 0 0 0 0
 -1 -1 -1 1 0 0 0
 1 1 -1 -1 1 0 0
 -1 1 -1 -1 -1 1 0
 1 1 1 -1 -1 -1 1
 6-204

-1 1 0 0 0 0 0
 -1 -1 1 0 0 0 0
 -1 -1 -1 1 0 0 0
 1 1 -1 -1 1 0 0
 1 1 -1 -1 -1 1 0
 1 1 -1 1 -1 -1 1
 6-191

-1 1 0 0 0 0 0
 -1 -1 1 0 0 0 0
 -1 -1 -1 1 0 0 0
 1 1 -1 -1 1 0 0
 -1 1 -1 -1 -1 1 0
 1 1 -1 1 1 -1 1
 6-198

-1 1 0 0 0 0 0
 -1 -1 1 0 0 0 0
 -1 -1 -1 1 0 0 0
 1 1 -1 -1 1 0 0
 -1 1 -1 -1 -1 1 0
 1 -1 1 -1 -1 -1 1
 6-205

-1 1 0 0 0 0 0
 -1 -1 1 0 0 0 0
 -1 -1 -1 1 0 0 0
 1 1 -1 -1 1 0 0
 1 1 -1 -1 -1 1 0
 -1 1 -1 1 -1 -1 1
 6-192

-1 1 0 0 0 0 0
 -1 -1 1 0 0 0 0
 -1 -1 -1 1 0 0 0
 1 1 -1 -1 1 0 0
 -1 1 -1 -1 -1 1 0
 1 -1 -1 1 1 -1 1
 6-199

-1 1 0 0 0 0 0
 -1 -1 1 0 0 0 0
 -1 -1 -1 1 0 0 0
 1 1 -1 -1 1 0 0
 -1 1 -1 -1 -1 1 0
 1 1 -1 -1 -1 -1 1
 6-206

-1 1 0 0 0 0 0
 -1 -1 1 0 0 0 0
 -1 -1 -1 1 0 0 0
 1 1 -1 -1 1 0 0
 1 1 -1 -1 -1 1 0
 1 1 1 -1 -1 -1 1
 6-193

-1 1 0 0 0 0 0
 -1 -1 1 0 0 0 0
 -1 -1 -1 1 0 0 0
 1 1 -1 -1 1 0 0
 -1 1 -1 -1 -1 1 0
 1 1 1 1 -1 -1 1
 6-200

-1 1 0 0 0 0 0
 -1 -1 1 0 0 0 0
 -1 -1 -1 1 0 0 0
 1 1 -1 -1 1 0 0
 -1 1 -1 -1 -1 1 0
 1 -1 -1 -1 -1 -1 1
 6-207

-1 1 0 0 0 0 0
 -1 -1 1 0 0 0 0
 -1 -1 -1 1 0 0 0
 1 1 -1 -1 1 0 0
 1 1 -1 -1 -1 1 0
 -1 1 1 -1 -1 -1 1
 6-194

-1 1 0 0 0 0 0
 -1 -1 1 0 0 0 0
 -1 -1 -1 1 0 0 0
 1 1 -1 -1 1 0 0
 -1 1 -1 -1 -1 1 0
 1 -1 1 1 -1 -1 1
 6-201

-1 1 0 0 0 0 0
 -1 -1 1 0 0 0 0
 -1 -1 -1 1 0 0 0
 1 1 -1 -1 1 0 0
 -1 1 -1 -1 -1 1 0
 -1 -1 -1 -1 -1 -1 1
 6-208

-1 1 0 0 0 0 0
 -1 -1 1 0 0 0 0
 -1 -1 -1 1 0 0 0
 1 1 -1 -1 1 0 0
 1 1 -1 -1 -1 1 0
 1 1 -1 -1 -1 -1 1
 6-195

-1 1 0 0 0 0 0
 -1 -1 1 0 0 0 0
 -1 -1 -1 1 0 0 0
 1 1 -1 -1 1 0 0
 -1 1 -1 -1 -1 1 0
 1 1 -1 1 -1 -1 1
 6-202

-1 1 0 0 0 0 0
 -1 -1 1 0 0 0 0
 -1 -1 -1 1 0 0 0
 1 1 -1 -1 1 0 0
 -1 -1 -1 -1 -1 1 0
 -1 1 1 1 1 -1 1
 6-209

-1 1 0 0 0 0 0
 -1 -1 1 0 0 0 0
 -1 -1 -1 1 0 0 0
 1 1 -1 -1 1 0 0
 1 1 -1 -1 -1 1 0
 -1 1 -1 -1 -1 -1 1
 6-196

-1 1 0 0 0 0 0
 -1 -1 1 0 0 0 0
 -1 -1 -1 1 0 0 0
 1 1 -1 -1 1 0 0
 -1 1 -1 -1 -1 1 0
 1 -1 -1 1 -1 -1 1
 6-203

-1 1 0 0 0 0 0
 -1 -1 1 0 0 0 0
 -1 -1 -1 1 0 0 0
 1 1 -1 -1 1 0 0
 -1 -1 -1 -1 -1 1 0
 1 1 -1 1 1 -1 1
 6-210

-1 1 0 0 0 0 0
 -1 -1 1 0 0 0 0
 -1 -1 -1 1 0 0 0
 1 1 -1 -1 1 0 0
 -1 -1 -1 -1 -1 1 0
 -1 1 -1 1 1 -1 1
 6-211

-1 1 0 0 0 0 0
 -1 -1 1 0 0 0 0
 -1 -1 -1 1 0 0 0
 1 1 -1 -1 1 0 0
 -1 -1 -1 -1 -1 1 0
 1 1 -1 -1 -1 -1 1
 6-218

-1 1 0 0 0 0 0
 -1 -1 1 0 0 0 0
 -1 -1 -1 1 0 0 0
 -1 1 -1 -1 1 0 0
 1 1 -1 1 -1 1 0
 1 -1 1 -1 -1 -1 1
 6-225

-1 1 0 0 0 0 0
 -1 -1 1 0 0 0 0
 -1 -1 -1 1 0 0 0
 1 1 -1 -1 1 0 0
 -1 -1 -1 -1 -1 1 0
 1 1 1 1 -1 -1 1
 6-212

-1 1 0 0 0 0 0
 -1 -1 1 0 0 0 0
 -1 -1 -1 1 0 0 0
 1 1 -1 -1 1 0 0
 -1 -1 -1 -1 -1 1 0
 -1 1 -1 -1 -1 -1 1
 6-219

-1 1 0 0 0 0 0
 -1 -1 1 0 0 0 0
 -1 -1 -1 1 0 0 0
 -1 1 -1 -1 1 0 0
 1 1 -1 1 -1 1 0
 1 1 -1 -1 -1 -1 1
 6-226

-1 1 0 0 0 0 0
 -1 -1 1 0 0 0 0
 -1 -1 -1 1 0 0 0
 1 1 -1 -1 1 0 0
 -1 -1 -1 -1 -1 1 0
 -1 1 1 1 -1 -1 1
 6-213

-1 1 0 0 0 0 0
 -1 -1 1 0 0 0 0
 -1 -1 -1 1 0 0 0
 1 1 -1 -1 1 0 0
 -1 -1 -1 -1 -1 1 0
 -1 -1 -1 -1 -1 -1 1
 6-220

-1 1 0 0 0 0 0
 -1 -1 1 0 0 0 0
 -1 -1 -1 1 0 0 0
 -1 1 -1 -1 1 0 0
 1 1 -1 1 -1 1 0
 1 -1 -1 -1 -1 -1 1
 6-227

-1 1 0 0 0 0 0
 -1 -1 1 0 0 0 0
 -1 -1 -1 1 0 0 0
 1 1 -1 -1 1 0 0
 -1 -1 -1 -1 -1 1 0
 1 1 -1 1 -1 -1 1
 6-214

-1 1 0 0 0 0 0
 -1 -1 1 0 0 0 0
 -1 -1 -1 1 0 0 0
 -1 1 -1 -1 1 0 0
 1 1 -1 1 -1 1 0
 1 -1 1 1 -1 -1 1
 6-221

-1 1 0 0 0 0 0
 -1 -1 1 0 0 0 0
 -1 -1 -1 1 0 0 0
 -1 1 -1 -1 1 0 0
 1 1 -1 1 -1 1 0
 -1 -1 -1 -1 -1 -1 1
 6-228

-1 1 0 0 0 0 0
 -1 -1 1 0 0 0 0
 -1 -1 -1 1 0 0 0
 1 1 -1 -1 1 0 0
 -1 -1 -1 -1 -1 1 0
 -1 1 -1 1 -1 -1 1
 6-215

-1 1 0 0 0 0 0
 -1 -1 1 0 0 0 0
 -1 -1 -1 1 0 0 0
 -1 1 -1 -1 1 0 0
 1 1 -1 1 -1 1 0
 1 1 -1 1 -1 -1 1
 6-222

-1 1 0 0 0 0 0
 -1 -1 1 0 0 0 0
 -1 -1 -1 1 0 0 0
 -1 1 -1 -1 1 0 0
 1 -1 -1 1 -1 1 0
 1 1 1 1 -1 -1 1
 6-229

-1 1 0 0 0 0 0
 -1 -1 1 0 0 0 0
 -1 -1 -1 1 0 0 0
 1 1 -1 -1 1 0 0
 -1 -1 -1 -1 -1 1 0
 1 1 1 -1 -1 -1 1
 6-216

-1 1 0 0 0 0 0
 -1 -1 1 0 0 0 0
 -1 -1 -1 1 0 0 0
 -1 1 -1 -1 1 0 0
 1 1 -1 1 -1 1 0
 1 -1 -1 1 -1 -1 1
 6-223

-1 1 0 0 0 0 0
 -1 -1 1 0 0 0 0
 -1 -1 -1 1 0 0 0
 -1 1 -1 -1 1 0 0
 1 -1 -1 1 -1 1 0
 1 -1 1 1 -1 -1 1
 6-230

-1 1 0 0 0 0 0
 -1 -1 1 0 0 0 0
 -1 -1 -1 1 0 0 0
 1 1 -1 -1 1 0 0
 -1 -1 -1 -1 -1 1 0
 -1 1 1 -1 -1 -1 1
 6-217

-1 1 0 0 0 0 0
 -1 -1 1 0 0 0 0
 -1 -1 -1 1 0 0 0
 -1 1 -1 -1 1 0 0
 1 1 -1 1 -1 1 0
 1 1 1 -1 -1 -1 1
 6-224

-1 1 0 0 0 0 0
 -1 -1 1 0 0 0 0
 -1 -1 -1 1 0 0 0
 -1 1 -1 -1 1 0 0
 1 -1 -1 1 -1 1 0
 1 1 -1 1 -1 -1 1
 6-231

-1 1 0 0 0 0 0
 -1 -1 1 0 0 0 0
 -1 -1 -1 1 0 0 0
 -1 1 -1 -1 1 0 0
 1 -1 -1 1 -1 1 0
 1 -1 -1 1 -1 -1 1
 6-232

-1 1 0 0 0 0 0
 -1 -1 1 0 0 0 0
 -1 -1 -1 1 0 0 0
 -1 1 -1 -1 1 0 0
 1 1 1 -1 -1 1 0
 1 1 1 1 -1 -1 1
 6-239

-1 1 0 0 0 0 0
 -1 -1 1 0 0 0 0
 -1 -1 -1 1 0 0 0
 -1 1 -1 -1 1 0 0
 1 1 1 -1 -1 1 0
 1 -1 -1 -1 -1 -1 1
 6-246

-1 1 0 0 0 0 0
 -1 -1 1 0 0 0 0
 -1 -1 -1 1 0 0 0
 -1 1 -1 -1 1 0 0
 1 -1 -1 1 -1 1 0
 1 1 1 -1 -1 -1 1
 6-233

-1 1 0 0 0 0 0
 -1 -1 1 0 0 0 0
 -1 -1 -1 1 0 0 0
 -1 1 -1 -1 1 0 0
 1 1 1 -1 -1 1 0
 1 -1 1 1 -1 -1 1
 6-240

-1 1 0 0 0 0 0
 -1 -1 1 0 0 0 0
 -1 -1 -1 1 0 0 0
 -1 1 -1 -1 1 0 0
 1 1 1 -1 -1 1 0
 -1 -1 -1 -1 -1 -1 1
 6-247

-1 1 0 0 0 0 0
 -1 -1 1 0 0 0 0
 -1 -1 -1 1 0 0 0
 -1 1 -1 -1 1 0 0
 1 -1 -1 1 -1 1 0
 1 -1 1 -1 -1 -1 1
 6-234

-1 1 0 0 0 0 0
 -1 -1 1 0 0 0 0
 -1 -1 -1 1 0 0 0
 -1 1 -1 -1 1 0 0
 1 1 1 -1 -1 1 0
 1 1 -1 1 -1 -1 1
 6-241

-1 1 0 0 0 0 0
 -1 -1 1 0 0 0 0
 -1 -1 -1 1 0 0 0
 -1 1 -1 -1 1 0 0
 1 -1 1 -1 -1 1 0
 1 1 1 -1 1 -1 1
 6-248

-1 1 0 0 0 0 0
 -1 -1 1 0 0 0 0
 -1 -1 -1 1 0 0 0
 -1 1 -1 -1 1 0 0
 1 -1 -1 1 -1 1 0
 1 1 -1 -1 -1 -1 1
 6-235

-1 1 0 0 0 0 0
 -1 -1 1 0 0 0 0
 -1 -1 -1 1 0 0 0
 -1 1 -1 -1 1 0 0
 1 1 1 -1 -1 1 0
 1 -1 -1 1 -1 -1 1
 6-242

-1 1 0 0 0 0 0
 -1 -1 1 0 0 0 0
 -1 -1 -1 1 0 0 0
 -1 1 -1 -1 1 0 0
 1 -1 1 -1 -1 1 0
 1 -1 1 -1 1 -1 1
 6-249

-1 1 0 0 0 0 0
 -1 -1 1 0 0 0 0
 -1 -1 -1 1 0 0 0
 -1 1 -1 -1 1 0 0
 1 -1 -1 1 -1 1 0
 1 -1 -1 -1 -1 -1 1
 6-236

-1 1 0 0 0 0 0
 -1 -1 1 0 0 0 0
 -1 -1 -1 1 0 0 0
 -1 1 -1 -1 1 0 0
 1 1 1 -1 -1 1 0
 1 1 1 -1 -1 -1 1
 6-243

-1 1 0 0 0 0 0
 -1 -1 1 0 0 0 0
 -1 -1 -1 1 0 0 0
 -1 1 -1 -1 1 0 0
 1 -1 1 -1 -1 1 0
 1 1 1 1 -1 -1 1
 6-250

-1 1 0 0 0 0 0
 -1 -1 1 0 0 0 0
 -1 -1 -1 1 0 0 0
 -1 1 -1 -1 1 0 0
 1 -1 -1 1 -1 1 0
 -1 -1 -1 -1 -1 -1 1
 6-237

-1 1 0 0 0 0 0
 -1 -1 1 0 0 0 0
 -1 -1 -1 1 0 0 0
 -1 1 -1 -1 1 0 0
 1 1 1 -1 -1 1 0
 1 -1 1 -1 -1 -1 1
 6-244

-1 1 0 0 0 0 0
 -1 -1 1 0 0 0 0
 -1 -1 -1 1 0 0 0
 -1 1 -1 -1 1 0 0
 1 -1 1 -1 -1 1 0
 1 -1 1 1 -1 -1 1
 6-251

-1 1 0 0 0 0 0
 -1 -1 1 0 0 0 0
 -1 -1 -1 1 0 0 0
 -1 1 -1 -1 1 0 0
 1 1 1 -1 -1 1 0
 1 -1 1 -1 1 -1 1
 6-238

-1 1 0 0 0 0 0
 -1 -1 1 0 0 0 0
 -1 -1 -1 1 0 0 0
 -1 1 -1 -1 1 0 0
 1 1 1 -1 -1 1 0
 1 1 -1 -1 -1 -1 1
 6-245

-1 1 0 0 0 0 0
 -1 -1 1 0 0 0 0
 -1 -1 -1 1 0 0 0
 -1 1 -1 -1 1 0 0
 1 -1 1 -1 -1 1 0
 1 1 -1 1 -1 -1 1
 6-252

-1 1 0 0 0 0 0 -1 -1 1 0 0 0 0 -1 -1 -1 1 0 0 0 -1 1 -1 -1 1 0 0 1 -1 1 -1 -1 1 0 1 -1 -1 1 -1 -1 1 6-253	-1 1 0 0 0 0 0 -1 -1 1 0 0 0 0 -1 -1 -1 1 0 0 0 -1 1 -1 -1 1 0 0 1 1 -1 -1 -1 1 0 1 1 1 -1 1 -1 1 6-260	-1 1 0 0 0 0 0 -1 -1 1 0 0 0 0 -1 -1 -1 1 0 0 0 -1 1 -1 -1 1 0 0 1 1 -1 -1 -1 1 0 1 -1 1 -1 -1 -1 1 6-267
-1 1 0 0 0 0 0 -1 -1 1 0 0 0 0 -1 -1 -1 1 0 0 0 -1 1 -1 -1 1 0 0 1 -1 1 -1 -1 1 0 1 1 1 -1 -1 -1 1 6-254	-1 1 0 0 0 0 0 -1 -1 1 0 0 0 0 -1 -1 -1 1 0 0 0 -1 1 -1 -1 1 0 0 1 1 -1 -1 -1 1 0 1 -1 1 -1 1 -1 1 6-261	-1 1 0 0 0 0 0 -1 -1 1 0 0 0 0 -1 -1 -1 1 0 0 0 -1 1 -1 -1 1 0 0 1 1 -1 -1 -1 1 0 1 1 -1 -1 -1 -1 1 6-268
-1 1 0 0 0 0 0 -1 -1 1 0 0 0 0 -1 -1 -1 1 0 0 0 -1 1 -1 -1 1 0 0 1 -1 1 -1 -1 1 0 1 -1 1 -1 -1 -1 1 6-255	-1 1 0 0 0 0 0 -1 -1 1 0 0 0 0 -1 -1 -1 1 0 0 0 -1 1 -1 -1 1 0 0 1 1 -1 -1 -1 1 0 1 1 1 1 -1 -1 1 6-262	-1 1 0 0 0 0 0 -1 -1 1 0 0 0 0 -1 -1 -1 1 0 0 0 -1 1 -1 -1 1 0 0 1 1 -1 -1 -1 1 0 1 -1 -1 -1 -1 -1 1 6-269
-1 1 0 0 0 0 0 -1 -1 1 0 0 0 0 -1 -1 -1 1 0 0 0 -1 1 -1 -1 1 0 0 1 -1 1 -1 -1 1 0 1 1 -1 -1 -1 -1 1 6-256	-1 1 0 0 0 0 0 -1 -1 1 0 0 0 0 -1 -1 -1 1 0 0 0 -1 1 -1 -1 1 0 0 1 1 -1 -1 -1 1 0 1 -1 1 1 -1 -1 1 6-263	-1 1 0 0 0 0 0 -1 -1 1 0 0 0 0 -1 -1 -1 1 0 0 0 -1 1 -1 -1 1 0 0 1 1 -1 -1 -1 1 0 -1 -1 -1 -1 -1 -1 1 6-270
-1 1 0 0 0 0 0 -1 -1 1 0 0 0 0 -1 -1 -1 1 0 0 0 -1 1 -1 -1 1 0 0 1 -1 1 -1 -1 1 0 1 -1 -1 -1 -1 -1 1 6-257	-1 1 0 0 0 0 0 -1 -1 1 0 0 0 0 -1 -1 -1 1 0 0 0 -1 1 -1 -1 1 0 0 1 1 -1 -1 -1 1 0 1 1 -1 1 -1 -1 1 6-264	-1 1 0 0 0 0 0 -1 -1 1 0 0 0 0 -1 -1 -1 1 0 0 0 -1 1 -1 -1 1 0 0 1 -1 -1 -1 -1 1 0 1 1 -1 1 1 -1 1 6-271
-1 1 0 0 0 0 0 -1 -1 1 0 0 0 0 -1 -1 -1 1 0 0 0 -1 1 -1 -1 1 0 0 1 -1 1 -1 -1 1 0 -1 -1 -1 -1 -1 -1 1 6-258	-1 1 0 0 0 0 0 -1 -1 1 0 0 0 0 -1 -1 -1 1 0 0 0 -1 1 -1 -1 1 0 0 1 1 -1 -1 -1 1 0 1 -1 -1 1 -1 -1 1 6-265	-1 1 0 0 0 0 0 -1 -1 1 0 0 0 0 -1 -1 -1 1 0 0 0 -1 1 -1 -1 1 0 0 1 -1 -1 -1 -1 1 0 1 -1 -1 1 1 -1 1 6-272
-1 1 0 0 0 0 0 -1 -1 1 0 0 0 0 -1 -1 -1 1 0 0 0 -1 1 -1 -1 1 0 0 1 1 -1 -1 -1 1 0 1 -1 -1 1 1 -1 1 6-259	-1 1 0 0 0 0 0 -1 -1 1 0 0 0 0 -1 -1 -1 1 0 0 0 -1 1 -1 -1 1 0 0 1 1 -1 -1 -1 1 0 1 1 1 -1 -1 -1 1 6-266	-1 1 0 0 0 0 0 -1 -1 1 0 0 0 0 -1 -1 -1 1 0 0 0 -1 1 -1 -1 1 0 0 1 -1 -1 -1 -1 1 0 1 1 1 -1 1 -1 1 6-273

-1 1 0 0 0 0 0 -1 -1 1 0 0 0 0 -1 -1 -1 1 0 0 0 -1 1 -1 -1 1 0 0 1 -1 -1 -1 -1 1 0 1 -1 1 -1 1 -1 1 6-274	-1 1 0 0 0 0 0 -1 -1 1 0 0 0 0 -1 -1 -1 1 0 0 0 -1 1 -1 -1 1 0 0 1 -1 -1 -1 -1 1 0 1 1 -1 -1 -1 -1 1 6-281	-1 1 0 0 0 0 0 -1 -1 1 0 0 0 0 -1 -1 -1 1 0 0 0 -1 1 -1 -1 1 0 0 -1 -1 -1 -1 -1 1 0 1 -1 1 -1 1 -1 1 6-288
-1 1 0 0 0 0 0 -1 -1 1 0 0 0 0 -1 -1 -1 1 0 0 0 -1 1 -1 -1 1 0 0 1 -1 -1 -1 -1 1 0 1 1 1 1 -1 -1 1 6-275	-1 1 0 0 0 0 0 -1 -1 1 0 0 0 0 -1 -1 -1 1 0 0 0 -1 1 -1 -1 1 0 0 1 -1 -1 -1 -1 1 0 1 -1 -1 -1 -1 -1 1 6-282	-1 1 0 0 0 0 0 -1 -1 1 0 0 0 0 -1 -1 -1 1 0 0 0 -1 1 -1 -1 1 0 0 -1 -1 -1 -1 -1 1 0 1 1 1 1 -1 -1 1 6-289
-1 1 0 0 0 0 0 -1 -1 1 0 0 0 0 -1 -1 -1 1 0 0 0 -1 1 -1 -1 1 0 0 1 -1 -1 -1 -1 1 0 1 -1 1 1 -1 -1 1 6-276	-1 1 0 0 0 0 0 -1 -1 1 0 0 0 0 -1 -1 -1 1 0 0 0 -1 1 -1 -1 1 0 0 1 -1 -1 -1 -1 1 0 -1 -1 -1 -1 -1 -1 1 6-283	-1 1 0 0 0 0 0 -1 -1 1 0 0 0 0 -1 -1 -1 1 0 0 0 -1 1 -1 -1 1 0 0 -1 -1 -1 -1 -1 1 0 1 -1 1 1 -1 -1 1 6-290
-1 1 0 0 0 0 0 -1 -1 1 0 0 0 0 -1 -1 -1 1 0 0 0 -1 1 -1 -1 1 0 0 1 -1 -1 -1 -1 1 0 1 1 -1 1 -1 -1 1 6-277	-1 1 0 0 0 0 0 -1 -1 1 0 0 0 0 -1 -1 -1 1 0 0 0 -1 1 -1 -1 1 0 0 -1 -1 -1 -1 -1 1 0 1 -1 1 1 1 -1 1 6-284	-1 1 0 0 0 0 0 -1 -1 1 0 0 0 0 -1 -1 -1 1 0 0 0 -1 1 -1 -1 1 0 0 -1 -1 -1 -1 -1 1 0 1 1 -1 1 -1 -1 1 6-291
-1 1 0 0 0 0 0 -1 -1 1 0 0 0 0 -1 -1 -1 1 0 0 0 -1 1 -1 -1 1 0 0 1 -1 -1 -1 -1 1 0 1 -1 -1 1 -1 -1 1 6-278	-1 1 0 0 0 0 0 -1 -1 1 0 0 0 0 -1 -1 -1 1 0 0 0 -1 1 -1 -1 1 0 0 -1 -1 -1 -1 -1 1 0 1 1 -1 1 1 -1 1 6-285	-1 1 0 0 0 0 0 -1 -1 1 0 0 0 0 -1 -1 -1 1 0 0 0 -1 1 -1 -1 1 0 0 -1 -1 -1 -1 -1 1 0 1 -1 -1 1 -1 -1 1 6-292
-1 1 0 0 0 0 0 -1 -1 1 0 0 0 0 -1 -1 -1 1 0 0 0 -1 1 -1 -1 1 0 0 1 -1 -1 -1 -1 1 0 1 1 1 -1 -1 -1 1 6-279	-1 1 0 0 0 0 0 -1 -1 1 0 0 0 0 -1 -1 -1 1 0 0 0 -1 1 -1 -1 1 0 0 -1 -1 -1 -1 -1 1 0 1 -1 -1 1 1 -1 1 6-286	-1 1 0 0 0 0 0 -1 -1 1 0 0 0 0 -1 -1 -1 1 0 0 0 -1 1 -1 -1 1 0 0 -1 -1 -1 -1 -1 1 0 1 1 1 -1 -1 -1 1 6-293
-1 1 0 0 0 0 0 -1 -1 1 0 0 0 0 -1 -1 -1 1 0 0 0 -1 1 -1 -1 1 0 0 1 -1 -1 -1 -1 1 0 1 -1 1 -1 -1 -1 1 6-280	-1 1 0 0 0 0 0 -1 -1 1 0 0 0 0 -1 -1 -1 1 0 0 0 -1 1 -1 -1 1 0 0 -1 -1 -1 -1 -1 1 0 1 1 1 -1 1 -1 1 6-287	-1 1 0 0 0 0 0 -1 -1 1 0 0 0 0 -1 -1 -1 1 0 0 0 -1 1 -1 -1 1 0 0 -1 -1 -1 -1 -1 1 0 1 -1 1 -1 -1 -1 1 6-294

-1 1 0 0 0 0 0 -1 -1 1 0 0 0 0 -1 -1 -1 1 0 0 0 -1 1 -1 -1 1 0 0 -1 -1 -1 -1 -1 1 0 1 1 -1 -1 -1 -1 1 6-295	-1 1 0 0 0 0 0 -1 -1 1 0 0 0 0 -1 -1 -1 1 0 0 0 -1 -1 -1 -1 1 0 0 -1 1 1 1 -1 1 0 1 1 1 -1 -1 -1 1 6-302	-1 1 0 0 0 0 0 -1 -1 1 0 0 0 0 -1 -1 -1 1 0 0 0 -1 -1 -1 -1 1 0 0 1 1 -1 1 -1 1 0 -1 1 1 1 -1 -1 1 6-309
-1 1 0 0 0 0 0 -1 -1 1 0 0 0 0 -1 -1 -1 1 0 0 0 -1 1 -1 -1 1 0 0 -1 -1 -1 -1 -1 1 0 1 -1 -1 -1 -1 -1 1 6-296	-1 1 0 0 0 0 0 -1 -1 1 0 0 0 0 -1 -1 -1 1 0 0 0 -1 -1 -1 -1 1 0 0 -1 1 1 1 -1 1 0 1 -1 1 -1 -1 -1 1 6-303	-1 1 0 0 0 0 0 -1 -1 1 0 0 0 0 -1 -1 -1 1 0 0 0 -1 -1 -1 -1 1 0 0 1 1 -1 1 -1 1 0 1 1 -1 1 -1 -1 1 6-310
-1 1 0 0 0 0 0 -1 -1 1 0 0 0 0 -1 -1 -1 1 0 0 0 -1 1 -1 -1 1 0 0 -1 -1 -1 -1 -1 1 0 -1 -1 -1 -1 -1 -1 1 6-297	-1 1 0 0 0 0 0 -1 -1 1 0 0 0 0 -1 -1 -1 1 0 0 0 -1 -1 -1 -1 1 0 0 -1 1 1 1 -1 1 0 1 1 -1 -1 -1 -1 1 6-304	-1 1 0 0 0 0 0 -1 -1 1 0 0 0 0 -1 -1 -1 1 0 0 0 -1 -1 -1 -1 1 0 0 1 1 -1 1 -1 1 0 -1 1 -1 1 -1 -1 1 6-311
-1 1 0 0 0 0 0 -1 -1 1 0 0 0 0 -1 -1 -1 1 0 0 0 -1 -1 -1 -1 1 0 0 -1 1 1 1 -1 1 0 1 1 1 1 -1 -1 1 6-298	-1 1 0 0 0 0 0 -1 -1 1 0 0 0 0 -1 -1 -1 1 0 0 0 -1 -1 -1 -1 1 0 0 -1 1 1 1 -1 1 0 1 -1 -1 -1 -1 -1 1 6-305	-1 1 0 0 0 0 0 -1 -1 1 0 0 0 0 -1 -1 -1 1 0 0 0 -1 -1 -1 -1 1 0 0 1 1 -1 1 -1 1 0 1 1 1 -1 -1 -1 1 6-312
-1 1 0 0 0 0 0 -1 -1 1 0 0 0 0 -1 -1 -1 1 0 0 0 -1 -1 -1 -1 1 0 0 -1 1 1 1 -1 1 0 1 -1 1 1 -1 -1 1 6-299	-1 1 0 0 0 0 0 -1 -1 1 0 0 0 0 -1 -1 -1 1 0 0 0 -1 -1 -1 -1 1 0 0 -1 1 1 1 -1 1 0 -1 -1 -1 -1 -1 -1 1 6-306	-1 1 0 0 0 0 0 -1 -1 1 0 0 0 0 -1 -1 -1 1 0 0 0 -1 -1 -1 -1 1 0 0 1 1 -1 1 -1 1 0 -1 1 1 -1 -1 -1 1 6-313
-1 1 0 0 0 0 0 -1 -1 1 0 0 0 0 -1 -1 -1 1 0 0 0 -1 -1 -1 -1 1 0 0 -1 1 1 1 -1 1 0 1 1 -1 1 -1 -1 1 6-300	-1 1 0 0 0 0 0 -1 -1 1 0 0 0 0 -1 -1 -1 1 0 0 0 -1 -1 -1 -1 1 0 0 1 1 -1 1 -1 1 0 -1 1 -1 -1 1 -1 1 6-307	-1 1 0 0 0 0 0 -1 -1 1 0 0 0 0 -1 -1 -1 1 0 0 0 -1 -1 -1 -1 1 0 0 1 1 -1 1 -1 1 0 1 1 -1 -1 -1 -1 1 6-314
-1 1 0 0 0 0 0 -1 -1 1 0 0 0 0 -1 -1 -1 1 0 0 0 -1 -1 -1 -1 1 0 0 -1 1 1 1 -1 1 0 1 -1 -1 1 -1 -1 1 6-301	-1 1 0 0 0 0 0 -1 -1 1 0 0 0 0 -1 -1 -1 1 0 0 0 -1 -1 -1 -1 1 0 0 1 1 -1 1 -1 1 0 1 1 1 1 -1 -1 1 6-308	-1 1 0 0 0 0 0 -1 -1 1 0 0 0 0 -1 -1 -1 1 0 0 0 -1 -1 -1 -1 1 0 0 1 1 -1 1 -1 1 0 -1 1 -1 -1 -1 -1 1 6-315

-1 1 0 0 0 0 0
-1 -1 1 0 0 0 0
-1 -1 -1 1 0 0 0
-1 -1 -1 -1 1 0 0
1 1 -1 1 -1 1 0
-1 -1 -1 -1 -1 -1 1
6-316

-1 1 0 0 0 0 0
-1 -1 1 0 0 0 0
-1 -1 -1 1 0 0 0
-1 -1 -1 -1 1 0 0
-1 1 -1 1 -1 1 0
1 1 1 -1 -1 -1 1
6-323

-1 1 0 0 0 0 0
-1 -1 1 0 0 0 0
-1 -1 -1 1 0 0 0
-1 -1 -1 -1 1 0 0
1 1 1 -1 -1 1 0
-1 1 -1 -1 1 -1 1
6-330

-1 1 0 0 0 0 0
-1 -1 1 0 0 0 0
-1 -1 -1 1 0 0 0
-1 -1 -1 -1 1 0 0
-1 1 -1 1 -1 1 0
1 1 -1 -1 1 -1 1
6-317

-1 1 0 0 0 0 0
-1 -1 1 0 0 0 0
-1 -1 -1 1 0 0 0
-1 -1 -1 -1 1 0 0
-1 1 -1 1 -1 1 0
1 -1 1 -1 -1 -1 1
6-324

-1 1 0 0 0 0 0
-1 -1 1 0 0 0 0
-1 -1 -1 1 0 0 0
-1 -1 -1 -1 1 0 0
1 1 1 -1 -1 1 0
1 1 1 1 -1 -1 1
6-331

-1 1 0 0 0 0 0
-1 -1 1 0 0 0 0
-1 -1 -1 1 0 0 0
-1 -1 -1 -1 1 0 0
-1 1 -1 1 -1 1 0
1 -1 -1 -1 1 -1 1
6-318

-1 1 0 0 0 0 0
-1 -1 1 0 0 0 0
-1 -1 -1 1 0 0 0
-1 -1 -1 -1 1 0 0
-1 1 -1 1 -1 1 0
1 1 -1 -1 -1 -1 1
6-325

-1 1 0 0 0 0 0
-1 -1 1 0 0 0 0
-1 -1 -1 1 0 0 0
-1 -1 -1 -1 1 0 0
1 1 1 -1 -1 1 0
-1 1 1 1 -1 -1 1
6-332

-1 1 0 0 0 0 0
-1 -1 1 0 0 0 0
-1 -1 -1 1 0 0 0
-1 -1 -1 -1 1 0 0
-1 1 -1 1 -1 1 0
1 1 1 1 -1 -1 1
6-319

-1 1 0 0 0 0 0
-1 -1 1 0 0 0 0
-1 -1 -1 1 0 0 0
-1 -1 -1 -1 1 0 0
-1 1 -1 1 -1 1 0
1 -1 -1 -1 -1 -1 1
6-326

-1 1 0 0 0 0 0
-1 -1 1 0 0 0 0
-1 -1 -1 1 0 0 0
-1 -1 -1 -1 1 0 0
1 1 1 -1 -1 1 0
1 1 -1 1 -1 -1 1
6-333

-1 1 0 0 0 0 0
-1 -1 1 0 0 0 0
-1 -1 -1 1 0 0 0
-1 -1 -1 -1 1 0 0
-1 1 -1 1 -1 1 0
1 -1 1 1 -1 -1 1
6-320

-1 1 0 0 0 0 0
-1 -1 1 0 0 0 0
-1 -1 -1 1 0 0 0
-1 -1 -1 -1 1 0 0
-1 1 -1 1 -1 1 0
-1 -1 -1 -1 -1 -1 1
6-327

-1 1 0 0 0 0 0
-1 -1 1 0 0 0 0
-1 -1 -1 1 0 0 0
-1 -1 -1 -1 1 0 0
1 1 1 -1 -1 1 0
-1 1 -1 1 -1 -1 1
6-334

-1 1 0 0 0 0 0
-1 -1 1 0 0 0 0
-1 -1 -1 1 0 0 0
-1 -1 -1 -1 1 0 0
-1 1 -1 1 -1 1 0
1 1 -1 1 -1 -1 1
6-321

-1 1 0 0 0 0 0
-1 -1 1 0 0 0 0
-1 -1 -1 1 0 0 0
-1 -1 -1 -1 1 0 0
1 1 1 -1 -1 1 0
-1 1 1 -1 1 -1 1
6-328

-1 1 0 0 0 0 0
-1 -1 1 0 0 0 0
-1 -1 -1 1 0 0 0
-1 -1 -1 -1 1 0 0
1 1 1 -1 -1 1 0
1 1 1 -1 -1 -1 1
6-335

-1 1 0 0 0 0 0
-1 -1 1 0 0 0 0
-1 -1 -1 1 0 0 0
-1 -1 -1 -1 1 0 0
-1 1 -1 1 -1 1 0
1 -1 -1 1 -1 -1 1
6-322

-1 1 0 0 0 0 0
-1 -1 1 0 0 0 0
-1 -1 -1 1 0 0 0
-1 -1 -1 -1 1 0 0
1 1 1 -1 -1 1 0
1 1 -1 -1 1 -1 1
6-329

-1 1 0 0 0 0 0
-1 -1 1 0 0 0 0
-1 -1 -1 1 0 0 0
-1 -1 -1 -1 1 0 0
1 1 1 -1 -1 1 0
-1 1 1 -1 -1 -1 1
6-336

-1 1 0 0 0 0 0 -1 -1 1 0 0 0 0 -1 -1 -1 1 0 0 0 -1 -1 -1 -1 1 0 0 1 1 1 -1 -1 1 0 1 1 -1 -1 -1 -1 1 6-337	-1 1 0 0 0 0 0 -1 -1 1 0 0 0 0 -1 -1 -1 1 0 0 0 -1 -1 -1 -1 1 0 0 -1 1 1 -1 -1 1 0 1 1 1 1 -1 -1 1 6-344	-1 1 0 0 0 0 0 -1 -1 1 0 0 0 0 -1 -1 -1 1 0 0 0 -1 -1 -1 -1 1 0 0 -1 1 1 -1 -1 1 0 1 -1 -1 -1 -1 -1 1 6-351
-1 1 0 0 0 0 0 -1 -1 1 0 0 0 0 -1 -1 -1 1 0 0 0 -1 -1 -1 -1 1 0 0 1 1 1 -1 -1 1 0 -1 1 -1 -1 -1 -1 1 6-338	-1 1 0 0 0 0 0 -1 -1 1 0 0 0 0 -1 -1 -1 1 0 0 0 -1 -1 -1 -1 1 0 0 -1 1 1 -1 -1 1 0 1 -1 1 1 -1 -1 1 6-345	-1 1 0 0 0 0 0 -1 -1 1 0 0 0 0 -1 -1 -1 1 0 0 0 -1 -1 -1 -1 1 0 0 -1 1 1 -1 -1 1 0 -1 -1 -1 -1 -1 -1 1 6-352
-1 1 0 0 0 0 0 -1 -1 1 0 0 0 0 -1 -1 -1 1 0 0 0 -1 -1 -1 -1 1 0 0 1 1 1 -1 -1 1 0 -1 -1 -1 -1 -1 -1 1 6-339	-1 1 0 0 0 0 0 -1 -1 1 0 0 0 0 -1 -1 -1 1 0 0 0 -1 -1 -1 -1 1 0 0 -1 1 1 -1 -1 1 0 1 1 -1 1 -1 -1 1 6-346	-1 1 0 0 0 0 0 -1 -1 1 0 0 0 0 -1 -1 -1 1 0 0 0 -1 -1 -1 -1 1 0 0 1 1 -1 -1 -1 1 0 -1 1 -1 1 1 -1 1 6-353
-1 1 0 0 0 0 0 -1 -1 1 0 0 0 0 -1 -1 -1 1 0 0 0 -1 -1 -1 -1 1 0 0 -1 1 1 -1 -1 1 0 1 1 1 -1 1 -1 1 6-340	-1 1 0 0 0 0 0 -1 -1 1 0 0 0 0 -1 -1 -1 1 0 0 0 -1 -1 -1 -1 1 0 0 -1 1 1 -1 -1 1 0 1 -1 -1 1 -1 -1 1 6-347	-1 1 0 0 0 0 0 -1 -1 1 0 0 0 0 -1 -1 -1 1 0 0 0 -1 -1 -1 -1 1 0 0 1 1 -1 -1 -1 1 0 1 1 1 -1 1 -1 1 6-354
-1 1 0 0 0 0 0 -1 -1 1 0 0 0 0 -1 -1 -1 1 0 0 0 -1 -1 -1 -1 1 0 0 -1 1 1 -1 -1 1 0 1 -1 1 -1 1 -1 1 6-341	-1 1 0 0 0 0 0 -1 -1 1 0 0 0 0 -1 -1 -1 1 0 0 0 -1 -1 -1 -1 1 0 0 -1 1 1 -1 -1 1 0 1 1 1 -1 -1 -1 1 6-348	-1 1 0 0 0 0 0 -1 -1 1 0 0 0 0 -1 -1 -1 1 0 0 0 -1 -1 -1 -1 1 0 0 1 1 -1 -1 -1 1 0 -1 1 1 -1 1 -1 1 6-355
-1 1 0 0 0 0 0 -1 -1 1 0 0 0 0 -1 -1 -1 1 0 0 0 -1 -1 -1 -1 1 0 0 -1 1 1 -1 -1 1 0 1 1 -1 -1 1 -1 1 6-342	-1 1 0 0 0 0 0 -1 -1 1 0 0 0 0 -1 -1 -1 1 0 0 0 -1 -1 -1 -1 1 0 0 -1 1 1 -1 -1 1 0 1 -1 1 -1 -1 -1 1 6-349	-1 1 0 0 0 0 0 -1 -1 1 0 0 0 0 -1 -1 -1 1 0 0 0 -1 -1 -1 -1 1 0 0 1 1 -1 -1 -1 1 0 1 1 -1 -1 1 -1 1 6-356
-1 1 0 0 0 0 0 -1 -1 1 0 0 0 0 -1 -1 -1 1 0 0 0 -1 -1 -1 -1 1 0 0 -1 1 1 -1 -1 1 0 1 -1 -1 -1 1 -1 1 6-343	-1 1 0 0 0 0 0 -1 -1 1 0 0 0 0 -1 -1 -1 1 0 0 0 -1 -1 -1 -1 1 0 0 -1 1 1 -1 -1 1 0 1 1 -1 -1 -1 -1 1 6-350	-1 1 0 0 0 0 0 -1 -1 1 0 0 0 0 -1 -1 -1 1 0 0 0 -1 -1 -1 -1 1 0 0 1 1 -1 -1 -1 1 0 -1 1 -1 -1 1 -1 1 6-357

-1 1 0 0 0 0 0 -1 -1 1 0 0 0 0 -1 -1 -1 1 0 0 0 -1 -1 -1 -1 1 0 0 1 1 -1 -1 -1 1 0 1 1 1 1 -1 -1 1 6-358	-1 1 0 0 0 0 0 -1 -1 1 0 0 0 0 -1 -1 -1 1 0 0 0 -1 -1 -1 -1 1 0 0 1 1 -1 -1 -1 1 0 -1 1 -1 -1 -1 -1 1 6-365	-1 1 0 0 0 0 0 -1 -1 1 0 0 0 0 -1 -1 -1 1 0 0 0 -1 -1 -1 -1 1 0 0 -1 1 -1 -1 -1 1 0 1 -1 -1 -1 1 -1 1 6-372
-1 1 0 0 0 0 0 -1 -1 1 0 0 0 0 -1 -1 -1 1 0 0 0 -1 -1 -1 -1 1 0 0 1 1 -1 -1 -1 1 0 -1 1 1 1 -1 -1 1 6-359	-1 1 0 0 0 0 0 -1 -1 1 0 0 0 0 -1 -1 -1 1 0 0 0 -1 -1 -1 -1 1 0 0 1 1 -1 -1 -1 1 0 -1 -1 -1 -1 -1 -1 1 6-366	-1 1 0 0 0 0 0 -1 -1 1 0 0 0 0 -1 -1 -1 1 0 0 0 -1 -1 -1 -1 1 0 0 -1 1 -1 -1 -1 1 0 1 1 1 1 -1 -1 1 6-373
-1 1 0 0 0 0 0 -1 -1 1 0 0 0 0 -1 -1 -1 1 0 0 0 -1 -1 -1 -1 1 0 0 1 1 -1 -1 -1 1 0 1 1 -1 1 -1 -1 1 6-360	-1 1 0 0 0 0 0 -1 -1 1 0 0 0 0 -1 -1 -1 1 0 0 0 -1 -1 -1 -1 1 0 0 -1 1 -1 -1 -1 1 0 1 1 -1 1 1 -1 1 6-367	-1 1 0 0 0 0 0 -1 -1 1 0 0 0 0 -1 -1 -1 1 0 0 0 -1 -1 -1 -1 1 0 0 -1 1 -1 -1 -1 1 0 1 -1 1 1 -1 -1 1 6-374
-1 1 0 0 0 0 0 -1 -1 1 0 0 0 0 -1 -1 -1 1 0 0 0 -1 -1 -1 -1 1 0 0 1 1 -1 -1 -1 1 0 -1 1 -1 1 -1 -1 1 6-361	-1 1 0 0 0 0 0 -1 -1 1 0 0 0 0 -1 -1 -1 1 0 0 0 -1 -1 -1 -1 1 0 0 -1 1 -1 -1 -1 1 0 1 -1 -1 1 1 -1 1 6-368	-1 1 0 0 0 0 0 -1 -1 1 0 0 0 0 -1 -1 -1 1 0 0 0 -1 -1 -1 -1 1 0 0 -1 1 -1 -1 -1 1 0 1 1 -1 1 -1 -1 1 6-375
-1 1 0 0 0 0 0 -1 -1 1 0 0 0 0 -1 -1 -1 1 0 0 0 -1 -1 -1 -1 1 0 0 1 1 -1 -1 -1 1 0 1 1 1 -1 -1 -1 1 6-362	-1 1 0 0 0 0 0 -1 -1 1 0 0 0 0 -1 -1 -1 1 0 0 0 -1 -1 -1 -1 1 0 0 -1 1 -1 -1 -1 1 0 1 1 1 -1 1 -1 1 6-369	-1 1 0 0 0 0 0 -1 -1 1 0 0 0 0 -1 -1 -1 1 0 0 0 -1 -1 -1 -1 1 0 0 -1 1 -1 -1 -1 1 0 1 -1 -1 1 -1 -1 1 6-376
-1 1 0 0 0 0 0 -1 -1 1 0 0 0 0 -1 -1 -1 1 0 0 0 -1 -1 -1 -1 1 0 0 1 1 -1 -1 -1 1 0 -1 1 1 -1 -1 -1 1 6-363	-1 1 0 0 0 0 0 -1 -1 1 0 0 0 0 -1 -1 -1 1 0 0 0 -1 -1 -1 -1 1 0 0 -1 1 -1 -1 -1 1 0 1 -1 1 -1 1 -1 1 6-370	-1 1 0 0 0 0 0 -1 -1 1 0 0 0 0 -1 -1 -1 1 0 0 0 -1 -1 -1 -1 1 0 0 -1 1 -1 -1 -1 1 0 1 1 1 -1 -1 -1 1 6-377
-1 1 0 0 0 0 0 -1 -1 1 0 0 0 0 -1 -1 -1 1 0 0 0 -1 -1 -1 -1 1 0 0 1 1 -1 -1 -1 1 0 1 1 -1 -1 -1 -1 1 6-364	-1 1 0 0 0 0 0 -1 -1 1 0 0 0 0 -1 -1 -1 1 0 0 0 -1 -1 -1 -1 1 0 0 -1 1 -1 -1 -1 1 0 1 1 -1 -1 1 -1 1 6-371	-1 1 0 0 0 0 0 -1 -1 1 0 0 0 0 -1 -1 -1 1 0 0 0 -1 -1 -1 -1 1 0 0 -1 1 -1 -1 -1 1 0 1 -1 1 -1 -1 -1 1 6-378

134

Appendix B: Dimensions of the open-loop chain

Figure A1 shows the configuration of the open-loop chain used in the simulation. It is assumed that the links are uniform and the mass center of each link is located in the middle of the link. The dynamic equations for the open-loop chain neglecting gravitational terms are given by:

$$\begin{aligned}
 \tau_1 &= [m_1 l_1^2 / 3 + m_2 (l_1^2 + l_2^2 c_2^2 / 3 + l_1 l_2 c_2) + m_3 (l_1 + l_2 c_2 + l_3 c_{23} / 2)^2 + \\
 &\quad m_3 l_3^2 c_{23}^2 / 12] \ddot{\theta}_1 + h_1 \\
 \tau_2 &= [m_2 l_2^2 / 3 + m_3 (l_2^2 + l_3^2 / 3 + l_2 l_3 c_3)] \ddot{\theta}_2 + [m_3 l_3^2 / 3 + m_3 l_2 l_3 c_3 / 2] \ddot{\theta}_3 + h_2 \\
 \tau_3 &= [m_3 (l_3^2 / 3 + l_2 l_3 c_3 / 2)] \ddot{\theta}_2 + (m_3 l_3^2 / 3) \ddot{\theta}_3 + h_3
 \end{aligned} \tag{A.1}$$

where

$$\begin{aligned}
 h_1 &= -m_2 \dot{\theta}_1 \dot{\theta}_2 [l_2 (l_1 + l_2 c_2 / 2) s_2 + l_2^2 c_2 s_2 / 6] \\
 &\quad - m_3 \dot{\theta}_1 \dot{\theta}_3 [(l_1 + l_2 c_2 + l_3 c_{23} / 2) l_3 s_{23} + l_3^2 s_{23} c_{23} / 6] \\
 &\quad - m_3 \dot{\theta}_1 \dot{\theta}_2 [(l_1 + l_2 c_2 + l_3 c_{23} / 2) (2l_2 s_2 + l_3 s_{23}) + l_3^2 c_{23} s_{23} / 6]
 \end{aligned}$$

$$\begin{aligned}
 h_2 &= m_2 (l_1 l_2 s_2 / 2 + l_2^2 c_2 s_2 / 3) \dot{\theta}_1^2 + m_3 (l_1 + l_2 c_2 + l_3 c_{23} / 2) (l_2 s_2 + l_3 s_{23}) \dot{\theta}_1^2 \\
 &\quad + m_3 l_3^2 \dot{\theta}_1^2 c_{23} s_{23} / 12 - m_3 l_2 l_3 (\dot{\theta}_2 + \dot{\theta}_3 / 2) s_3 \dot{\theta}_3
 \end{aligned}$$

$$h_3 = m_3 l_3 s_{23} \dot{\theta}_1^2 [(l_1 + l_2 c_2 + l_3 c_{23} / 2) + l_3 c_{23} / 6] / 2 + m_3 l_2 l_3 s_3 \dot{\theta}_2^2 / 2$$

and where $s_2 = \sin \theta_2$, $s_3 = \sin \theta_3$, $c_2 = \cos \theta_2$, $c_3 = \cos \theta_3$, $s_{23} = \sin(\theta_2 + \theta_3)$, and $c_{23} = \cos(\theta_2 + \theta_3)$.

The following numerical values are used for the simulation:

$m_1 = 90$ gm, $m_2 = m_3 = 100$ gm; $l_1 = 3$ cm, $l_2 = l_3 = 4$ cm; joint axis pulley radius: $r_1 = r_2 = r_3 = 0.8$ cm, spooler radius of the i^{th} motor: $r_{m_i} =$

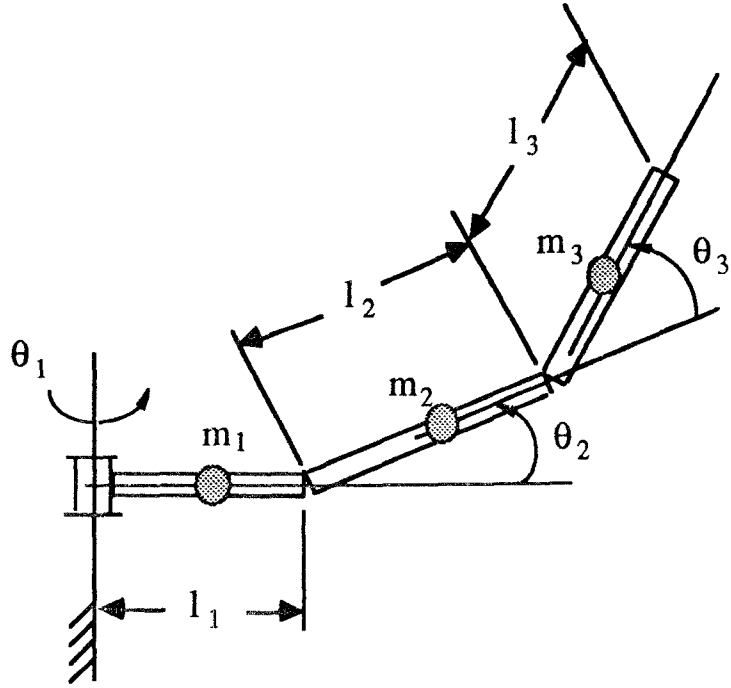


Fig. A1 Schematic of the open-loop chain

0.8 cm, gear ratio $n_i=12$, motor rotor inertia $j_{m_i} = 12.78 \text{ dyne} - \text{cm} - \text{sec}^2$, viscous damping coefficient $b_{m_i} = 68.5 \text{ dyne-cm-sec/rad}$, and maximum motor torque=215400 dyne-cm, for all motors.

The simulation package SIMNON (Åström, 1985) is used to simulate the system. The plant is integrated under the continuous time system and the time step for integration is 0.005 sec.